The Influence of Neck Stiffness, Impact Location, and Angle on Peak Linear Acceleration, Shear Force, and Energy Loading Measures of Hockey Helmet Impacts

By: Stephen Carlson

MSc.
School of Kinesiology
Lakehead University
Thunder Bay, Ontario

Submitted in partial fulfillment
of the requirements of
Master's of Science
In
Kinesiology

Supervisor: Dr. Carlos Zerpa

Committee: Dr. Siamak Elyasi, Dr. Eryk Przysucha

ABSTRACT

Head and brain injuries like concussion affect many hockey players throughout their playing careers. Hockey helmets remain to be the best form of head protection available as they function well to reduce the occurrence of skull fracture by minimizing linear accelerations and force transfer to the head. Currently, among helmet testing protocols and the literature, there is a large focus on peak linear acceleration reduction and the comparison of injury risk across impact conditions relative to linear accelerations felt by the brain. Additionally, gaps exist analyzing how certain impact characteristics like impact angle and neck stiffness influence injury risk. The purpose of this study was to examine the influence that impact angle, neck stiffness, and impact location have on commonly analyzed variables such as peak linear acceleration and Severity Index, while also analyzing differences in shear force and energy loaded onto the head and neck. The study served to create a model to compute the amount of energy loaded into the system composed of head, neck and helmet and to determine the strength of the relationship between the amounts of energy loaded into the system and the risk of injury estimated by Severity Index values. The study involved an analysis of 18 impacts at different velocities per helmet impact locations using a combination of three neck stiffness and two impact angles. In total, 540 impacts were conducted and analyzed. The findings were analyzed and an interaction effect with a medium effect size was observed between impact angle and impact location when measuring peak linear acceleration, $F(8, 510)= 16.174$, $p< .005$, $\eta^2= .113$. Also, interaction effects with small effect sizes were determined between impact angle and impact location, $F(4, 510)= 11.977$, $p< .005$, $\eta^2= .086$, as well as between neck torque and impact angle when measuring the amount of energy loaded onto the system, $F(2, 510)=3.700$, $p= .025$, $\eta^2= .014$. An interaction effect with a medium effect size was also observed between impact angle and impact location

when measuring Severity Index, $F(4, 510)= 12.795$, $p<0.005$, $\eta^2= .091$. Finally, a three-way interaction with a small effect size was observed between the variables when measuring shear force applied to the headform, $F(8, 510)= 5.550$, $p< .005$, $\eta^2= .080$. A model to predict energy loaded was also created using impact location, angle of impact, peak linear acceleration, and peak shear force as predictors, $F(5, 535)= 54.190$, $p< .005$. In addition to these findings, a moderate correlation between Severity Index and the amount of energy loaded onto the system was determined, $r= .340$, $p< .05$. This study served to build on previous research analyzing helmeted impacts in an attempt to improve understanding of injury mechanisms.

ACKNOWLEDGEMENTS

I would like to thank and acknowledge the help and support of Dr. Zerpa and the rest of my thesis committee. I would like to thank Dr. Zerpa for being very supportive, for his edits, suggestions, guidance, knowledge and for the help in overcoming the many roadblocks that arose through the study, and for all the help with the calculations. I would also like to thank him for the opportunity and for making sure I had everything I needed to complete this study. I would also like to thank Dr. Elyasi for providing his valued expertise and opinions on the methods and study as a whole. Dr Prsysucha: thank you for providing your valued opinion and effort to get the document to the point it is today. I would also like to acknowledge the senior fourth year Mechanical Engineering students for designing and building the drop system under the supervision of Dr. Meilan Liu, Dr. Kefu Liu, and Dr. Zerpa. I would also like to thank Mr. Glen Paterson for the incredible amount of help he provided on ensuring the drop system was functioning properly; without him the study would have never been possible to complete within the desired timeframe. Without your experience and creativity, the study would not have happened. I would also like to thanks Mr. Thomas Hoshizaki for helping me throughout my directed study and in using your connections to acquire helmets for testing; you saved me a lot of money. I would like to thank Mary and all of those who helped hold the neckform while I was torqueing it or helped problem solve through all the many issues that arose. All of your help was greatly appreciated.

Table of Contents

List of Figures

List of Tables

Chapter One - Introduction

Hockey is a fast and aggressive sport with large potential for injury (Flik, Lyman, & Marx, 2005). The inherent risk of injury has led to the development of new equipment for injury prevention (Wennberg & Tator, 2003). In the sport of hockey, helmets serve as the primary form of head protection (Kis et al., 2013), however, injuries to the head and brain remain commonplace (Benson, Mieeuwisse, Rizos, Kang, & Burke, 2011). Head and brain injuries can be very severe in nature as they may lead to neurological dysfunction and in rare cases, death (Post, Oeur, Hoshizaki, & Gilchrist, 2011).

Hockey helmets, in their current form, are designed to best protect against traumatic brain injuries (TBIs) such as skull fractures and subdural hematomas (Kis et al., 2013). These severe injuries are caused by sudden accelerations and decelerations on the head and brain, resulting from a large mechanical impact (Namjoshi et al., 2013). Designing a hockey helmet to prevent head injuries involves many tradeoffs between performance, comfort, and appearance (Graham, Rivara, Ford, & Spicer 2014), making helmet design a difficult task to master.

There is little doubt that hockey helmets have been very effective in reducing the occurrence of head and brain injuries, especially those traumatic in nature (Hoshizaki & Chartrand, 1995), which has led to the development of helmet testing protocols. Current methods for testing helmets involve a pass or fail criteria based on a single, large impact (Post et al., 2011). To conduct this testing, the helmet is usually mounted on a surrogate “headform”, designed to respond closely to an actual human head. Accelerometers instrumented in the headform measure the linear acceleration felt by the headform during an impact (Post et al., 2011). The maximum threshold value accepted for peak linear impact acceleration ranges from 275 to 300gs. This range was obtained from human cadaver research conducted on skull

fractures (Gurdjian, Roberts, & Thomas, 1966).The unit “g” is used for any linear acceleration analysis and is simply a multiple of the acceleration due to gravity ($g=9.81\ m/s^2$). If the peak linear acceleration measured during the impact is less than the threshold acceleration measure, the helmet is deemed appropriately protective. While this measure of peak linear acceleration is based on the acceleration experienced by the brain through the centre of mass, along the plane of impact, this testing method may not be indicative of the rigor of the sport of hockey.

Current research in hockey helmet testing has also determined that rotational accelerations contribute to the occurrence of concussion and diffuse axonal injuries in the brain (King et al., 2003).These rotational accelerations are caused in part by shear forces applied to the head during impact (Kleiven, 2013). These rotational or angular accelerations are measured in a similar fashion as linear accelerations; but, are expressed in $rads/s^2$, or radians per second squared, which is a measure of changes in angular velocity over time. This type of acceleration is not generally included in initial helmet testing protocols.

The relationship between angle of impact and acceleration measures during hockey helmet impact testing has also been studied in the past (Walsh, Rousseau, & Hoshizaki, 2011; Zhang, Yang, & King, 2011). The influence that the angle of impact has on brain tissue response, however, is not well understood and the research has focused mainly on measures of peak linear or angular acceleration. By focusing solely on the peak linear or angular acceleration felt by the headform, the information obtained before and after the peak acceleration values is ignored. Incorporating an analysis to examine the helmet performance throughout a greater proportion of the impact may provide a greater insight into the protective abilities of the helmet to dissipate energy away from the brain during an impact.

Energy analysis has been employed in examining the protective ability of bicycle face

protection and soccer headgear but not of hockey helmet performance(Marsh, McPherson, & Zerpa, 2008; Monthatipkul, Iovenitti, & Sbarski, 2012).An energy analysis focusing on energy transferred to the head and neck during impact may provide more information on hockey helmet ability to protect the head against impacts. This type of energy loading analysis can focus on quantifying the amount of energy transferred or applied to the head due to the energy management ability of the helmet and neck; as opposed to focusing on the maximum acceleration felt by the headform or brain. Using the entire loading phase of energy transfer, the impact injury risk can be more accurately analyzed as opposed to focusing on its ability to reduce a large peak linear or angular acceleration.

A helmet energy loading analysis may also provide better insight into head and brain injuries, which are a severe problem in ice hockey; most common of these injuries are concussions (Agel & Harvey, 2010). Indeed, ice hockey has been identified as having the highest incidence of concussion and head injury per participant of all sports (Kelly, Lissel, Rowe, Vincenten, & Voaklander, 2001; Kendall et al., 2012). Although awareness of such injuries continues to grow, the occurrence of injury shows no signs of slowing down, which may be due to limitations of current peak linear acceleration testing criteria for hockey helmets (Kelly et al., 2001; Kendall et al., 2012). In recent years, there has been an increasing awareness for the need for more versatile measures or indices with which to judge the degree of injury hazard, pointing out the fact that traditional methods may not provide enough insight into injury risk (Gadd, 1966).

The effect of neck stiffness on helmet impact acceleration and energy loading measures on the testing dynamic of helmets has not yet been studied extensively in helmet design and performance. Based on these concerns the purpose of this study was: to examine the influence of

neck stiffness, impact location, and angle of impact on the energy and shear force characteristics of hockey helmet impacts as opposed to traditional methods of linear impact accelerations during simulated free falls. The second purpose of this study was to examine the degree of relationship between helmet impact energy loading and the risk of head injury, as estimated by the NOCSAE Severity Index.

The findings of the study revealed that an interaction effect was existed between impact angle and impact location when measuring peak linear acceleration. Also, interaction effects were observed between impact angle and impact location as well as between neck torque and impact angle when measuring the amount of energy loaded onto the system. An interaction effect was also observed between impact angle and impact location when measuring Severity Index. Finally, a three-way interaction was observed between the variables when measuring shear force applied to the headform. These interaction effects reveal the fact that the helmet and neckform manage the impacts differently, depending on the exact impact condition. This suggests that helmets cannot protect the head against injury equally for all impacts, rather, there are significant differences in the risk of injury depending on neck stiffness, the angle of impact, and where the impact occurred on the head. The differences that arise may be due to the helmets itself as well as the asymmetry of the anatomically correct head and neckform used in the study (Foreman, 2010), resulting in different dynamic response upon impact.

In addition to the previously mentioned findings, a moderate correlation between the amount of energy loaded onto the head and Severity Index was determined. This finding shows the relationship between the amount of energy loaded onto the head and the risk of injury as estimated by Severity Index. The results show a relation between the variables in that impacts with a large amount of energy loaded onto the system tended to be at a higher risk of injury.

Conducting an analysis that includes the effect of neck stiffness, shear forces, and energy loading will build on the existing knowledge and provide insight to better understand helmet materials and neck influence in reducing the probability of head and brain injuries in hockey. The results could also provide data for the development of new criteria for helmet design.

Chapter Two - Literature Review

Head and Brain Injuries in Hockey

Hockey is a sport with a high probability for the occurrence of head and brain injuries (Post et al., 2011; Wennberg & Tator, 2003). It has also been identified as having an elevated risk for concussion and other chronic brain injuries due to repetitive head impacts (Chamard et al., 2012). To reduce these injuries, various types of protective equipment have been developed (Biasca, Wirth, & Tegner, 2002). Despite improvements of the overall protective equipment set, head injuries have not been eliminated, but rather the types and patterns of injury changed. It has been reported that changes in protective equipment, such as the addition of larger padding, has paradoxically resulted in an increased risk of head and neck injuries (Biasca et al., 2002).

Even since the mandatory wearing of helmets, head injuries began to rise to become the most common location of injury in hockey (Benson et al., 2011). This increase may be due to the lack of improvement in helmet impact testing as the safety demands of the athletes increased; testing protocols have changed very little over the past 50 years (Rowson, Rowson, & Duma, 2015) and should be improved as soon as possible (Halstead, Alexander, Cook, & Drew, 1998). As stated in the literature, direct contact with an object during a fall or collision can cause serious brain injuries and skull fracture (Yoganandan & Pintar, 2004). That is if the deformation is pushed past its threshold, mechanical failure can occur in the skull, causing fracturing. Fracturing of the skull can cause subsequent injuries such as brain bleeds and pressure gradients created within the skull producing great amount of intracranial damage (Gurdjian, Webster, & Lissner, 1955). Injuries like skull fractures and epidural and subdural hematomas have been largely eliminated (Post et al., 2011), however, do still occur in rare cases (Honey, 1998).

According to the International Ice Hockey Federation (IIHF), there are 577 thousand

hockey players registered and competing in different age groups and levels of competitiveness throughout Canada (Kendall, Post, Rousseau, Gilchrist, & Hoshizaki, 2012). It was reported in 1999 that 3.78% of all sport-related emergency room visits in Canada were due to head injuries that occurred while playing hockey. Most common of all these injuries were concussions; in fact, ice hockey has been identified as having the highest incidence of concussion and head injury per participant of all sports (Kelly et al., 2001; Kendall et al., 2012). When describing head injuries, they are generally categorized as focal, such as skull fracture, where a specific location has been damaged, or as diffuse (e.g., concussion), where a more widespread portion of the brain is affected.

Focal injuries. A focal injury, like skull fracture, is caused by a direct impact to the head with another object, leading to a transfer of mechanical forces (Ouckama, 2013). The breaking of the skull can cause fragments of bone to enter the head and contact the brain. A linear fracture may also occur. That is, the fracture occurs without any depression or distortion of the bones of the skull. Open fractures are also possible, exposing the brain to the external environment, leaving it vulnerable to infection (Aldman, 1984; Hardy et al., 2001). During a head impact, the high levels of strain produced during impact can lead to rupture and bleeding near the dura, referred to as subdural/epidural haematomas (Andriessen, Jacobs, & Vos, 2010). When the injuries are this severe in nature, in the literature, they are referred to as traumatic brain injuries or TBIs. Another type of focal injury is traumatic subarachnoid hemorrhage, which is the result of a contusion or focal damage. This type of head injury is also seen as a delocalized diffuse injury, which poses a threat to brain health and functioning (Andriessen et al., 2010).

Diffuse Injuries. Diffuse brain injuries broadly encompass distributed damage to axons, vascular damage, hypoxic-ischemic injury, and swelling in the brain (Andriessen, Jacobs, & Vos,

2010). The mechanism from which these types of injuries arise are generally rapid accelerations and decelerations to the brain. One reason this occurs is the heterogeneity of the brain structures themselves (Andriessen et al., 2010). Since some structures of the brain may be anchored and fixed by certain structures of the skull such as the brain stem during impact, some portions move more rapidly than others, causing irregular strains, tension, and compressive forces throughout the brain, which may lead to a concussion (Shaw, 2002).

Concussion. A concussion can be defined simply as "an alteration in brain function, or evidence of brain pathology, caused by an external force" (Menon, Schwab, Wright, & Maas, 2010).In terms of brain injuries, a concussion is considered to fall into the category of mild traumatic brain injury (mTBI) and can be seen as such among the existing literature. Injuries classified as mTBI are diagnosed when transient neurophysiologic brain dysfunction, sometimes along with structural axonal and neuronal damage is seen in patients (Katz, Cohen, & Alexander, 2015). The deficits produced from mTBI are generally more subtle than those produced from TBIs like skull fracture, however, in a small number of people, the cognitive, physical, behavioral, and emotional effects may persists beyond one year post-injury (Arciniegas, Anderson, Topkoff, & McAllister, 2005). Concussions can be considered a diffuse brain injury due to the delocalization of damage and has become a major point of focus when considering the safety of athletes throughout all levels of sport. Determining the occurrence of concussion in sports like hockey can be difficult, especially with the large number that go unreported (Daneshvar, Nowinski, McKee, & Cantu, 2011).In the past, when an athlete sustained a concussion, it was regarded as a minor injury and sometimes referred to as having had "your bell rung", sometimes with the recommendations by coaches to simply "walk it off" (Graham et al., 2014). In recent years, there has been a growing awareness for head injuries, especially

concussion, in that all concussions involve some level of brain injury and athletes should be removed immediately following a suspected injury (Halstead et al., 2010). A culture change has been seen in terms of acknowledgement of concussions, treatment, and management, leading to rule changes in an attempt to reduce their occurrence (USA Hockey, 2011).

Benson et al. (2011) attempted to gain a greater understanding of concussion in hockey. Over the course of seven NHL seasons (1997-2004), an inclusive cohort of NHL players and teams were included to examine the occurrence of concussions at the professional rank. In this study, 559 concussions occurred over this time span as diagnosed by a group of physicians. Another study conducted by Flik et al. in 2005 revealed that concussion accounted for 18.6% of all injuries, making it the most common type of injury among collegiate athletes. The findings of Benson et al. (2011) demonstrated that concussions are a major concern to the health and well being of hockey players, accounting for the largest amount of time lost due to injury.

In hockey, the most common causes of concussions are falls to the ice, shoulder to the head and punches to the head (Graham et al., 2014; Kendall et al., 2012). Common side effects include headaches, issues concentrating, antero- and/or retrograde memory loss, balance issues, and motor control loss (Mayo Clinic, 2010). The physiological changes to the brain may include a reduction in cerebral blood flow, over-firing of neurons, imbalances of ions across cells, and an increase in glucose metabolism (Giza & Hovda, 2001). The changes in brain functioning and symptoms may last from hours to months depending on severity (McAllister, Sparling, Flashman, & Saykin, 2001). Hall, Hall, and Chapman (2005) defined three categories in which concussion severity can be graded from the Cantu guidelines, Colorado Medical Society Guidelines, and the America Academy of Neurology Guidelines. Using loss of consciousness, confusion, and amnesia, concussions can be graded on a scale of 1 to 3 based on severity of these

symptoms, 3 being the most severe. The agencies and classes of concussion are shown in Table 1, adapted from Hall, Hall, and Chapman (2005). As depicted in Table 1, each agency relies on certain symptoms when diagnosing and grading a concussion. For example, the Cantu guidelines pay no attention to confusion while the American Academy of Neurology Guidelines do not consider amnesia experienced following a concussion when grading the injury. These discrepancies when diagnosing a concussion highlight the difficulty and general disagreement of concussion severities.

Table 1

Classification of Concussion

Source and Concussion Grade		Confusion	Amnesia	Loss of Consciousness
Cantu Guidelines	I	N/A	Resolving in 30 minutes	No loss of consciousness
	II	N/A	Lasting longer than 30 minutes but less than 24 hours	Resolving in 5 minutes
	III	N/A	Lasting longer than 24 hours	Lasting longer than 5 minutes
Colorado Medical Society	I	+	-	-
	II	+	+	-
	III	+	+	+
American Academy of Neurology	I	Resolving in 15 minutes	N/A	No loss of consciousness
	II	Lasting longer than 15 minutes	N/A	No loss of consciousness
	III	Any level	N/A	Loss of consciousness for any period of time

Concussions, along with any injury to the brain should never be taken lightly, even if it falls into the loosely defined category of "mild". The symptoms may vary greatly in terms of severity and longevity. Furthermore, concussions should always be considered serious, as the potential for long-term effects may rise if poor choices are made based on recovery and a return to play (Hoshizaki, Post, Kendall, Karton, & Brien, 2013).

Head Impacts and Mechanisms of Injury

Occurrence of impacts. An important aspect of understanding head injuries is to examine how often athletes are at risk and how often impacts to the head actually occur. Understanding how often athletes are exposed to injurious situations and head impacts can help to improve the understanding of injury mechanisms, establish reliable injury risk assessment tools, and reduce the prevalence of head injury in sports (Cobb, 2013).

In a study conducted by Brainard et al. (2012) on the number of impacts sustained by collegiate hockey players, the researchers recruited 51 female and 37 male participants to wear helmets instrumented with six single-axis linear accelerometers along with a portable battery powered unit for data collection during two competitive seasons. The study revealed that over the course of a collegiate hockey season, female athletes were exposed to an average M=105, standard deviation (SD)=17.5 impacts per season while the males sustained a higher average of M=347.3,SD=170.2 impacts to the head per season. A similar study by Wilcox et al. (2014) was conducted on collegiate aged hockey players to quantify the number of head impacts sustained by male and female hockey players. The researchers followed 99 players (41 male, 58 female) over the course of three competitive seasons. In this study, players' helmets were instrumented with a head impact telemetry system composed of six single-axis accelerometers to measure and record acceleration induced to the brain during impacts. The median number of head impacts sustained by female athletes was found to be 170 with a maximum value of 489 while the male athletes sustained a median of 287 impacts to the head with a maximum value of 785. Both studies described here provide valuable information on the number of impacts athletes encounter across gender during competitions.

The issue of a large number of head impacts that athletes are exposed to during

competitive games is not only a problem among adult players but also youth players. Mihalik et al. (2012) conducted a study attempting to gain a better understanding of the number and severity of head impacts sustained by youth players during competitions. Fifty-two youth players aged 13-16 were included in the study. Using accelerometer-instrumented helmets, the researchers measured and recorded 12,253 impacts over the course of two seasons with an average of 117.8 impacts per player per season. Although all these impacts are usually below concussive threshold values, there is still a concern that the effects of these repetitive impacts may translate into subconcussive impacts leading to neurological impairment (Bailes, Petraglia, Omalu, Nauman, & Talavage, 2013).

Subconcussive impacts. Subconcussive impacts can also lead to similar effects as those caused by a severe concussion (Bailes et al., 2013). There is clinical evidence suggesting that subconcussive or repetitive impacts cause similar long-term effects and conditions leading to post-concussion syndrome and chronic traumatic encephalopathy (CTE) (Petraglia, Dashnaw, Turner, & Bailes, 2014). CTE is a rare progressive neurological disorder that can result in cognitive, mood, behavioral, and neurological symptoms negatively affecting the lives of athletes (Concannon, Kaufman, & Herring, 2014). Unfortunately, diagnosis can only be determined post-mortem.

Some researchers agree that subconcussive impacts "reflect the lowest level of trauma related to concussion", meaning that these impacts can be considered concussive impacts but with different magnitudes and mechanisms of injury (Hoshizaki, Post, Kendall, Karton, & Brien, 2013, p. 4). Indeed, these repetitive impacts have been shown to produce neuropsychological and functional impairment with axonal damage, which has been detected via diffusion tensor imaging even when there were not visible signs of injury (Bailes et al., 2013). In essence,

significant axonal injury, neuroinflammation, and blood-brain barrier permeability changes have also been observed to occur following these impacts creating a major concern in contact sports like hockey (Bailes et al., 2013). These observations suggest that the occurrence of these impacts during competitions should not be taken lightly and should be given equal consideration as those impacts that produce higher energy dissipation in the brain to better understand the mechanisms of injury that affect the athlete's quality of life.

Mechanisms of injury. Head injuries can be the result of two main mechanisms: direct impacts and inertial loading (Meaney & Smith, 2011). Direct impacts to the head can produce pressure waves through the head and brain due to the large amounts of linear acceleration (Gurdjian, Hodgson, Thomas, & Patrick, 1968) while the inertial loading is associated with greater levels of rotational acceleration and shear forces (Gurdjian, 1972). These injuries arise typically from impacts applied either directly to the head or indirectly to the torso when it is decelerated abruptly (King, Yang, Zhang, & Hardy, 2003).

Direct impacts and inertial loadings to the head cause concussions due to rapid deformation of the brain tissue resulting in diffuse mechanically induced depolarization of the cortical neurons connected in the white matter (Shaw, 2002). In more severe trauma like TBIs, axonal injury occurs throughout the white matter of the brain by the stretching of axons beyond their physiological injury threshold (Graham, Adams, Nicoll, Maxwell, & Genarelli, 1995).

In more profound definition, white matter constitutes about half of the human brain and provides essential connectivity between neural networks (Filley, 2012) and is considered to be the center for movements, intellect, cognition, and sensations (Schmahmann, Smith, Eichler, & Filley, 2008). Through the use of diffusion tensor imaging, researchers have found that college level athletes who sustained a concussion showed evidence of damage clustered in the left

hemisphere white matter fiber tracts (Schmahmann et al., 2008). This damage was incurred to areas such as the inferior/superior longitudinal and fronto-occupital fasciculi, the retrolenticular part of the internal capsule, and posterior thalamic and acoustic radiations (Schmahmann et al., 2008).

There are a few mechanical factors that influence the level of strain and potential for white matter damage during an impact including "head impact versus non-head-impact scenarios, rotational versus linear acceleration, and centroidal versus non-centroidal impacts" (Graham et al., 2014). A head impact can be defined as any instance where the head contacts an external object such as the ice or an opposing player in hockey (Graham et al., 2014). The non-head-impact scenario would be an instance where a rapid acceleration or deceleration may be applied to the head without any direct contact to the head with an external object but may occur when another portion of the body is impacted. When referring to centroidal or non-centroidal impacts, the centre of mass of the head and brain is used as a reference point (Graham et al., 2014). Centroidal impacts are those where energy is directed through the centre of mass, while non-centroidal impacts are not, resulting in a rotation of the head. Upon impact, the head and brain experience a combination of linear and rotational accelerations depending on the location and direction, causing deformation to the brain (King et al., 2003).

Linear acceleration. Head impacts and helmet performance are measured based on peak linear acceleration and white matter brain tissue damage or strain (Post et al., 2011). When measuring linear acceleration, the unit of measure "g" is used. A g is the experimentally determined acceleration due to gravity (about 9.81 m/s^2), thus, measuring acceleration in gs means measuring acceleration as a multiple of this value. Peak linear accelerations have been found to be associated with head and brain injuries that are more traumatic in nature such as

skull fracture and subdural hematoma (Gurdjian, Lissner, & Evans, 1961); a break or depression of the cranial skull bone and a complication of aneurysmal subarachnoid hemorrhage respectively (Biesbroek, Ringel, Algra, & van der Sprenkel, 2012). The impacts resulting in these high levels of linear acceleration produce focal brain injuries and severe damage affecting specific areas of the brain responsible for cognition and sensations (King et al., 2003).

In the past, linear accelerations were viewed as the major cause of head and brain injuries (Gurdjian & Webster, 1945).It has been shown, however, that the translation of the head resulting in high levels of linear acceleration is only associated with focal injuries and not with diffuse injuries produced by rotational accelerations (Gennarelli, Ommaya, & Thibault, 1971).

Rotational accelerations. It has been hypothesized by Holbourn (1943) that shear and tensile strain generated by rotation alone could cause cerebral concussion, white matter tissue damage as well as countercoup contusion. Other researchers in the literature hypothesize this as well, as it is the general consensus that large amounts of rotational accelerations contribute to the occurrence of concussion and diffuse axonal injuries (King et al., 2003). Gennarelli (1983) stated that rotational acceleration could produce most types of primary head injury if it is applied with the right magnitude and to the right location of the head. A conflicting perspective by Omaya et al. (1971) stated that rotational acceleration alone cannot produce the severity of injury that direct impacts cause. Acceleration on the brain without direct impact to the head suggests a whiplash-like incident as it has been argued that the neck cannot produce enough energy transfer to the brain to cause acceleration capable of these injuries (King et al., 2003). In the literature, the term rotational acceleration has been used interchangeably with angular acceleration. Rotational acceleration is measured using the unit "rads/s^2" or radians per second squared. It is evident, however, that there is debate over whether rotational acceleration alone can cause injury

or not. Furthermore, researchers argue that it is rare that an individual would be exposed exclusively to rotational acceleration as it is a consequence of linear acceleration during head impacts (King et al., 2003).

Combined mechanism. Latest research studies indeed support the notion that head impacts causing brain white matter tissue damage and concussion generally result from the effect of both linear and rotational accelerations (Graham et al., 2014; Halstead, 2001; Higgins, Halstead, Snyder-Mackler, & Barlow, 2007). In a study conducted by Mihalik et al. (2012) on youth hockey players, the researchers found that all recorded head impacts over the two seasons involved a combination of both linear and rotational accelerations. In hockey, impacts to the head are not always directed through the centre of mass of the head. In some situations, the impact to the head is generated after contact with other parts of the body or when the head bounces off the object or player following the impact (Graham et al., 2014) all of which include some magnitude of rotational acceleration. Since real world head impact involve the interaction of both linear and rotational acceleration, the negative effects applied to the brain may result in skull and brain deformation, which are induced and exacerbated by the intensity of both linear and rotational accelerations. As stated by Post et al. (2011) moderate levels of both types of acceleration combined have the potential for a severe brain injury (King et al., 2003).

Location of impact. Along with the effects produced by rotational accelerations, impact location to the head has been shown to influence the dynamic response felt by the human brain and white matter tissue. In a study by Zhang et al. (2011), it was demonstrated that the effect of lateral impacts increased the chances of skull deformation and white matter stress and strain felt by intracranial tissue. This finding was previously recorded using primate subjects, where lateral head movement during impact was found to result in more serious diffuse damage when

compared to movement in the sagittal plane (Gennarelli et al., 1982).

A similar relationship between impact location and changes in peak linear accelerations has been found in multiple studies. Walsh, Rousseau, and Hoshizaki (2011) demonstrated that impact location revealed differences in peak linear accelerations. The side location revealed the largest peak linear acceleration (132.8g), more than the front (121.3g) and rear locations (116.9g). In a study by Daniel, Rowson, and Duma (2012), the same relationship was observed when analyzing real-life football impacts among youth participants.

Angle of impact. While the location of the impact and the type of linear or rotational acceleration contribute to the severity of the white matter tissue damage and degree of concussion, statistics about the occurrence and incidence of head injuries also revealed that the extent to which the angle of impact affects the degree of concussion and tissue damage depends on the steepness of the angle and the amount of friction present at the moment of impact (Haldin & Kleiven, 2013). If friction is large, the angle of impact will result in a high rotation and shear force being applied to the head. Previous studies for example have indicated that impacting a surrogate headform at a 45° angle resulted in higher rotational accelerations felt by the head, as compared to similar head impacts at no angle of inclination (Walsh et al., 2011).The literature, however, lacks information on the degree to which shear forces differ due to changing the angle of impact.

The relationship between brain tissue response and angle of impact when measuring linear and rotation accelerations, however, needs further research, especially for helmet designs to protect against concussions. As stated by Walsh et al. in 2011, evaluation of helmet performance when exposed to various angles of impact, rather than locations alone, could prove to be a more thorough form of evaluation in helmet design to better protect athletes against head

and brain injuries.

When evaluating a helmet impact angle, if the angle is too steep the helmet may glance off the impact surface and effectively limit the ability of the test to measure linear and rotational accelerations (Mills, Wilkes, Derler, & Flisch, 2009). As stated in an article by Halldin and Kleiven (2013), "the angle should probably be between 30-45 degrees in order to result in a normal force between the helmet and the ground large enough to avoid slippage" (pg. 10).

Neck influence. Another aspect of impact mechanics that has been overlooked in the literature is the influence of neck stiffness during head impacts (Rousseau & Hoshizaki, 2009). Some researchers have hypothesized that an athlete with a stiffer or stronger neck can mitigate the accelerations felt by the brain by resisting the impact (Rousseau & Hoshizaki, 2009). This resistance to impact is accomplished by increasing their effective mass and conditioning through training their head, neck, and upper torso to work together to absorb impact accelerations, as opposed to exposing the head to all the impact acceleration experienced by the athlete, which may lead to injury, especially for those athletes with less stiff necks (Rousseau, & Hoshizaki, 2009).

The response of human neck stiffness during head collision has only been investigated via simulation by using a headform with a mechanical neck attached to it, especially for helmet testing. The research finding had indicated, however, that the stiffness of the neckform could affect the motion and response of the head during impact (Halldin & Kleiven, 2013). Consequently, the neck response behaviour could influence the head response acceleration transferred to the head and brain during collision (Rousseau & Hoshizaki, 2009).

Other researchers had examined neck stiffness in relation to neck compliance to simulate athlete preparedness for an impact (Rousseau &Hoshizaki, 2009). That is, if an athlete

anticipates an impact, the athlete will be able to stiffen and brace his or her neck prior to impact. On the other hand, if the athlete does not anticipate the impact, he or she will not be able to stiffen their neck to the same magnitude, which creates more neck compliance and higher risk of injury (Rousseau & Hoshizaki, 2009). Rousseau and Hoshizaki (2009) investigated the effect of neck compliance on head impact acceleration measures to better understand the behavior of neck stiffness during collision. To conduct this study, the researchers used a Hybrid III surrogate headform, along with three different neck stiffness (50^{th} percentile Hybrid II neckform as well as a 30% more compliant and 30% less compliant version) applied to three different mechanical neckforms connected to a surrogate headform, impacted at three different velocities (5 m/s, 7 m/s, and 9 m/s). They defined neck compliance as "the ability of the neck to resist motion (in this case, bending, torsion, and compression), where a higher compliance would offer less resistance and less compliance would indicate more resistance" (Rousseau & Hoshizaki, 2009, pg. 91). The results revealed differences in peak linear acceleration when analyzing the three different neck compliances at impact velocities of 9 m/s and 5 m/s. Impacts collected at the velocity of 7 m/s did not show significant differences in peak linear acceleration across neck stiffness. The researchers stated that the influence of the neck on head accelerations requires further investigation to include this concept in future helmets designs to provide better protection to athletes against brain injury (Halldin & Kleiven, 2013; Rousseau & Hoshizaki, 2009).

Hockey Helmets and Current Testing Procedures

Hockey helmets. Helmets are traditionally viewed as the best way to protect the head against brain trauma and have become the primary instrument for head protection in hockey (Kis et al., 2013). Despite the importance of the brain to the body's functioning and well-being, the helmet was one of the last pieces of equipment to be made mandatory for participation in the

sport of hockey (Hoshizaki & Brien, 2004). Proper helmet fit for each individual player, however, is not always possible due to the high demand in the mass production of helmets to protect the head against injuries. Consequently, more attention had been paid to the shape and size of helmets to fit an average human head and little consideration has been given to those individuals in the low and high percentiles, exposing them to higher risk.

In spite of helmet limitations to properly accommodate all human head sizes, the main function of a hockey helmet design is to mitigate the chance of an injury occurring by minimizing linear accelerations upon impact (Gimbel & Hoshizaki, 2008; Graham et al, 2014). Another important purpose of head protection is to block object penetration during collision so that the object cannot breach the surface of the skull. Regardless of these protective abilities of helmets, there are conflicting opinions among researchers on the potential of helmets in reducing the occurrence of concussions. There are researchers who suggest that concussion reduction is possible when wearing a helmet (Benson, Hamilton, Meeuwisse, McCrory, & Dvorak, 2009). That is, if the linear acceleration during impact can be reduced, it is hypothesized that the rotational acceleration could also be reduced, resulting in fewer concussions (Halstead, Alexander, Cook, & Drew, 1998; Rowson & Duma, 2011).

The constituents of a hockey helmet include a comfort liner, an energy attenuation liner, a restraint system (chin strap, size adjustments), and an outer shell (Gimbel & Hoshizaki, 2008; Graham et al., 2014). The materials used in these helmets are designed to deform and minimize linear impact accelerations. In hockey helmets, the materials are chosen due to their ability to deform and return to normal following an impact (Hoshizaki & Brien, 2004). That is, the helmet material should be able to withstand many impacts over multiple competitive seasons.

Outer shell. The outer shell of the hockey helmet is made up of lightweight plastics and

composites that ensure durability and protection (Graham et al., 2014). Acceleration transferred to the head is reduced by the outer shell through deformation, which spreads the impact energy throughout the helmet (Higgins et al., 2007). By deforming, the shell can spread the impact energy over a larger surface area, reducing the incidence of focal injuries (Rousseau, Post, & Hoshizaki, 2009). The shell is traditionally designed in two halves, a front portion and a rear portion (Halstead et al., 1998). This division allows for helmet size adjustment, meaning they can be enlarged in an attempt to create a better fit for the user. Halstead et al. (1998) stated that it appears as though the helmet shells were developed as a sales tool to keep cost down but not with the intention to provide proper fit and retention when mounted on a human head.

The outer shell defines the unique geometry of hockey helmet designs seen today. This geometry has proven to be of some concern in terms of reducing the overall effectiveness of the helmet (Halstead et al., 1998). The "traditional" design of hockey helmets involves certain portions of the helmet that are flatter than others, particularly in the crown area. A flat portion poses some issues in terms of the energy attenuation ability of the helmet. The flatter portions are not as effective at spreading the energy away from the point of impact, meaning impact energy will be more focal at these points (Halstead et al., 1998).

Attenuation lining. The liner serves as the primary form of energy management (Gimbel & Hoshizaki, 2008). The inner lining crushes to absorb and dissipate the energy transferred to the helmet during impact. Selecting the thickness of liner can be of particular difficulty to helmet manufacturers as increasing the density and thickness would certainly reduce the peak linear acceleration transferred to the head, however, increasing the overall diameter could lead to an increase in the potential rotational accelerations transferred, decreased aerodynamics, increased mass, and decreased aesthetic appeal (Landro, Sala,& Olivieri, 2002).

The main types of materials used for the liners are vinyl nitrile (VN) and expanded polypropylene (EPP) foams (Rousseau et al., 2009). The EPP foams used in "higher-end" helmets is thought to manage higher energies than VN foams, however, tends to degrade quicker. The ability of these foams to prevent mTBIs like concussions remains relatively unclear. Rousseau et al. (2009) conducted a study attempting to compare the two types of foams in terms of their ability to reduce peak linear acceleration and peak rotational acceleration. By impacting helmets using the different types of foam, EPP foams were indeed found to reduce the peak linear acceleration in greater amounts than the VN foam, however, VN proved to reduce rotational acceleration better than its EPP counterpart. EPP foam was implemented to perform better than VN foam, but it is clear it may not be as effective in reducing rotational acceleration, which is a major mechanism in mTBIs like concussion.

Helmet Testing

Hockey helmets are designed to pass specific testing protocols to measure their protective ability (Gimbel & Hoshizaki, 2008). Peak linear acceleration has become the accepted dependent variable in measuring the protective ability of hockey helmets (Post et al., 2011). Current helmet designs have proven to be effective in reducing the incidence of injuries more traumatic in nature like skull fracture by greatly reducing the peak linear accelerations transferred to the head (Kis et al., 2013). Despite these reductions in TBIs, there is little evidence suggesting that helmets can protect against concussions. It is widely known that rotational acceleration is an important mechanism in concussion, however, this aspect of impact kinematics is ignored in current helmet testing protocols (Halstead et al., 1998).

The standards used to test hockey helmets have remained relatively unchanged since the 1960s (Gwin, Chu, McAllister, & Greenwald, 2009). Hockey helmet protocols involve a

measure of peak linear acceleration. The helmets are dropped from predetermined heights to have a calculated impact velocity against a standardized surface. The maximum value allowed is set around 275-300gs, depending on the agency (Halstead et al., 1998).This g value was obtained from human cadaver research and it is based on the accepted threshold standard for a skull fracture to occur during a head impact (Gurdjian, Roberts, & Thomas, 1966).

The American Society for Testing Materials (ASTM) is one of the organizations that implement hockey helmet testing protocols. The protocol as defined by the ASTM F1045 involves the helmet mounted on a surrogate headform attached to a monorail drop rig and dropped with an inbound velocity of 4.5 m/s (Gimbel & Hoshizaki, 2008). The peak linear acceleration felt by the headform cannot exceed 300gs for three consecutive impacts, meaning that if the helmet passes this test, it can sufficiently protect the head against a skull fracture at an impact of 4.5 m/s.

The National Operating Committee on Standards for Athletic Equipment (NOCSAE) in Canada has also developed testing standards by which they evaluate helmets. Testing is done at 6 different locations on the helmet: front, right side, right front boss, right rear boss, rear, and top (NOCSAE, 2014), as depicted in Figure 1. Impacts at each location involve testing at 3.46 m/s, 4.88 m/s, and 5.46 m/s. The helmet must pass all impact conditions and remain intact and ready for use (NOCSAE, 2014). It has been stated that the NOCASE standards are “perhaps better suited to research, development, and the potential prediction of serious injury onset” (Halstead, 2001, pg. 324).

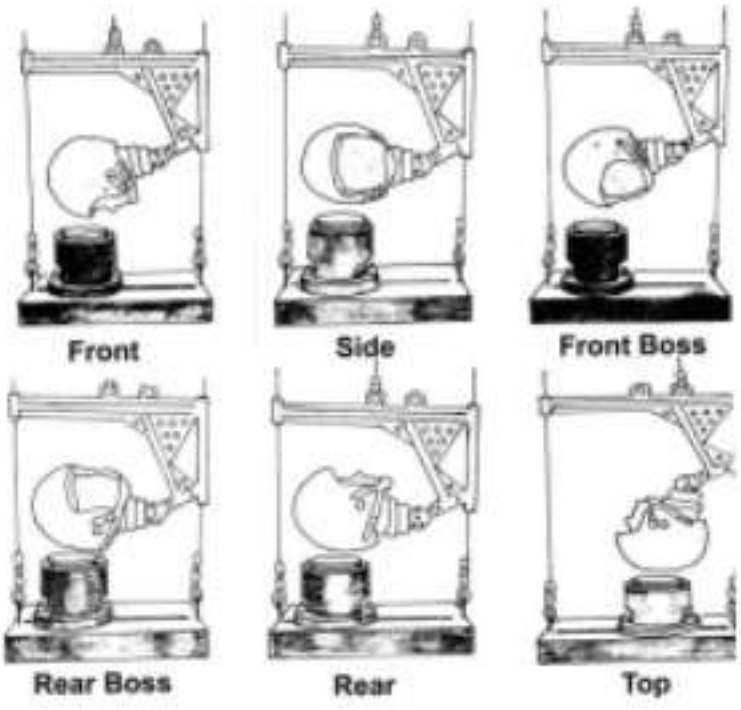

Figure 1. Impact locations as defined by NOCSAE standards (NOCSAE, 2014). Adapted from "Standard test method and equipment used in evaluating the performance characteristics of headgear/equipment", National Operating Committee on Standards for Athletic Equipment (2014), Overland Park, USA: NOCSAE. Copyright 2014 by the National Operating Committee on Standards for Athletic Equipment.

Current testing protocols such as those defined by NOCSAE and ASTM may have reduced the occurrence of skull fractures due to the acceleration restriction during the testing protocol impact velocity, however, Hoshizaki (1995) demonstrated that the liners commonly used in hockey helmets may not be as effective at reducing acceleration and energy transfer during impacts above and below the impacts induced during testing. Unfortunately, hockey helmet standards created to account for high-energy impacts when testing the helmet's ability to prevent skull fractures "are not designed to ensure the same degree of protection at low- and medium-energy impacts" (Gimbel & Hoshizaki, 2008, p. 154). Furthermore, the research finding indicate that the impact velocity defined by ASTM does not even reflect the highest level of energy impacts sustained during play (Halstead et al., 1998), bringing into question the

usefulness of current testing protocols.

It is unclear whether or not current helmet testing protocols accurately reflect the protection needs of athletes. The main concern is that helmet-testing protocols have become focused on a pass or fail criteria based on linear impact accelerations but such test does not reflect the wide range of impacts that will an athlete commonly experiences during playing (Gimbel & Hoshizaki, 2008). Helmets that are designed to withstand a single impact velocity can jeopardize the safety of the athletes as the materials chosen function well only within a range of impact energy absorption (Avalle, Belingardi, & Montanini, 2001). Another major downfall to the testing protocol is that it does not reflect the number of impacts commonly sustained by hockey players. Furthermore, there is little research conducted on "wear-and-tear" of helmets over time (Pearsall & Hakim-Zadeh, 2002). Some researchers have suggested that in order to determine if the helmet can sufficiently protect an athlete over the course of a season or multiple seasons, the testing should include a larger number of impacts and different evaluation techniques (Pearsall & Hakim-Zadeh, 2002).

Current evaluation techniques. Currently, there is a widespread use of quantitative evaluation techniques by helmet manufacturers (Caswell & Deivert, 2002).These include tolerance curves such as the Wayne State Tolerance Curve (WSTC), the Head Injury Criterion (HIC), and Severity Index. All of these measures were developed in an attempt to quantify risk of severe head and brain injury, including an attempt to estimate when said injuries are most likely to occur (Greenwald, Gwin, Chu, & Crisco, 2008).

The WSTC was developed initially to understand head injury thresholds during automotive crashes using curves depicting linear acceleration over time (Greenwald et al., 2008). This model has lead to expansions and development of other measures like the HIC. The curve

data was established using animal and human cadaver data and presents a curve that is set to determine the peak linear acceleration that would cause a skull fracture for a given impact duration (Greenwald, et al., 2008) as shown in Figure 2.

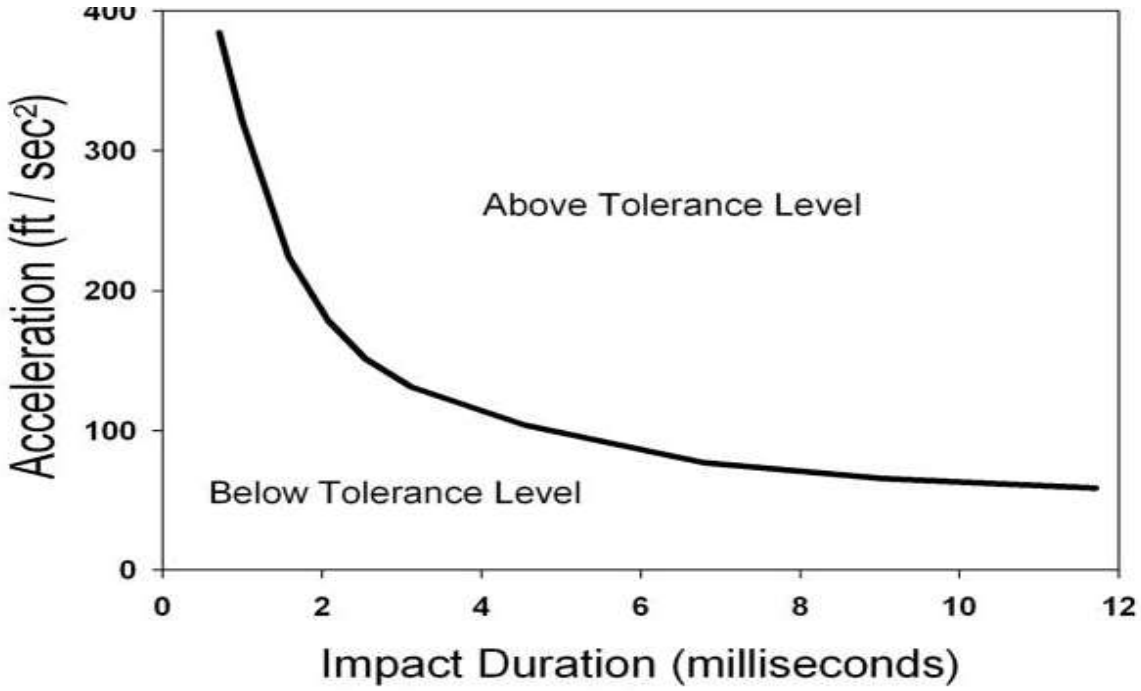

Figure 2. The Wayne State Tolerance Curve. The curve shown is based off animal and cadaver data and determines risk for skull fracture during impacts at different peak linear accelerations and time duration. Adapted from "Head impact severity measures for evaluating mild traumatic brai injury risk exposure", R. Greenwald, J. Gwin, J. Chu, and J. Crisco, 2008, *Neurosurgery, 63*(4), p. 789-798.

The HIC, as depicted in Equation 1, is an effective and accepted criterion for determining head injury risk for linear accelerations placed on the head and brain (Kimpara & Iwamoto, 2012). HIC is used to predict TBIs such as skull fracture and brain contusion.

$$HIC = \left\{ (t_2 - t_1) \left[\frac{1}{t_2 - t_1} \int_{t_1}^{t_2} a(t)dt \right]^{2.5} \right\} \max \quad (1)$$

where:

a = linear acceleration

t_2-$t_1 \leq$ 36ms

t_2-t_1 = time interval where peak acceleration occurs

Time in the formula is measured in seconds. The 2.5 weighting factor was determined by Lissner et al. in 1960 as the slope of the WSTC. There has not been exact thresholds developed to determine the exact risk of injury, however, The National Highway Traffic Safety Administration has identified 700 as the tolerable upper limit (Eppinger et al., 1999).

NOCSAE uses Severity Index (SI), as stated in Equation 2, to determine risk of injury for a given impact during their testing protocol. The index is based on accelerations measured by the headform and SI measures cannot exceed the acceptable levels (NOCESAE, 2014).

$$SI = \int_{t_0}^{t_1} A^{2.5} dt \tag{2}$$

where:

A= head acceleration impulse function
t_1= impulse duration

The formula is similar to that of HIC with one notable difference. That is, the exclusion of multiplying the integral by the inverse change in time, and then multiplying this outcome by the change in time. Integration to calculate SI is carried out over the duration of the acceleration pulse. According to NOCSAE "Standard Performance Specifications for Newly Manufactured Hockey Helmets" (2014), the peak SI of any impact during testing protocol cannot exceed 1200. It is also a stipulation that any impact at 3.46 m/s cannot exceed 300 SI. This index was developed based on correlations with historic injury data for impacts 1-50ms in duration. The SI is not a perfect measure but it "can provide useful correlations to previous injuries" (Oukama, 2013, p. 27). Despite these correlations, the usefulness of SI in determining concussion risk has yet to be proven and it has been stated that "more advanced methods will be needed to design helmets and other protective gear to optimize injury risk reduction (O'Brien & Meehan, 2015, p. 97). Determining the integral of acceleration, as SI attempts to do, may give an estimate of

protective ability, however, other measures such as energy and force transferred during impact may be able to quantify the injury risk in terms of impact energy directed through head and brain. As stated by Chajari and Galvanetto (2013) current testing methods focusing on peak linear acceleration should be improved by including other measures such as force and energy to provide better guidelines for helmet designers and therefore, possibly reduce the occurrence of injuries.

Energy Loading and Force Measures during Impact

Force measures during impact. Researchers have made a great attempt to develop additional measuring techniques to assess helmet ability to protect athletes against concussions by including measures of shear forces and energy loading when testing helmet materials. In a study conducted by Bishop and Arnold (1993), the researchers assessed the ability of helmets to distribute forces during puck impacts by applying pressure sensitive film to the helmet at the impact site. Their results revealed that none of the helmets used had the ability to adequately distribute forces at the side location, even though peak linear accelerations decreased below the acceptable range (Bishop & Arnold, 1993). This force distribution is of particular concern to areas like the "thinner, more vulnerable temporal squamous bone such that the adjacent neurovascular structures may in turn sustain high focal tissue distress" (Oukama & Pearsall, 2012, pg. 77). Distribution of a focal force over a larger area results in smaller compressive stress making penetration of forces in the brain tissue much less likely (Hannon & Knapp, 2006).Some other researchers have stated that measuring deceleration, as depicted in Equation 3, after the brain and head have been accelerated, is a key determinant in the brain exposure to impact forces (Barth, Freeman, Broshek, & Varney, 2001).

$$a = (v^2 - v_0^2)/2sg \quad (3)$$

where:

a = acceleration
v = final velocity
v_2 = initial velocity
s = change in position
g = acceleration due to gravity

The formula represented in Equation 3 explains the relationship between acceleration (a), velocity (v), position (s), and gravity (g) during falling impacts. The use of "g" in the formulas 3 and 4 allows for the expression of results to be in multiples of the acceleration due to gravity, or "g force". V_0 is concerned with the initial velocity before the deceleration begins, whereas v is the direction velocity at the end of the deceleration (Barth et al., 2001). The position refers to the change in displacement after impact during the deceleration and g is the acceleration due to gravity (9.812 m/s^2). At impact, the final velocity (v) is expected to be 0 m/s. Therefore; Equation 3 is simplified, resulting in Equation 4:

$$a = -v_0^2/2sg \quad (4)$$

where:

a= acceleration
v_0= initial velocity
s= change in position
g= acceleration due to gravity

Newton's Second Law of motion states that force is equal to mass times acceleration:

$$F = ma \quad (5)$$

where:

F = force acting on object
m = mass of object
a = acceleration

In an impact situation, the acceleration felt by the brain is due to a force being applied to the head. By making a substitution of Equation 4 into Equation 5, we have:

$$F = mv^2 / 2s \quad (6)$$

where:

F = force
m = mass
v = velocity
s = change in position

From the algorithm depicted in Equation 6, the relationship between force, acceleration, mass, and displacement can be gleaned (Barth et al., 2001). Furthermore, from Equation 6, we can deduce that if all variable except displacement were held constant, a lower stopping distance would result in a significantly higher force experienced by the brain, suggesting that compliance of materials at impact have a significant effect on brain injury, even though an exact threshold for force and injury occurrence has not yet been established for the brain (Barth et al., 2001).

Studies measuring force dispersal during a simulated fall have not been conducted to a greater extent, however, it is known that the manner in which helmets can manage and distribute force within the "local dynamic boundary of helmet/cranium contact site" can greatly influence the risk for and severity of brain injury (Oukama & Pearsall, 2012, pg. 82). In a study conducted by Bishop and Arnold (1993), it was found that the force measures recorded on the head during impact were sometimes contradictory to the head injury risk as calculated by traditional measures, warranting the inclusion of impact force management as an analysis of performance during a simulated fall when using a drop rig system. In an attempt to measure impact forces using forces sensors inside the helmet, Oukama and Pearsall (2012) found that peak focal force through the impact location did not correlate well with peak linear acceleration, meaning that peak focal force could not be predicted using peak linear acceleration as both have separate

impact characteristics.

Energy loading. Besides force dispersal not being included in helmet standard testing protocols to assess if the helmet passes or fails before being sent to the market, another relevant variable not included in this helmet testing protocols is energy loaded onto the head. Energy that is loaded is dissipated by the helmet mainly through the attenuation layer, wherein energy is "absorbed" by the crushable foam (Cui, Kiernan, & Gilchrist, 2009). Energy dissipation is defined as the conversion of mechanical energy into another form of energy, such as heat ("Dissipation", 2015). An ideal energy absorbing material will involve a loading and unloading curve (McLean et al., 1997). In an ideal situation, the foam would be loaded with the entirety of the incoming impact energy and all the energy would be dissipated out of the system during the unloading phase. This concept would suggest that all incoming energy generated during an impact would be absorbed and directed away from the head and brain, however, helmets are not perfect energy absorbers.

While the concept of energy loading have not been used to develop a helmet pass or fail criteria, some researchers have conducted studies to better understand how energy is dissipated through helmets when exposed to an impact. For example, Monthatipkul, Iovenitti, and Sbarski (2012) conducted a study to measure energy absorption during impacts of bicycle headgear. Using a drop rig, headgears were impacted according to the Australia and Standards New Zealand protocol in place for bicycle helmets (AS/NZS standards). Impacting the headgear allowed for the creation of force versus displacement curves for each impact. The force during impact was determined by using the known impactor mass and the acceleration captured from an accelerometer. The foam material crushing (loading) and the bouncing (unloading) phase of impacts were plotted, as shown in Figure 3. The area between the loading and unloading curves

in Figure 3 represents the energy dissipated by the foam during the impact. Using this approach, the amount of energy dissipated by the helmet could be analyzed to better understand the protective ability of the foam. It is important to keep in mind that according to the second law of thermodynamics (law of conservation), energy cannot be created nor destroyed, meaning that it is conserved over time (Vatansever & Hamblin, 2013). That is, the energy dissipated into helmet does not stay in the helmet because it gets converted into another source of energy such as heat.

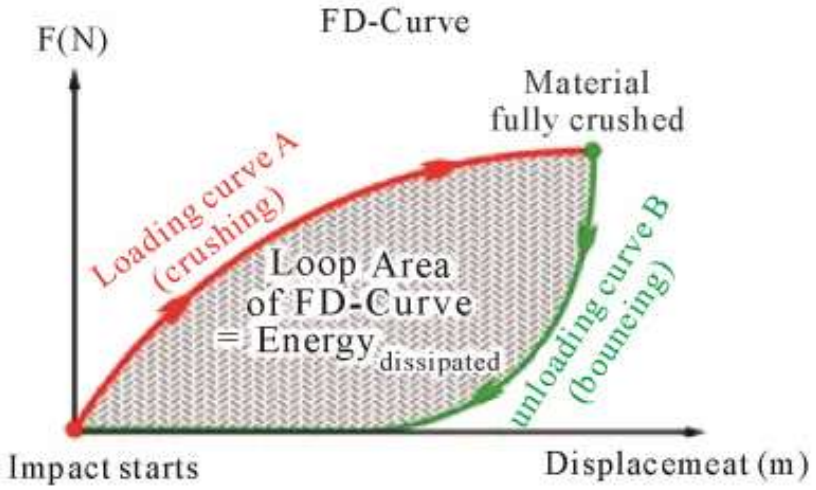

Figure 3. Energy from Force-Displacement Curve. The figure shows an example of the loading and unloading during impact along with the area representing the total energy dissipated by the helmet. Adapted from "Design of facial impact protection gear for cyclists", S. Monthatipkul, P. Iovenitti, and I. Sbarski, 2012, *Journal of Transportation Technologies,* 2, 204-212.

To better understand the helmet capability to dissipate energy during an impact, the area under the loading curve as depicted in Figure 3 represents the work applied to the helmet. Since work is equal to the change in kinetic energy of the system, this input energy can be represented by Equation 7 as the kinetic energy (KE) transferred to the helmet during the impact.

$$KE = \frac{1}{2}mv^2 \quad (7)$$

where:

m= mass of system
v= velocity

The area under the unloading curve as depicted in Figure 3 can be defined as the energy returning from the impact back to the impactor, which can also be calculated using Equation 7 (Monthatipkul et al., 2012). The energy dissipated during impact, however, can be defined as the initial input energy minus the returning energy, as shown in Equation 8. This can be seen as the area between the two curves.

$$E_{dissipated} = E_{loading} - E_{unloading} \quad (8)$$

The efficiency of the helmet in absorbing energy (E_{ab}) during the impact relative to the total amount of energy inputted into the head and helmet can be calculated using Equation 9.

$$E_{ab} = \frac{Energy_{\ dissipated}}{Energy_{\ input}} * 100\% \quad (9)$$

Based on Equation 7, a material or foam with a high capability for energy absorption will allow little energy to be transferred directly to the head during impact and a lower rebound velocity (Monthatipkul et al., 2012). A helmet with a lower rebound velocity will minimize the risk for a secondary impact mechanism to occur. This lower rebound velocity also affects the risk for countercoup injury, which is produced when the brain rebounds in the direction of the deceleration contacting the rear portion of the skull (Barth et al., 2001).

Given that energy dissipation analysis have not been conducted extensively to test the effectiveness of helmet in protecting against head injuries and concussions, some prior studies conducted on bicycle and soccer headgear have provided meaningful information in assessing

the ability of helmet material to absorb energy when impacted a different speeds (Marsh, McPherson, & Zerpa, 2008; Monthatipkul et al., 2012). The previous studies, however, did not attempt to measure the energy dissipation in a real-life simulation. One issue that arises when simulating real-life impacts, is the influence the neck has. During an impact, the neck will allow the head to bend away from the object it is contacting, making the determination of energy dissipated by the helmet during that impact difficult to isolate. Measuring energy loading may allow for accurate comparisons of impact severity and the total amount of energy transferred to the head, neck, and helmet from the impacting surface.

Since there are limitations with current testing protocols to assess helmet ability to minimize head injuries and trauma, an energy loading analysis technique may offer an avenue to better assess hockey helmets impact pass and fail criteria, and better understand the performance of helmet materials in minimizing head trauma. By focusing on the energy loaded onto the system, the impact severity can be determined by incorporating the entire impact. Currently, there is no specific value for energy loading or transfer used as a criterion for injury risk. No prior studies could be found using energy loaded as a dependent variable in hockey helmet analysis for single or multiple impact analysis. The usefulness of implementing an energy loading analysis technique to assess hockey helmet performance is based on the notion that the entire duration of the energy transfer during impact is taken into consideration as opposed to traditional measuring techniques, which rely on a single peak linear acceleration value.

In summary, linear acceleration criteria and injury risk criteria have proven to be useful in the prediction of risk of skull fracture and other severe trauma, however, they remain poor predictors of mTBI risk. A test focusing on force and energy loading besides peak linear acceleration should be examined to better understand the effect of neck strength and material

properties of helmets. This study can assist in defining more robust guidelines for helmet designers to mitigate the occurrence of head and brain injuries

Chapter Three - Method

Purpose

Based on the above rationale, the first purpose of this study was to examine the influence of neck stiffness, impact location, and angle of impact on the energy and shear force characteristics of hockey helmet impacts in addition to traditional methods of linear impact accelerations during simulated free falls. The second purpose of this study was to examine the degree of relationship between helmet impact energy loading and the risk of head injury, as estimated by the NOCSAE Severity Index.

Research Questions

The following research questions were used to guide the study:

1) What is the interaction effect of impact angle, impact location, and neck stiffness when measuring peak linear acceleration, shear force, Severity Index, and energy loading?
2) To what extent can helmet impact energy loading be predicted based on shear force, impact angle, neck stiffness, and impact location?
3) What is the relationship between helmet impact energy loading and Injury Severity Index?

Instruments

Headform. A medium sized NOCSAE headform, as depicted in Figure 11 (see page 55), was used for all trials. The headform was developed in order to simulate the dynamic response that a human head experiences during impact (Hodgson, 1975). This headform is considered to be more anatomically correct than the Hybrid III headform, which is another commonly used headform in the field of impact research. The NOCSAE headform is considered more

anatomically correct due to the inclusion of appropriate facial features and bone structure (McAllister, 2013). The NOCSAE headform is instrumented with an array of accelerometers to measure the acceleration felt at impact in the anterior-posterior direction, the superior-inferior direction and the left-right direction (McAllister, 2013; NOCSAE, 2011). This headform has been used in the literature to simulate the dynamic response of impact including both linear and rotational accelerations (Rowson & Dumas, 2013; Rowson, Dumas, Beckwith, et al., 2012).

Accelerometers, Power Supply, and Software Interface. The headform is instrumented with triaxial accelerometers. The accelerometers were connected to a PCB model 482A04 integrated circuit piezoelectric sensor (ICP) amplifier and power supply unit to maintain power supply to the accelerometers and produce accelerometer analog outputs in x, y, and z directions. The accelerometer analog signals were sent from the amplifier unit to an A/D Instruments Powerlab 16/30 analog to digital converter at a sampling frequency of 20 kHz. The 16/30 Powerlab unit consists of 16 input analog channels with an input voltage range of +/- 2 mV to +/- 10 V. The analog input from each channel was converted to digital and the signal was read into the Lab Charts computer acquisition software. The acquired data was then processed using a Chart Reader Software module. For this study, only three analog input channels were used to collect accelerometer data. Channel 1 recorded the acceleration data in the x-axis, Channel 2 recorded acceleration in the y-plane, and Channel 3 recorded acceleration data gathered in the z-direction. A fourth channel was dedicated to compute the resultant acceleration felt by the headform using Equation 10. A low pas filter at a cut-off frequency of 1000 Hz was applied to the resultant acceleration data to minimize high frequency noise due to vibrations induced to the headform during free falling.

$$\text{Resultant Acceleration} = \sqrt{x^2 + y^2 + z^2} \quad (10)$$

where:

x = linear acceleration in the x-direction
y = linear acceleration in the y-direction
z = acceleration in the z-direction

Mechanical neckform. The neckform, as depicted in Figure 4, was made of neoprene rubber with steel end plates in order to emulate the 50th percentile of a human neck. The neoprene rubber was designed to fit between circular steel disks. To prevent slippage between the steel and rubber disks, the constituent materials have a protruded cylindrical offset. The offset allows the steel and rubber disks to be pressed tightly together while a top plate and base bracket secure the components together.

The neoprene rubber, with steel end plates in the form of a neck, was also designed to simulate neck inertial effects that occur during loading. The rubber disks were designed with two features of the human neck in mind. Firstly, a cutout of the cross-section of the disk was made. Secondly, a larger cutout in the back of the neck was made, see in Figure 4. These two processes were conducted to better mimic the features of a human neck and the response and loading a neck would experience during an impact.

Figure 4. Neckform assembly. This figure shows the assembly of the neckform along with the posterior cutouts in the neoprene rubber, seen between the circular steel plates.

To keep the steel plates and rubber firmly pressed together, a "wire-rope" runs

longitudinally through the neckform, shown in Figure 5. The neckform can also be adjusted to different torque levels using this wire-rope, which allows the user to limit neck rotation and flexion during impacts. The cable can be tightened to adjust the level of neck stiffness and rotation. The cable is made of galvanized stainless steel, ultra-flexible 7x19 strand right lay rope with a machined end-shank made from 303 stainless steel welded to the top of the wire and press-fit into the top plate of the neckform.

Figure 5. Wire-rope cable. The figure shows a rendering of the wire-rope cable that runs longitudinally through the centre of the neckform.

The neck and headform is mounted first to a circular steel plate complete with eight holes arranged around the edge of the plate to allow for mounting to the drop carriage, shown in Figure 6. The main purpose of the plate, however, is to allow for rotation of the neck and headform relative to the impact surface. This plate allows for the control of impact location on the helmet used for this experiment. The plate required rearrangement when a new location was desired.

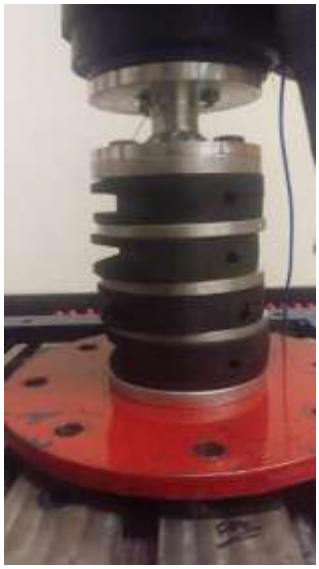

Figure 6. Neckform and circular steel plate. This figure depicts the final segmented neckform along with the circular plate, complete with eight holes to allow for rotation. Cross-sectional cutouts in the neck can be seen at the front of the neckform.

Helmet

Six medium sized identical CCM Vector V08 helmets were used for the study. The number of identical helmets needed for this study was determined by conducting a preliminary helmet wear and tear test to identify if the helmet properties were compromised due to the a large number of impacts per location. More details of the wear and tear protocol are outlined in the procedures.

The medium CCM Vector V08 helmet (22.5 to 24.25 inch head circumference) contains a dual-density VN liner along with a lightweight (518 grams) and ventilated outer shell. The helmet uses a tool-free adjustment system located on each side of the helmet. The helmet was made to its smallest fit in order to optimally fit the NOCSAE headform.

Drop Testing

Drop system. The testing involved a dual rail drop system, as depicted in Figure 7, constructed by students from the Lakehead Mechanical Engineering Department and staff from

the faculty of the School of Kinesiology. The rig incorporates a drop carriage to which the headform can be mounted, secured on a railing system with little friction, such that the motion of the headform can be regarded as free fall. The weight of the headform, neckform, and drop carriage is 30.6kg and remained as such throughout the entire procedures. A 110-volt AC winch with a wire connected to a magnetic plate was used to elevate the drop rig to the correct height prior to each impact. The winch was controlled by a wall mounted electronic controller and a raise/lower switch. When energized, the magnetic plate remains in contact with the steel drop carriage. When the release switch on the controller is pressed, the magnets are deenergized and the rig falls freely to the contact surface completely unbound and free to rebound from the surface (Gimbel & Hoshizaki, 2008). The rig is mounted on rubber matting which is bolted into the floor to minimize noise and vibration caused during impact.

Figure 7. Lakehead University drop system. The controller can be seen to the left of the system. The forward/reverse switch to control raising and lowering is attached by cable to the controller. The neck and headform are mounted, along with the circular steel plate, to the circular blue plate seen above.

Reliability and concurrent-related evidence of validity for linear impact acceleration measures of the Lakehead University impact drop system was examined via a pilot study.

Concurrent validity is studied when the measures of a test are proposed to be a substitute for the measures of another test, previously established as criteria (Cronbach & Meehl, 1955). In this case, the Lakehead University impact drop system was compared to the University of Ottawa Neurotrauma Science research lab impact acceleration measures drop system to provide concurrent-related evidence of validity. The results indicated strong intraclass correlation (ICC) between both systems; ICC=0.922, $p<0.005$ for frontal impacts; ICC=0.844, $p<0.005$ for front boss impacts; ICC=0.934, $p<0.005$ for side impacts; ICC=0.952, $p<0.005$ for rear boss locations; and ICC=0.932, $p<0.005$ for rear impacts.

To provide evidence of reliability, 100 identical rear impacts at 3.13 m/s were conducted. Strong evidence of reliability was found across replication of protocol using correlations between the system measures, r=0.922, $p<0.005$ when using the split-half technique. This technique involves the comparison of even and odd number impacts and testing for consistency in the measures. This correlation result provides evidence of consistency of the drop system and acceleration measures across identical trials. For more detailed information on the pilot study, see Appendix A.

For the current study, the impact surface of the Lakehead University Drop System was instrumented with an Advance Mechanics Technologies Incorporated (AMTI) force platform. This plate is equipped with a steel impact surface and angled steel bracket. All impacts were conducted in such a way that the headform was impacted near the centre of the plate.

Force platform. The AMTI OR6-5-1 force plate, as depicted in Figure 8, is designed with six degrees of freedom to measure three components of force and three moments along the x, y, and z axes. There are four proprietary load cells located at the four corners of the platform that are measured by foil strain gauges. The strain gauges form six Wheatstone bridges to

produce six output voltages: three voltages for forces (x, y, and z) and three for the moments along the x, y, and z axes to measure impacts applied to the surface of the force plate.

The force plate was mounted to a frame at the base of the drop system and a steel angle bracket was fastened onto the plate to measure shear forces and energy loading. The plate was firmly mounted to eliminate crosstalk and resonance, provide maximum linearity, and provide isolation from the external environment.

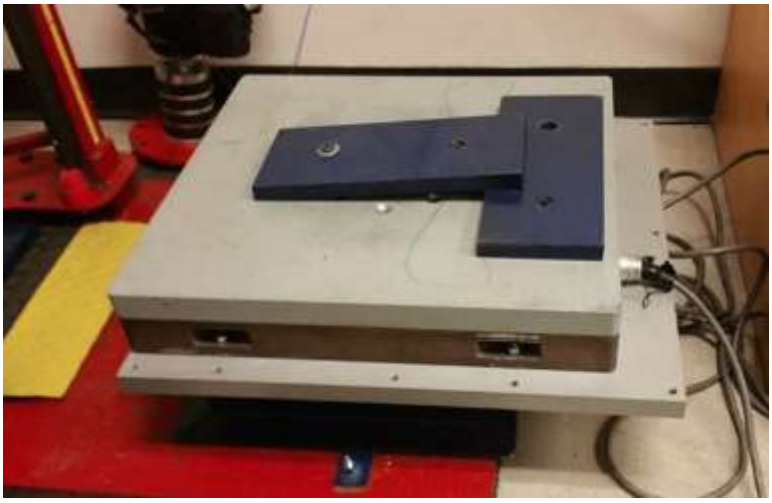

Figure 8. AMTI force platform. This figure shows the force platform with a wedge mounted on the surface to achieve an impact angle of 13.5 degrees.

The upper limit for loading the AMTI forceplate is 9800 N in the vertical direction when force is applied anywhere on the surface of the plate. A maximum of 6700 N can be applied anywhere in the x or y directions. Values from impacts conducted in the current study were not near these limits. Due to sensitivity of measurement, the platform was calibrated before all testing sessions. Data were acquired using LabCharts computer software and analyzed using Microsoft Excel computer software. The mass of the headform and helmet in addition to the resultant force measures collected were used to calculate energy loaded onto the system during impact.

Procedures

Prior to beginning the actual experimentation, the static stiffness, or neck compliance was determined. To accomplish this, the neck was tightened to different torque values and flexion loading tests were conducted to examine the stiffness of the headform for flexion, extension, and lateral flexion. Forces and neck length changes required to flex the neck through a range of motion were determined. The range of motion was limited to the maximum flexion that can be caused by manually pulling on the neck using a strain gauge. During the testing, pictures were taken and analyzed using Kinovea computer software to determine changes in neck length, angle, and force applied perpendicularly to the neckform. Forces and neck length measures were used to create moment-angle of flexion curves to be fit using a regression model. This approach was very similar to the testing protocol implemented by Spittle, Miller, Shipley and Kaleps (1992) to calibrate the stiffness of a Hybrid III neckform as depicted in Figure 9.

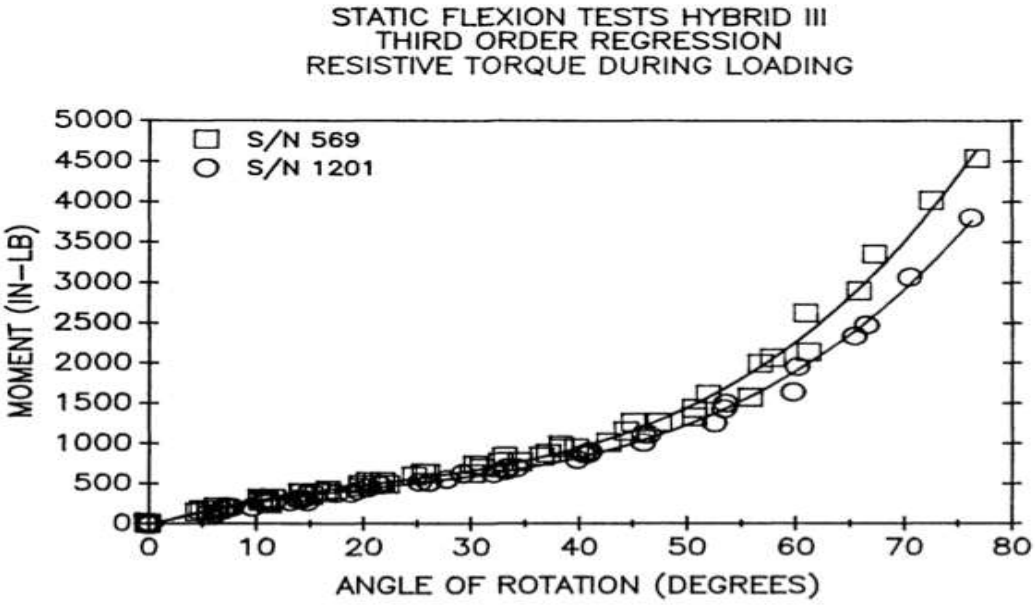

Figure 9. Static flexion test of Hybrid III neckform. The angle of flexion is plotted against the moment. A similar plot was created for the flexion, extension, and lateral flexion of the custom neckform used during the experiment. The amount of torque required to bend the three different neck tightness (8.4, 12, and 15.6 in-lb) was measured.

In addition to neck stiffness and compliance standardization, the performance deterioration of the helmets was also examined before conducting the actual testing. In order to measure the change in performance, the CCM Vector V08 helmet was impacted 200 times using a repetitive impactor, shown in Figure 10. An identical CCM V08 helmet to the ones that were used in the testing protocol was exposed to 200 impacts to the front and rear locations to measure deterioration over the proposed number of impacts per impact location, outlined in the procedures section. The impact surface was an AMTI forceplate, which allowed for the measurement of resultant force across the impacts. The number of impacts at which a significant increase in peak force was observed determined the threshold value of how many impacts the helmet could sustain to a single location before its protective ability was compromised. This approach allowed the researcher to predict helmet deterioration and gave insight into how often the helmet should be replaced in order to maintain the integrity of the results obtained during the procedure.

Figure 10. Repetitive impactor used to measure helmet deterioration. The helmet is mounted to a headform and piston that can repetitively impact the helmet against the previously described AMTI forceplate.

All data was collected in at a sampling frequency of 20 kHz in room 1028 of the C.J. Sanders Building on the Lakehead University campus. To ensure safety, the impact area was cleared while data was being collected.

The drop testing protocol for this study was conducted according to the NOSCAE drop test standards protocol, which states that the "headgear is positioned on a headform and then dropped in order to achieve an accepted free fall velocity. At impact, the instantaneous acceleration is measured by triaxial accelerometers and the resultant acceleration shall be used for Severity Index calculations" (NOCSAE, 2014, p. 2). During all simulated impacts, linear acceleration over time was collected for SI calculations. Resultant force data was also collected to calculate the energy loaded onto the system during each impact. Data collection was initiated once acceleration passed a 3g threshold value (Walsh et al., 2011).

In order to ensure a proper fit of the helmet on the headform, manufacturers fitting instructions were followed to obtain a reasonable fit, shown in Figure 11. The distance between the brim and the helmet and the bridge of the nose was measured to 5.5 cm to maintain consistency. In any case, fit is a subjective measure on a humanoid headform and the best judgment of the researcher was used along with these specifications.

Figure 11. NOCSAE headform with properly fitted helmet. This figure shows the NOCSAE headform that was fitted with a CCM Vector V08 helmet. This fit was maintained throughout the entire procedure.

The helmet was impacted a single time (Post, Oeur, Hoshizaki, & Gilchrist, 2011) for each combination of simulee, neck torque, angle, and location. This approach was used since

strong evidence of reliability and validity was found through the pilot study and to minimize wear and tear of the wire-rope cable that runs axially through the neckform. The helmet was impacted at 5 locations as defined in NOCSAE drop test standards for each impact velocity, similar to the helmet testing protocol implemented by Walsh et al. (2011). These locations included: front, front boss, side, rear boss, and rear. In Figure 1, the front (F) location is situated "in the median plane approximately 1 inch above the anterior intersection of the median and reference plane" (Higgins, Halstead, Snyder-Mackler, & Barlow, 2007, pg. 7). The front boss (FB) is defined as "a point approximately in the 45 degree plan from the median plane measured clockwise and located approximately above the reference plane" (Higgins, Halstead, Snyder-Mackler, & Barlow, 2007, pg. 7). Side (S) refers to the location "approximately at the intersection of the reference and coronal planes on the right side of the headform" (Higgins, Halstead, Snyder-Mackler, & Barlow, 2007, pg. 7). Rear boss (RB) is found "approximately at the posterior intersection of the median and the reference planes" (Higgins, Halstead, Snyder-Mackler, & Barlow, 2007, pg. 7). And finally, rear (R) is the location found "approximately at the intersection of the median and reference planes" (Higgins, Halstead, Snyder-Mackler, & Barlow, 2007, pg. 7).

In addition to changing location, the angle of inclination during impact was also adjusted. Impact angles of 0° and 13.5° were implemented in this testing protocol. A zero angle of inclination was achieved by contacting the force plate perpendicularly. The angle of 13.5-degrees was achieved using an impact wedge, mounted to the surface of the force plate at the desired angle. Furthermore, the neckform tightness was also adjusted to analyze the influence of neck compliance characteristics on dynamic response. Similar to the protocol by Rousseau and Hoshizaki (2009), neck compliance was adjusted to 30% above and below the standard setting of

the neckform (12 in-lb). See Table 2 for exact stiffness torques.

Table 2

Stiffness Conditions and Torques Required

Stiffness	Torque (in-lb)	Torque (Nm)
Low	8.4	0.949
Standard	12	1.356
High	15.6	1.763

When conducting the actual helmet testing procedure, each helmet location was impacted by dropping the helmet mounted on the NOCSAE headform onto the surface of the AMTI force plate at zero angle of inclination with the neckform torqued to the standard 12 in-lb. All impacts with each neck torque were completed before moving to the next location. The order of impacts were as follows: front, front boss, side, rear boss, followed by rear (as defined by NOCSAE standards). Each helmet was subjected to 1 impact per location at each of the 18 selected drop heights, similar to the research protocol of Marsh et al. (2004) as shown in Table 3. The inbound velocities were determined based on measures of vertical height using Equation 11. Eighteen drop heights, and estimated impact velocities were chosen at 5 cm increments between the lower limit of 2.62 m/s at a height of 0.35 m and upper limit of 4.85 m/s at a height of 1.20 m as shown in Table 3. With these protocols, a total of 90 impacts were simulated per neck torque condition for each of the two impact angles.

Following the completion of the zero degree angle of inclination impacts across the five helmet locations on the force plate, the procedure was repeated again for a 13.5 degree impact angle. The helmets were tested using the same 18 impact velocities for each angle condition and impact location. The headform was adjusted accordingly to ensure that the impact occurs at the desired location.

In addition to changing angle conditions and locations, the testing procedures described above was repeated for two additional neck torques (higher stiffness of 15.6 in-lb and lower stiffness of 8.4 in-lb), see Table 2. With the addition of two more neck stiffness, the total number of impacts required to sufficiently answer the research questions was 540.

Table 3 summarizes drop heights of the 18 simulees used in the study as well as the expected inbound velocities. Each simulee experienced identical impacts for all location, neck torque, and angle conditions. The drop heights range from 0.35 m to 1.2 m, with corresponding expected inbound velocities ranging from 2.62 m/s to 4.85 m/s.

Table 3

Simulee Inbound Velocities and Drop Heights

Simulee Number	Drop Height (m)	Impact Velocity (m/s)
1	0.35	2.62
2	0.40	2.80
3	0.45	2.97
4	0.50	3.13
5	0.55	3.28
6	0.60	3.43
7	0.65	3.57
8	0.70	3.71
9	0.75	3.84
10	0.80	3.96
11	0.85	4.08
12	0.90	4.20
13	0.95	4.32
14	1.00	4.43
15	1.05	4.54
16	1.10	4.64
17	1.15	4.75
18	1.20	4.85

Energy loading values were calculated from the force plate information. All necessary processing was conducted using Microsoft Excel computer software. Energy loading, shear force, Severity Index, and peak linear acceleration data were then input into IBM SPSS computer

software for hypothesis testing.

Energy during the loading phase of impact was calculated using the impact force data captured by the force plate based on Equation 11.

$$F = ma \tag{11}$$

where:

F = force
m = mass
a = acceleration

Equation 12 explains the relationship between force (impulse) and momentum:

$$F \cdot dt = m \cdot dV \tag{12}$$

where:

F = force
dt = time interval
m = mass
dV= velocity increment

Equation 12 was used to derive Equation 13, which explains the relationship between the final velocity and the force captured by the force plate.

$$V_f(t) = V_i + \frac{1}{m}\int_0^t F \cdot dt \tag{13}$$

where:

$V_f(t)$= final velocity
V_i = initial velocity
m = mass
F = force
t = time

Velocity is defined as the rate of change in position with respect to time. An integration technique was used to convert the velocity data during the impact into position data, as shown in Equation 16.

$$s(t) = s(t_0) + \int_{t_0}^{t} V_f(t) d\,t \tag{14}$$

where:

$s(t)$ = position at t
$s(t_0)$= initial position at t_0
t_0 = time at beginning of interval
t = time at end of interval
V_f = velocity

According to the work-energy theorem, the work applied to the helmet was equal to the change in kinetic energy. Equation 14 was used along with the force during impact to determine the energy during the loading phase of the impact, as seen in Equation 15.

$$E_{Loading} = \int_{0}^{s} F_1 \cdot d\,s \tag{15}$$

where:

$E_{Loading}$ = energy during loading
F_1 = force during loading
ds = compression or position increment

This formula computes the energy loaded onto the system (helmet, headform, and neckform) during the energy loading phase of impact. This energy loaded onto the system represents the amount of energy transferred during the impact and in effect, quantifies the severity of the impact and may represent potential for injury for the given impact condition.

Data Analysis

Inferential statistical analyses were conducted to answer each of the research questions formulated for this study. To answer research question 1, **what is the interaction effect of neck stiffness, impact angle, and impact location when measuring peak linear acceleration, shear force, Severity Index, and energy loading?** four 5 (impact location) x 2 (impact angle) x 3

(neck torque) factorial ANOVAs were conducted to examine the interaction effect between these factors on peak linear acceleration, shear force, severity index, and energy loading as dependent variables.

To answer research question 2, **to what extent can energy loading be predicted using shear force, impact angle, neck stiffness, impact location, and peak linear acceleration?** a multiple regression analysis was conducted using energy loaded as the dependent variable; shear force, impact angle, neck stiffness, and impact location as predictors. This analysis allowed for the determination of the power of each of the predictors, as well as the overall model, in predicting energy loaded onto the system. The ability of the overall model to predict the dependent variable could be determined by the R squared value. This value represents the proportion of the variance in the dependent variable that can be explained by the predictors used in the model.

Prior to running the analyses, the nominal variables with more than two levels (impact location and neck torque) were transformed into dummy variables, similar to the procedure by Alkharusi (2012). The dummy coded variables allowed for the determination of unique contributions for the levels of these variables. In addition, individual coefficients were created to determine how significantly each contributes to the model.

Creating a model to predict energy loaded onto the system can allow for the determination of the energy transferred to the helmet, head, and neck without having to perform the time consuming process of integrating the force data. In order to create an accurate and effective model, certain assumptions of the multiple regression analysis must be met and tested for, including: there are no significant outliers, there is independence of observation, no multicollinearity of the predictors, and there should be a linear relationship between each

predictor and the dependent variable.

Prior to creating the regression model, significant outliers or high leverage points were tested for using box-plot analysis, ensuring they do not negatively influence the predictive ability of the model. To test if there was a linear relationship between each predictor and the dependent variable, scatter plots were created and Pearson's product-moment correlations were calculated. The data was also checked to ensure there was no multicollinearity among the predictors. Checking for multicollinearity ensured that the predictors included in the model were linearly independent. Multicollinearity was tested by conducting a Pearson's product-moment correlation analysis between predictors. If predictors were found to be highly correlated, they were removed from the model. Multicollinearity was also tested using Variance Inflection Factor (VIF). VIF is used to quantify how much the variance was inflated by the presence of a given variable. A VIF value of 1 would imply no correlation among predictors, while a VIF exceeding 10 may require correction or removal of the predictor.

Independence of observation also needed to be tested to ensure there was no autocorrelation in the residuals. This assumption of multiple regressions was tested using the Durbin-Watson statistic. That is, if a value of 2 is obtained, there is no autocorrelation in the sample, while deviations toward 0 or 4 suggests a positive and negative autocorrelation, respectively.

To determine the unique contribution of each factor, partial correlations were conducted. This approach allowed for the determination of correlation between the predictor and dependent variable while controlling for the influence of the other predictors.

To answer research question 3**, what is the relationship between helmet impact energy loading and Injury Severity Index?** a Pearson's product-moment correlation analysis was

conducted to examine the degree of relationship between energy loading and severity index. Since a strong correlation was found between these two variables, a regression analysis was also conducted to create an interpolation function to predict injury Severity Index levels from energy loading to better assess helmet ability to protect against injuries during impact testing.

Chapter Four - Results

Repetitive Impact Testing

Before conducting the impact analysis using the Lakehead University impact drop system, the ability of the helmet to withstand impact forces was assessed over 200 impacts. The performance deterioration was observed using the repetitive impactor shown in Figure 10. The peak resultant force was measured over the 200 high-energy impacts for the front and rear location as shown in Figures 12 and 13 to observe any changes in peak force.

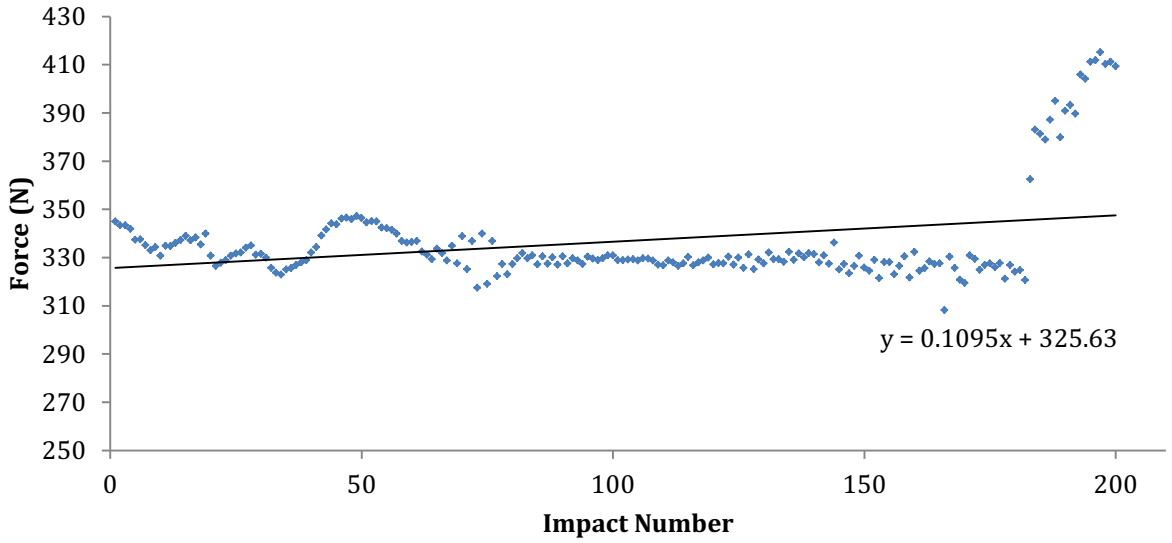

Figure 12. Repetitive impact testing at the front location. The figure shows the peak resultant force measured during repetitive impacts to the front location over the course of 200 impacts.

Figure 12 shows the peak force over the 200 impacts to the front location. The peak force remains relatively stable until impact 189, where there is a rapid increase in the peak force. This rapid increase suggests that the helmet performance decreased significantly for impacts beyond 189 impacts for the frontal location, but remained very stable until that point. From the equation of the line of best fit, even including the values after the spike, there is a very small slope, suggesting that the performance change over time is very small. Repetitive impact testing was also conducted to the rear location to determine if performance deterioration occurred similarly

to other locations. The results are shown in Figure 13.

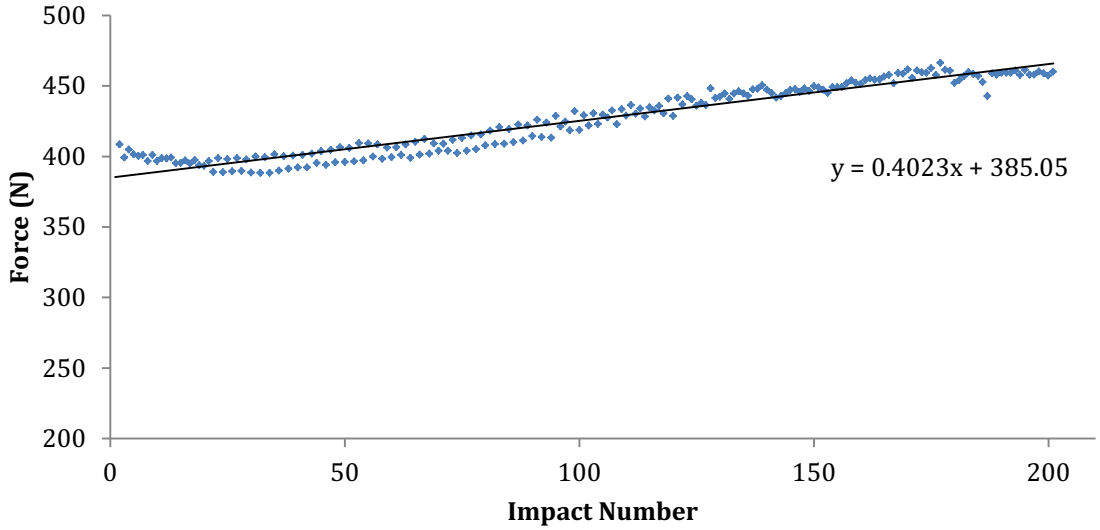

Figure 13. Repetitive impact testing to the rear location. The figure shows the peak force measured across 200 impacts to the rear location using the repetitive impactor.

The impacts to the rear location show a significantly different trend in performance deterioration than to the front location. There is no rapid spike in impact force, rather there is a gradual decline in performance. The decline in performance appears to begin around impact 90, where the impact force exceeds 410N and begins to climb further. The slope of the line-of-best-fit suggests that there is an increase of 0.4023N for every impact sustained to the helmet when including all 200 impacts. Although no rapid decline in performance is observed, there appears to be a decline in performance over a large number of impacts at the rear location.

The results from the repetitive impact testing revealed that helmet performance deteriorated over time, suggesting that the helmet should be replaced following to large number of impacts. To eliminate the possibility of helmet deterioration affecting the results of the study, a new helmet was used for each combination of neck torque and angle. That is, a new helmet was used after 90 impacts. A total of 6 helmets were used in the procedures.

Each helmet was impacted 18 times for each location, a number that was not expected to

cause significant performance deterioration. This design resulted in each impact condition beginning with a brand new helmet.

Static Neck Testing

The next objective of the study was to quantify the difference in neck stiffness of the three different neck torque settings used in the study. The testing was conducted manually using a hand-held strain gauge to pull the neckform in each direction. The range of motion for most tests was limited to 20 degrees, due to the amount of force required to cause further bending being too great to achieve manually. Figures 14, 15, and 16 show the torque results for the static extension, lateral flexion, and flexion testing procedures as well as the equation for the line-of-best-fit.

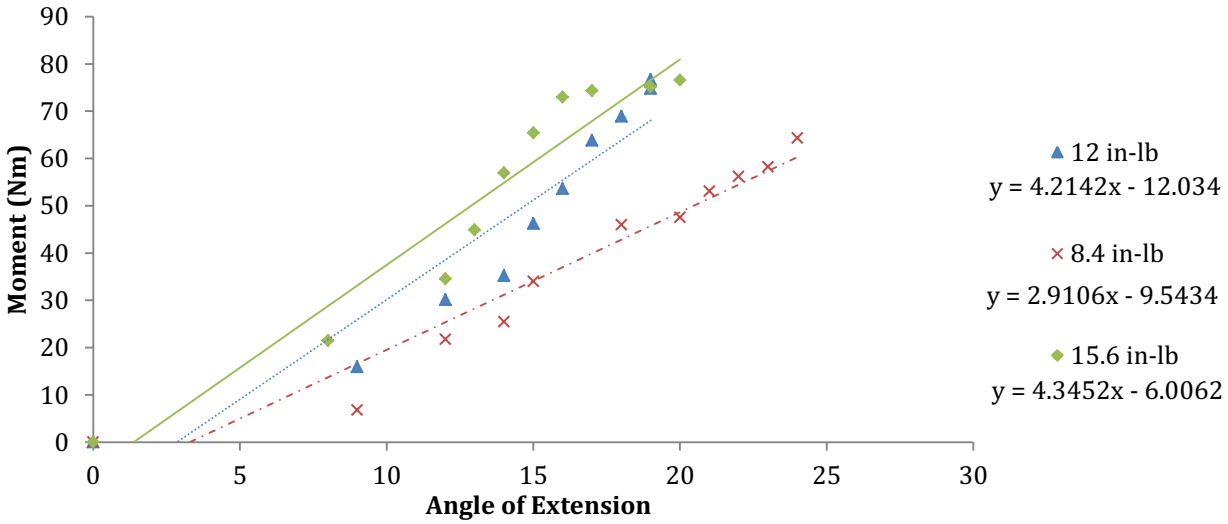

Figure 14. Static extension testing for the three neck torque settings used. The figure shows the resulting torque required to bend the neckform through a short range of motion. For each torque equation, x represents the angle of neck extension and y represents the moment or torque.

Figure 14 shows that as the tightness of the neck was increased, more torque was required to manually extend the neck through the short range of motion. The equation for the line-of-best-fit is shown for each neck torque to allow for the predicted amount of torque required to bend the neck to a given angle. The same testing was also conducted for lateral flexion, shown in Figure

15.

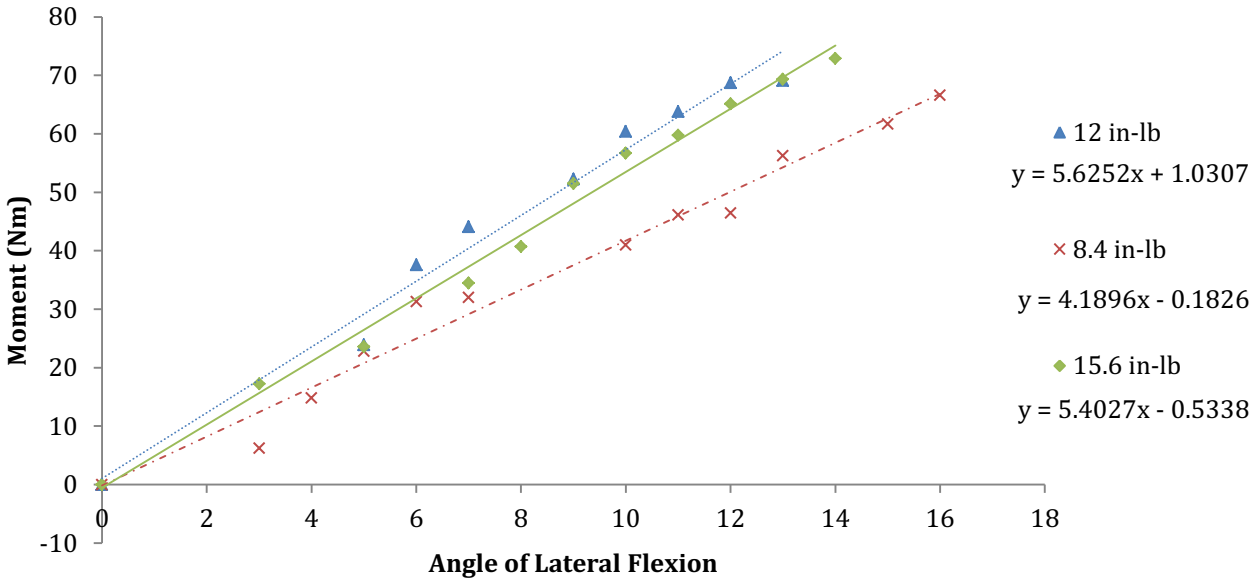

Figure 15. Static lateral flexion testing for the three neck torque settings used. The figure shows the resulting torques required to bend the neckform through a short range of motion. For each torque equation, x represents the angle of lateral flexion and y represents the moment or torque.

Figure 15 shows a less pronounced difference between the three neck torque settings. The lowest setting (8.4 in-lb) shows the lowest torque requirement to bend it through the range while the other two setting, 15.6 in-lb and 12 in-lb, appear to be very similar in terms of torque required to laterally flex the neck through the manually achievable range. The equation for the line-of-best fit is shown for each neck setting. In addition, the same protocol was repeated for flexion, shown in Figure 16.

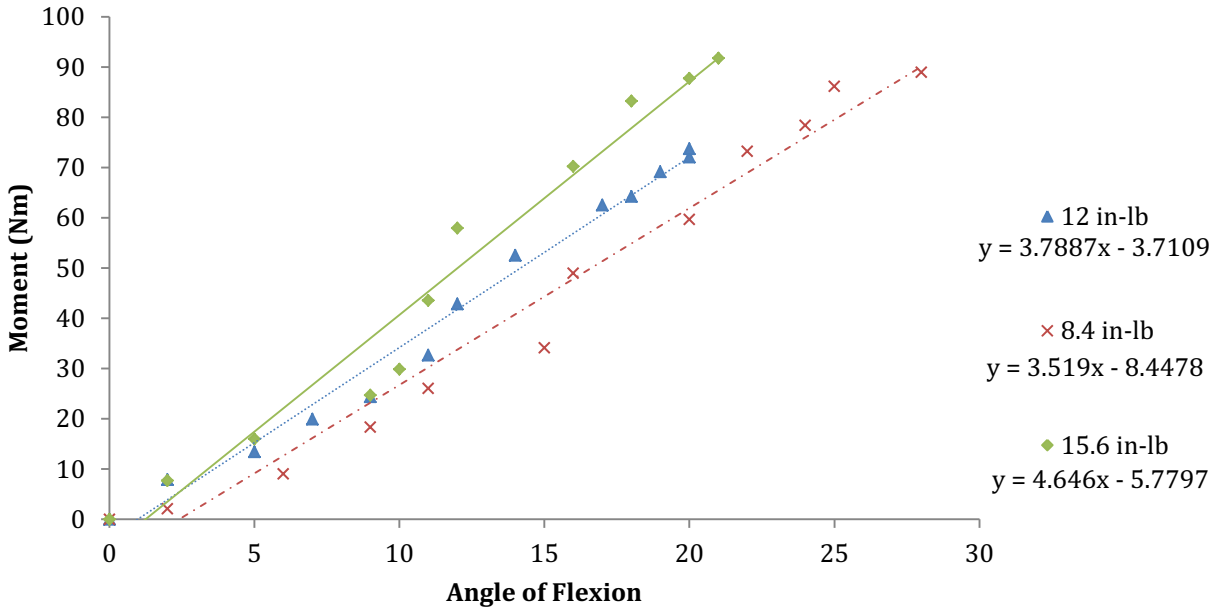

Figure 16. Static flexion testing for the three neck torque settings used. The figure shows the resulting torques required to bend the neckform through a short range of motion. For each torque equation, x represents the angle of lateral flexion and y represents the moment or torque.

Figure 16 shows a difference between the three setting in regards to the amount of torque required to bend the neckform through the manually achievable range. From the figure, it appears that the amount of torque required to bend the neck increases to a large degree when the neck is tightened from 8.4 in-lb to 12 in-lb and 15.6 in-lb. The equation for the line-of-best fit is shown for each neck setting to allow for the determination of the torque required to bend the neck through a given range of motion.

The following results are presented based on the statistical analyses conducted to answer each research question as stated in the methodology.

Research Question #1:

Helmet impact testing. The main objective of the study was to examine the influence of impact angle and neck torque on the dynamic response of a NOCSAE headform using a drop system to determine differences in impact characteristics for helmeted falls. A total of 540

unique impacts were conducted and peak linear acceleration, peak shear force, severity index, and loading energy were recorded. The results from the head drop impacts at zero degree and 13.5-degree angle of inclination are shown in Table 4 and Table 5, respectively. The results are expressed in terms of mean values and standard deviations, shown in parentheses, for each dependent variable.

Table 4

Dependent variable summary table for zero-degree impacts

Neck Torque (in-lb)	Location	Peak Linear Acceleration (g)	Peak Shear Force (N)	Severity Index (SI)	Loading Energy (J)
8.4	Front	134.24 (33.45)	1270.1 (173.17)	611.86 (273.53)	170.26 (43.68)
	Rear	113.61 (22.91)	1239.02 (284.87)	429.09 (172.29)	119.87 (48.59)
	Side	121.89 (35.50)	1347.01 (492.57)	427.37 (227.07)	92.87 (24.53)
	Front Boss	173.05 (66.51)	1870.29 (352.18)	833.57 (493.51	120.89 (20.75)
	Rear Boss	116.19 (32.04)	1223.22 (284.42)	408.15 (197.36)	119.99 (39.49)
12	Front	137.65 (38.35)	1048.88 (229.59)	610.28 (311.21)	150.05 (34.12)
	Rear	120.28 (29.56)	1331.06 (375.34)	452.66 (226.24)	124.99 (40.72)
	Side	118.23 (30.71)	2150.19 (787.26)	405.64 (205.47)	107.34 (30.65)
	Front Boss	146.61 (56.43)	2025.62 (239.33)	612.59 (390.92)	128.12 (16.19)
	Rear Boss	109.79 (35.58)	1335.71 (150.43)	383.34 (207.14)	132.49 (36.34)
15.6	Front	139.18 (40.23)	1391.4 (273.03)	633.31 (325.84)	200.72 (75.42)
	Rear	119.27 (22.90)	1485.30 (318.22)	434.92 (176.76)	140.28 (62.33)
	Side	125.11 (33.98)	1549.5 (671.57)	443.63 (225.45)	100.32 (32.54)
	Front Boss	191.56 (74.4)	1801.7 (371.34)	920.09 (603.83)	114.34 (14.62)
	Rear Boss	112.22 (29.15)	1408 (305.32)	385.86 (185.78)	136.54 (47.56)

Table 5

Dependent variable summary table for 13.5-degree impacts

Neck Torque (in-lb)	Location	Peak Linear Acceleration (g)	Peak Shear Force (N)	Severity Index (SI)	Loading Energy (J)
8.4	Front	101.14 (40.99)	1834.07 (494.97)	418.15 (267.41)	155.29 (60.29)
	Rear	105.78 (28.23)	2235.23 (591.74)	387.03 (196.36)	187.31 (38.23)
	Side	116.50 (34.07)	1954.49 (363.79)	405.99 (220.98)	106.89 (28.53)
	Front Boss	95.83 (34.75)	1689.94 (416.36)	374.19 (263.19)	142.19 (39.42)
	Rear Boss	100.99 (34.04)	2249.24 (598.46)	362.84 (212.21)	163.81 (52.29)
12	Front	104.29 (46.42)	2091.70 (755.99)	419.28 (289.64)	151.93 (69.47)
	Rear	104.83 (30.30)	2361.81 (525.86)	396.81 (212.48)	199.44 (39.21)
	Side	102.87 (31.05)	1694.59 (257.75)	363.54 (215.16)	112.84 (39.67)
	Front Boss	90.17 (33.15)	1778.14 (371.09)	322.89 (212.07)	142.83 (48.66)
	Rear Boss	103.77 (25.78)	2181.64 (415.48)	368.58 (184.19)	186.09 (65.98)
15.6	Front	98.83 (35.85)	1645.13 (373.25)	389.15 (247.16)	145.48 (55.45)
	Rear	114.65 (28.66)	2319.53 (797.37)	447.02 (195.96)	158.48 (42.67)
	Side	119.88 (34.37)	2000.18 (304.73)	416.61 (226.79)	111.45 (27.13)
	Front Boss	94.94 (36.12)	1876.94 (489.09)	321.43 (216.73)	141.57 (41.26)
	Rear Boss	101.79 (34.46)	2245.40 (493.93)	371.09 (209.97)	166.38 (48.17)

Peak linear acceleration. After conducting a 5 (impact location) x 2 (impact angle) x 3 (neck torque) factorial ANOVA with alpha level of 0.05, the results revealed a not significant three-way interaction effect between the independent variables, F(8, 510)= 0.714, p= .679 on peak linear acceleration. Significant main effects were observed for impact angle, F(1, 510)= 74.143, p< .005, as well as for impact location, F(4, 510)= 6.236, p< .005, but not for neck torque, F(2, 510)= 1.941, p= .145. The main effect of impact angle, see Figure 17, shows that the impacts to the zero-degree angle resulted in a greater amount of peak linear acceleration (M= 131.926g, SD= 46.266g) than the 13.5-degree impacts (M= 103.751g, SD= 34.242g).

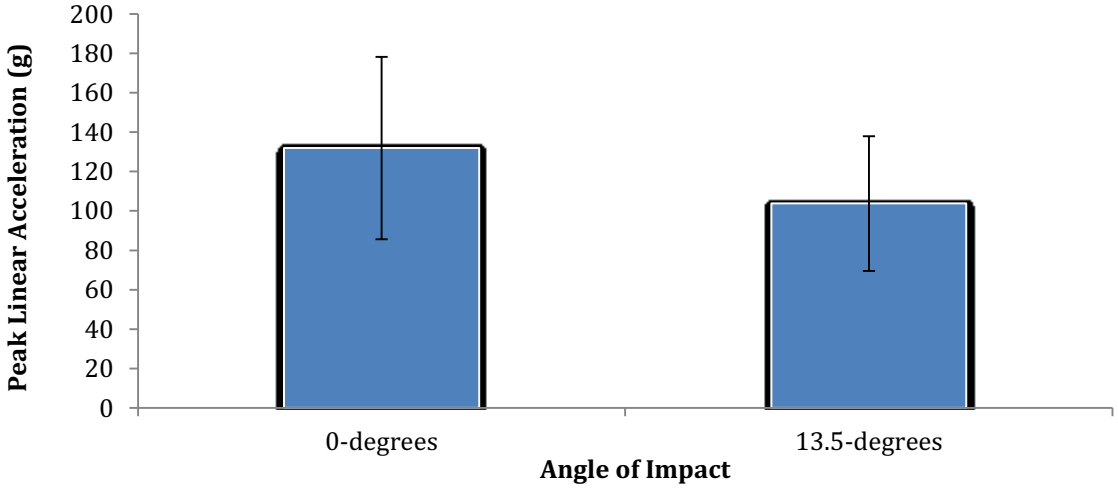

Figure 17. Main effect of impact angle when measuring peak linear acceleration. The figure shows the mean peak linear acceleration for the zero and 13.5-degree impacts.

The main effect of impact location revealed that there were statistically significant differences in peak linear acceleration across locations as well, see Figure 18. The greatest amount of peak linear acceleration occurred during the impacts to the Front Boss location (M= 132.027g, SD= 65.756g) followed by the Front (M= 119.224g, SD= 42.508g), Side (M= 117.412g, SD= 33.399g), Rear (M= 113.069g, SD= 27.288g), and the Rear Boss (M= 107.462g, SD= 31.778g).

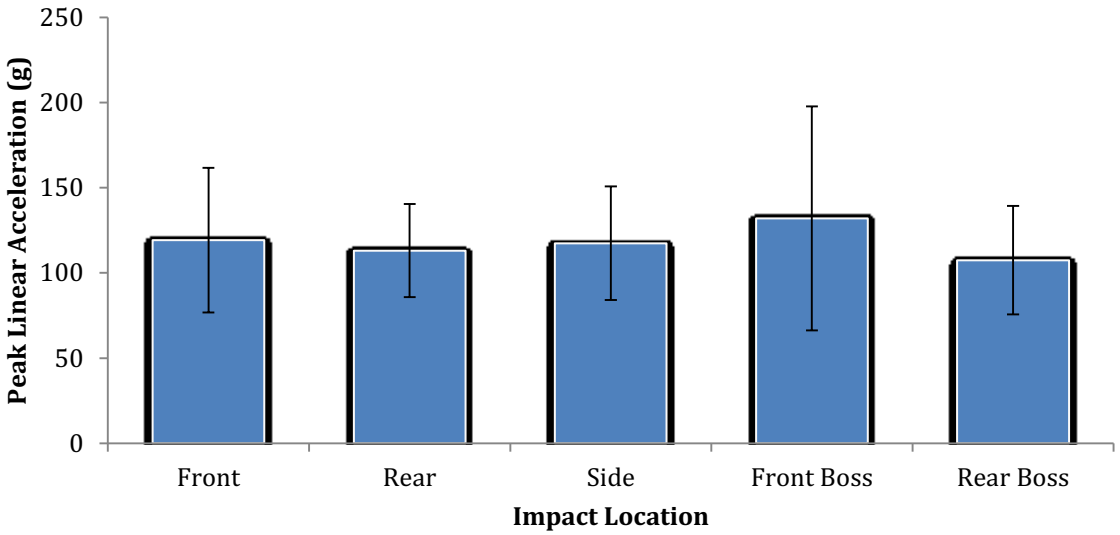

Figure 18. Main effect of impact location when measuring peak linear acceleration. The figure shows the differences in mean peak linear acceleration across the five impact locations.

There was, however, a statistically significant interaction effect between impact angle and impact location, $F(8, 510)= 16.174$, $p< .005$, $\eta^2= .113$. The η^2 value indicated a medium effect size. This interaction effect is illustrated in Figure 19, which indicates that as the impact angle increases from zero to 13.5 degrees, the mean peak linear acceleration decreases and converges for all impact locations. As depicted in Figure 19, the Front Boss location decreases from M= 170.407g to M= 93.647g, which represents the largest decrease in peak linear acceleration of all impact locations. The Side, Rear, and Rear Boss locations appear to only decrease slightly as the angle of impact increases from zero to 13.5 degrees, while the Front exhibits a much steeper decline, but not to the extent of the Front Boss location.

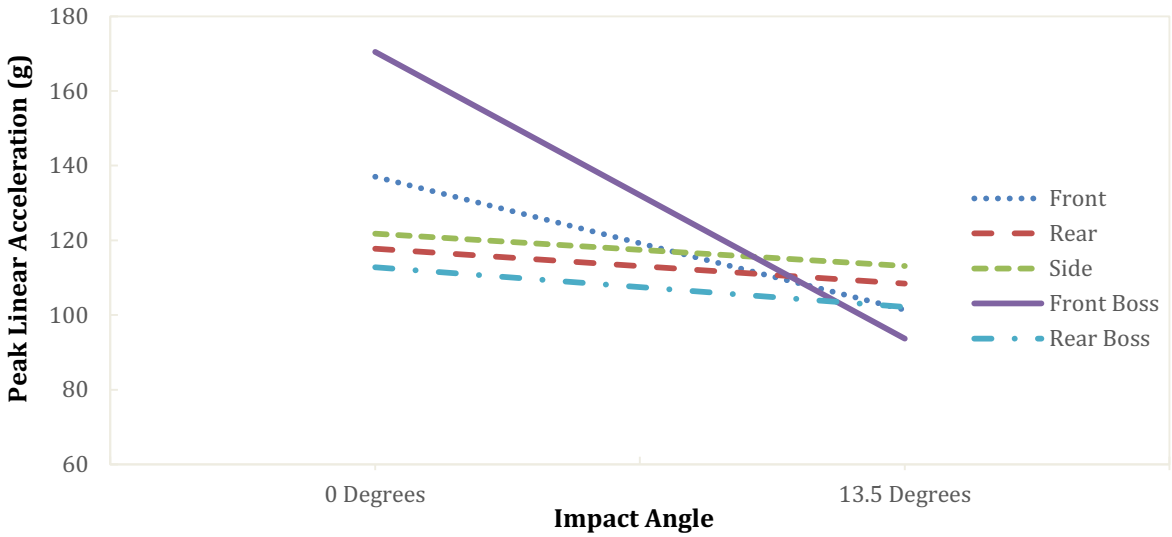

Figure 19. Impact angle and impact location interaction effect when measuring peak linear acceleration. The figure shows the difference in mean peak linear acceleration across impact location and impact angle.

Simple main effect analyses were conducted for the impact angles and locations to help explain the interactions. The results indicate that the simple main effect analysis across impact angles for each location was statistically significant for the Front location, $F(1, 510)= 23.680$, $p<0.05$, and the Front Boss location, $F(1, 510)= 110.063$, $p<0.005$. All pairwise comparisons were made for the Front and Front Boss impact locations across angles using a Bonferroni adjustment. For the Front location, the statistically significant difference was of 35.605g, 95% Confidence Interval (CI) [21.230, 49.979], $p< .005$. For the Front Boss impact location, the statistically significant difference was of 76.76g, 95% CI [62.385, 91.134], $p< .005$ across impact angles.

The simple main effect analysis across impact locations for each impact angle was only statistically significant for the zero-degree impacts, $F(4, 510)= 20.366$, $p< .005$. All pairwise comparisons were made using a Bonferroni adjustment. A statistically significant difference was observed between the Front and Front Boss impact locations (33.381g, 95% CI [12.753, 54.008], $p< .005$), Front and Rear Boss impact location (24.288g, 95% CI [3.660, 44.916], $p=0.01$), the

Rear and Front Boss impact locations (52.689g, 95% CI [32.061, 73.317], p<0.005), the Side and Front Boss impact locations (48.665g, 95% CI [28.037, 69.293], p<0.005) and the Front Boss and Rear Boss locations (57.669g, 95% CI [37.041, 78.297], p<0.005).

Energy loaded. A 5 (impact location) x 2 (impact angle) x 3 (neck torque) factorial ANOVA revealed that there was not a statistically significant three-way interaction effect between the independent variables, $F(8, 510)= 1.33$, $p= .224$ on energy loading. Statistically significant main effects were observed for impact angle, $F(1, 510)= 29.453$, $p< .005$, and impact location, $F(4, 510)= 28.589$, p<0.005. The main effect for neck torque was found to be not significant, $F(2, 510)= .745$, $p= .475$. The main effect of impact angle, see Figure 20, shows that the impacts to the 13.5-degree angle resulted in a greater amount of energy loading (M= 151.465 J, SD= 53.763 J) than the zero-degree impacts (M= 131.822 J, SD= 47.423 J).

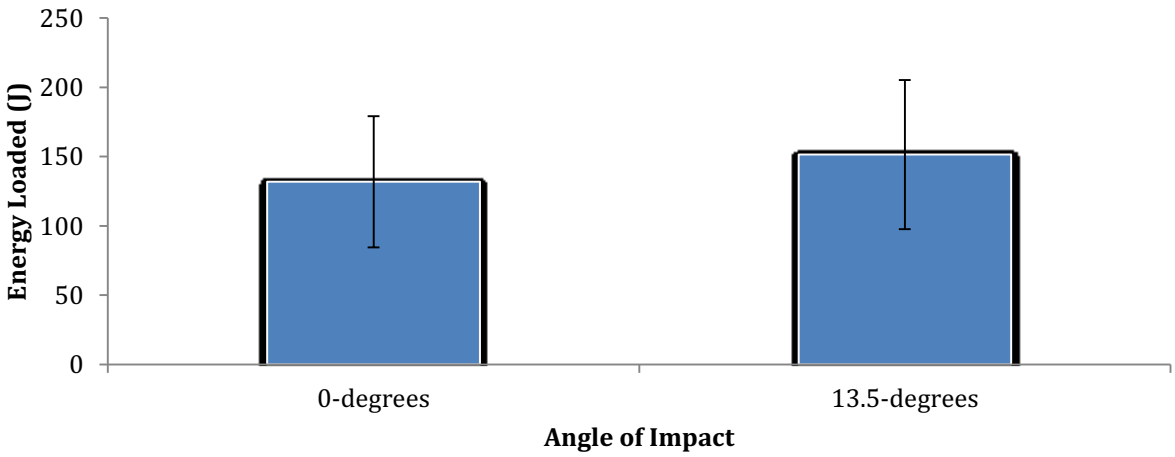

Figure 20. Main effect of impact angle when measuring the amount of energy loaded. The figure shows the mean amount of energy loaded during zero-degree and 13.5-degree impacts.

The main effect of impact location revealed that there were statistically significant differences in energy loading across locations as well, see Figure 21. The greatest amount of energy loading occurred during the impacts to the Front location (M= 162.290 J, SD= 59.855 J) followed by the Rear (M= 155.060 J, SD= 54.104 J), Rear Boss (M= 150.883 J, SD= 53.301 J),

Front Boss (M= 131.657 J, SD= 34.142 J), and the Side (M= 105.284 J, SD= 30.929 J).

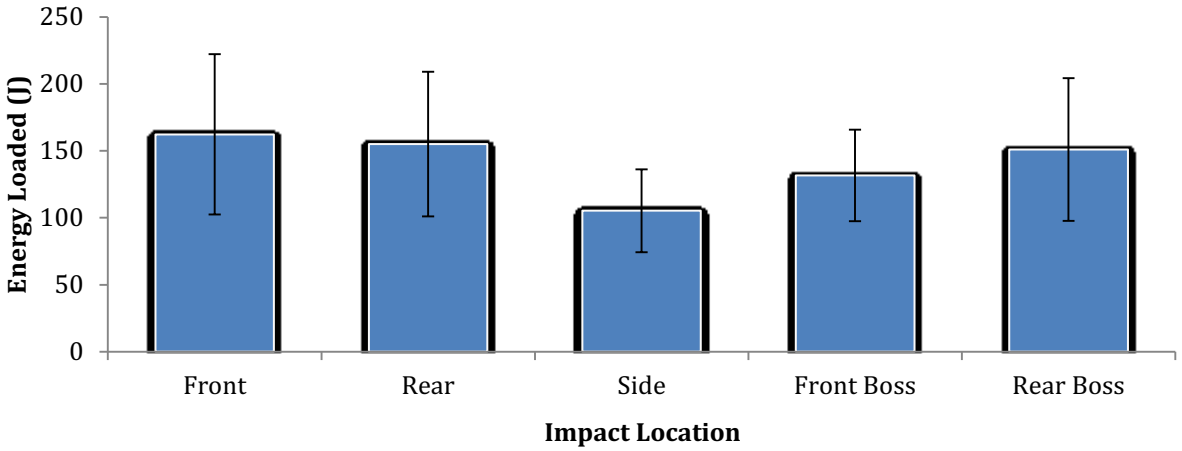

Figure 21. Main effect of impact location when measuring the amount of energy loaded onto the system. The figure shows the mean amount of energy loaded for the five impact locations.

There was, however, a statistically significant two-way interaction effect between impact location and impact angle with a medium effect size, $F(4, 510)= 11.977$, $p< .005$, $\eta^2= .086$. Figure 22 shows the interaction effect between angle and location when measuring the mean energy loaded onto the system during impact. As depicted in Figure 22, energy loading increases across locations when the impact angle is increased with the exception of the Front impact location. At the Front location, there is a decrease in energy loading from M=173.679 J to M=150.900 J. The location that shows the greatest increase in energy loading when the angle was increased is the Rear location as it experienced an increase from M=128.384 J to M=181.744 J when compared to any other impact location.

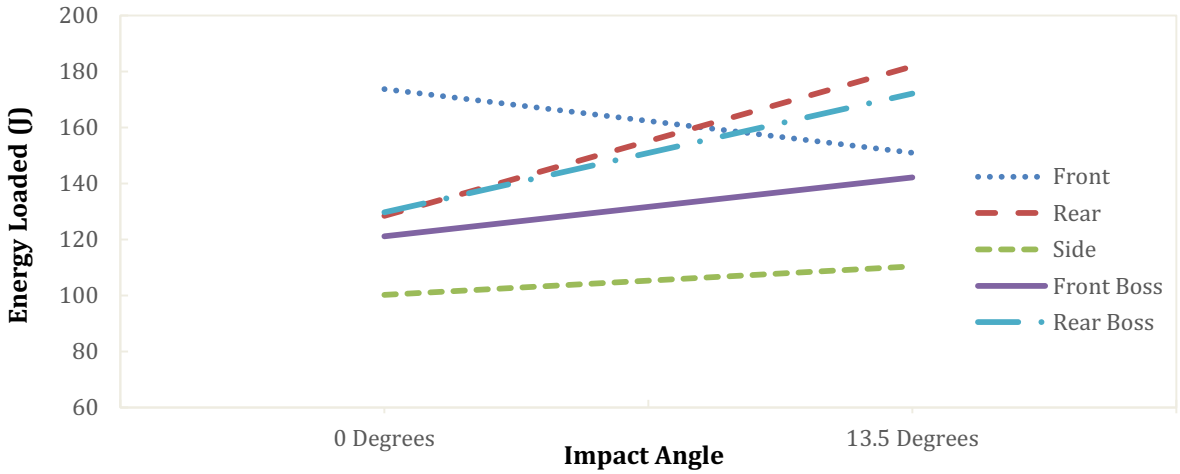

Figure 22. Impact angle and impact location interaction effect when measuring mean energy loading. The figure shows the difference in mean peak linear acceleration across impact location and impact angle.

Simple mean effects analyses were conducted to help explain the interactions. The simple main effect across impact angles was statistically significant for the Front location, $F(1, 510)= 7.025$, $p=0.008$, Rear location, $F(1, 510)= 38.549$, $p<0.005$, Front Boss location, $F(1, 510)= 6.014$, $p=0.015$, and the Rear Boss location, $F(1, 510)= 24.351$, $p<0.005$. All pairwise comparisons were completed for these impact locations using a Bonferroni adjustment across impact angles. There were statistical significant differences of 22.779 J, 95% CI [5.894, 39.663], $p= .008$ for the Front location, 53.360 J, 95% CI [36.475, 70.244], $p<0.005$ for the Rear location, 21.076 J, 95% CI [4.191, 37.960], $p=0.015$ for the Front Boss location, and 42.418 J, 95% CI [25.534, 59.302], $p<0.005$ for the Rear Boss location.

The simple main effect across impact locations was statistically significant for the zero-degree impacts, $F(4, 510)= 19.477$, $p<0.005$, as well as the 13.5-degree impacts, $F(4, 510)= 21.089$, $p<0.005$. All pairwise comparisons were completed for these impact angles using a Bonferroni adjustment between locations. For zero-degree impacts, there were statistically significant difference in energy loading of 28.210 J, 95% CI [3.980, 52.439], $p= .011$ between

the Rear and Side impact locations, 29.499 J, 95% CI [5.269, 53.729], p= .06 between the Rear Boss and Side impact locations.

For the 13.5-degree impacts, there were also statistically significant differences in energy loading of 30.844 J, 95% CI [6.614, 55.074], p= .004 between the Front and Rear impact locations, 40.506 J, 95% CI [16.276, 64.735], p<0.005 between the Front and Side impact locations, 71.350 J, 95% CI [47.120, 95.579], p<0.005 between the Rear and Side locations, 39.549 J, 95% CI [15.319, 63.778], p<0.005 between the Rear and Front Boss locations, 31.801 J, 95% CI [7.571, 56.031], p= .002 between the Side and Front boss locations, 61.697 J, 95% CI [37.468, 85.927], p< .005 between the Side and Rear Boss impact locations and 29.896 J, 95% CI [5.667, 54.126], p=0.005 between the Front Boss and Rear Boss impact locations.

A statistically significant two-way interaction effect was also observed between neck torque and angle, $F(2, 510)= 3.700$, p= .025. Figure 23 shows the interaction effect of neck torque and impact angle when measuring the energy loaded onto the system. From Figure 32, it can be seen that for the zero-degree impacts, there is an increase in the mean energy loaded as the neck torque increases from 8.4 in-lb (M=124.779 J) to the 12 in-lb (M=128.599 J) and the 15.6 in-lb settings (M=138.441 J). The trend for the 13.5-degree impact condition is much different, in the mean energy loaded increases from M=151.097 J at the 8.4 in-lb neck torque setting to M=158.627 J with the 12 in-lb and back down to 144.671 J with the 15.6 in-lb neck torque settings, respectively. The interaction shows that as the neck torque was increased, the mean energy loaded onto the system converges for either a direct or tangential impact.

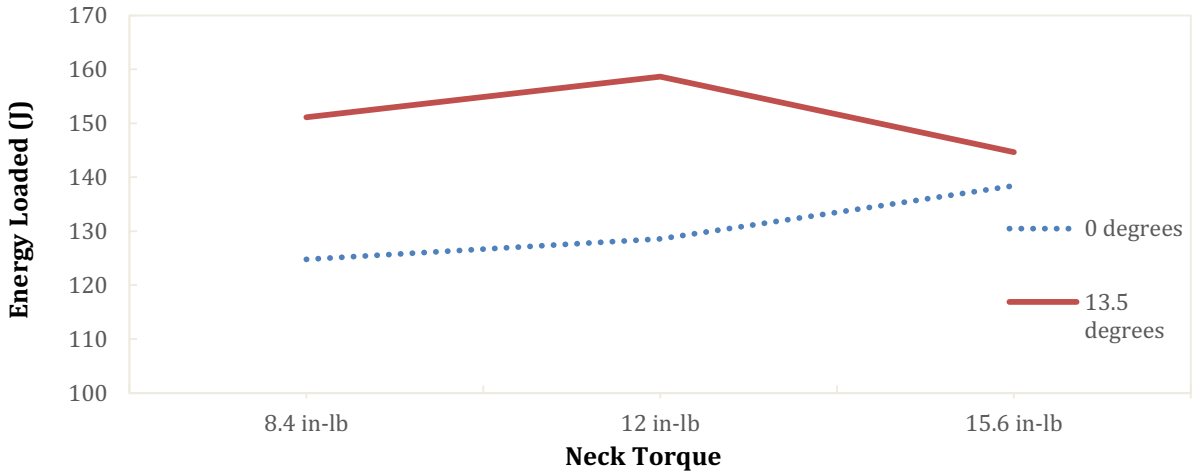

Figure 23. Impact angle and neck torque interaction effect when measuring mean energy loading. The figure shows the difference in mean peak linear acceleration across impact location and neck torque.

The simple main effect between impact angle was observed for the 8.4 in-lb neck torque, $F(1, 510)= 15.629$, $p< .005$, and the 12 in-lb neck torque, $F(1, 510)= 20.347$, $p< .005$. All pairwise comparisons were completed for these neck torque settings using a Bonferroni adjustment. A statistically significant difference of 26.318 J, 95% CI [13.239, 39.397], $p<0.005$ was observed for the 8.4 in-lb torque setting between the impact angle conditions. A statistically significant difference of 30.029 J, 95% CI [16.950, 43.107], $p<0.005$ was also observed for the 12 in-lb neck torque setting between the impact angle conditions. No statistically significant simple main effects were observed across the neck torque settings for this interaction effect.

Severity Index. From the linear acceleration data, the Severity Index for each impact was calculated for all zero degree impacts. A 5 (impact location) x 2 (impact angle) x 3 (neck torque) factorial ANOVA revealed that there was no statistically significant three-way interaction effect between the independent variables, $F(8, 510)= .699$, $p= .692$ on Severity Index measures. Statistically significant main effects were observed for impact angle, $F(1, 510)= 40.953$, $p< .005$, as well as for impact location, $F(4, 510)= 8.847$, $p< .005$. The main effect for neck torque was

found to be not significant, $F(2, 510)= 1.229$, $p= .294$. The main effect of impact angle, see Figure 24, shows that the impacts to the zero-degree angle resulted in a greater risk of injury as estimated by Severity Index (M= 532.825 SI, SD= 339.661 SI) than the 13.5-degree impacts (M= 383.090 SI, SD= 222.360 SI).

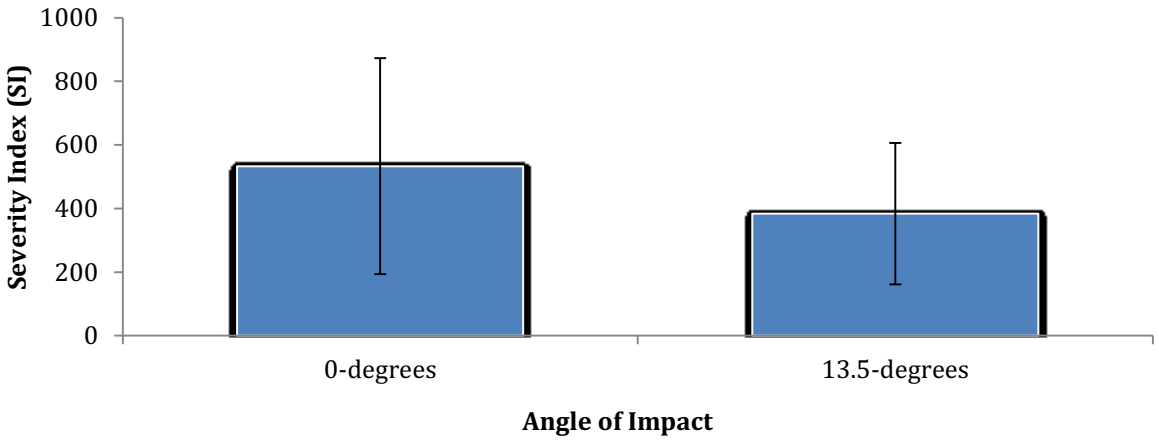

Figure 24. Main effect of impact angle when measuring Severity Index. The figure shows the mean Severity Index for the zero and 13.5-degree impacts.

The main effect of impact location revealed that there were statistically significant differences in energy loading across locations as well, see Figure 21. The greatest amount of energy loading occurred during the impacts to the Front Boss location (M= 564.129 SI, SD= 454.102 SI) followed by the Front (M= 513.670 SI, SD= 299.653 SI), Rear (M= 424.590 SI, SD= 194.469 SI), Side (M= 410.461 SI, SD= 216.511 SI), and the Rear Boss (M= 379.977 SI, SD= 195.612 SI).

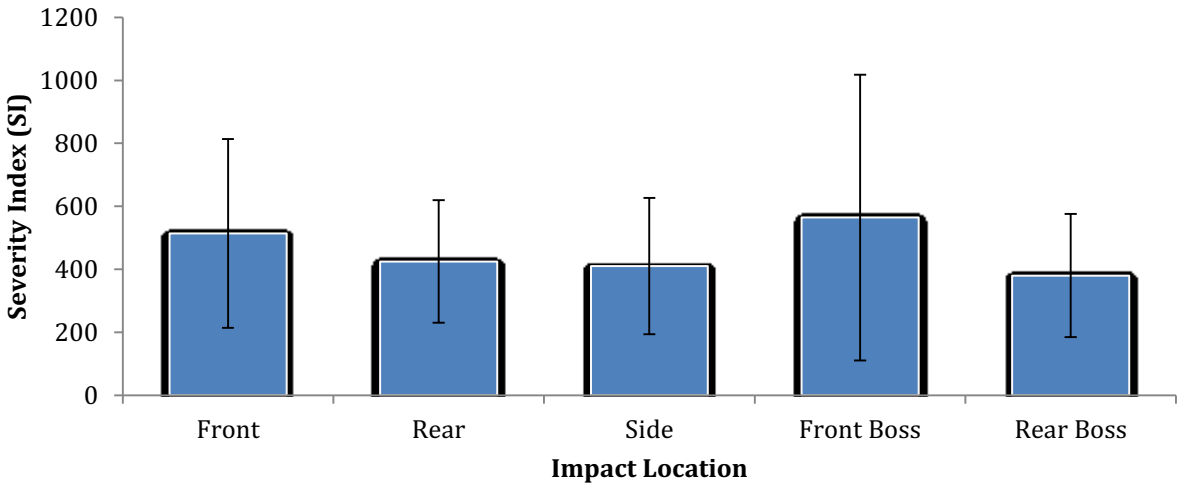

Figure 25. Main effect of impact location when measuring Severity Index. The figure shows the mean Severity index for the five impact locations.

There was, however, a statistically significant two-way interaction effect between impact location and impact angle with a medium effect size, $F(4, 510)= 12.795$, $p<0.005$, $\eta^2= .091$ on Severity Index measures. When looking at Figure 26, it can be noticed that as the impact angle increased from zero to 13.5 degrees, there was a decrease in the injury risk and all impact locations converge at 13.5 degrees. At the Side, Front Boss, and Rear Boss locations, the decrease on injury risk is slight, however, at the Front and Front Boss locations, there is a more pronounced decrease in the calculated Severity index when the angle changes from the zero-degree to the 13.5-degree impacts. The largest decrease on injury risk can be seen at the Front boss location changing from a mean Severity Index of M=788.753 SI during zero-degree impacts to a mean Severity Index of M=339.506 SI during the 13.5-degree impacts.

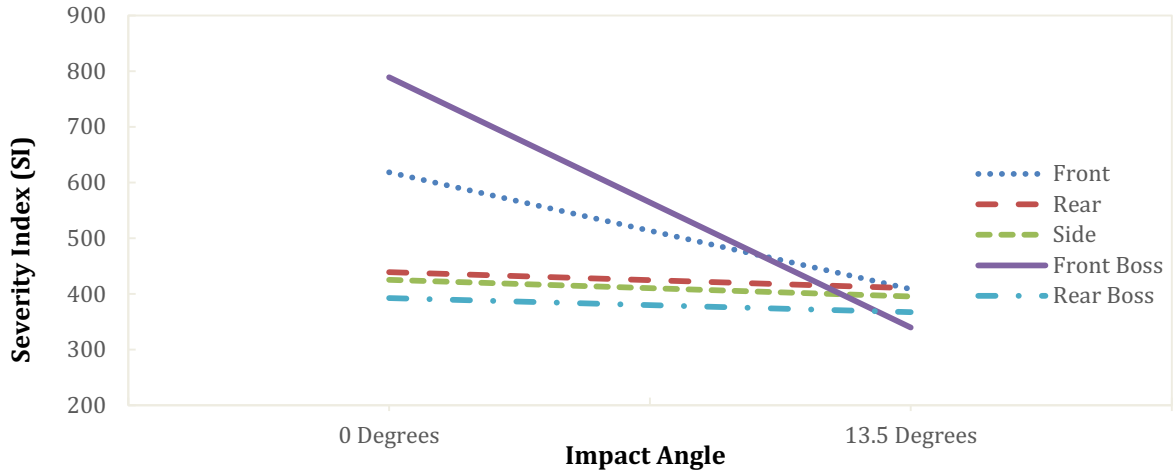

Figure 26. Impact angle and impact location interaction effect when measuring mean Severity Index. The figure shows the difference in mean Severity Index across impact location and impact angle.

The simple main effect across impact location was statistically significant for the zero-degree impact angle, $F(4, 510)= 20.957$, $p< .005$, but not for the 13.5 degree impact angle, which supports the rational that the Severity Index measures converge at 13.5 degrees across all impact locations. All pairwise comparisons were completed for these impact locations using a Bonferroni adjustment. A statistically significant difference of 209.623 SI, 95% CI [107.670, 311.575], $p< .005$ for the Front location across impact angles. A statistically significant difference of 449.247 SI, 95% CI [347.294, 551.200], $p< .005$ was also observed at the Front Boss location across impact angle conditions.

The simple main effect for impact location was statistically significant for the zero-degree impact angle, $F(4, 510)= 20.957$, $p< .005$. All pairwise comparisons were completed for these impact locations using a Bonferroni adjustment. A statistically significant difference was observed for the Front location when compared to all other locations. A statistically significant difference was observed between the Front location and the Rear location (179.592 SI, 95% CI [33.287, 325.898], $p= .006$), the Front location and the Side (192.940 SI, 95% CI [46.634,

339.246], p= .002), the Front and Front Boss locations (170.269 SI, 95% CI [23/963, 316.575], p= .011). In addition, a difference of 226.032 SI, 95% CI [79.727, 372.338], p< .005 was observed between the Front and Rear Boss impact locations. The same can be said for the Front Boss location. That is, a statistically significant difference was observed between the Front Boss and Rear impact locations (349.861 SI, 95% CI [203.556, 496.167], p< .005), the Front Boss and Side impact locations (363.209 SI, 95% CI [216.904, 542.607], p< .005) and between the Front Boss and Rear Boss impact location (396.301 SI, 95% CI [249.996, 542.607], p< .005).

Shear force. The shear force measures were determined using the force platform data from the x and y axes during each impact. A 5 (impact location) x 2 (impact angle) x 3 (neck torque) factorial ANOVA revealed that there was a statistically significant three-way interaction effect between the independent variables when measuring mean peak shear force with a small effect size, $F(8, 510)= 5.550$, $p< .005$, $\eta^2= .080$. To help explain the three way interaction effect, simple two way ANOVA designs were used. With the simple two way ANOVA designs, the neck torque factor was represented on the horizontal axis, the angle factor was represented by different graphs and the location factor was represented by different lines. That is, there was a simple two way interaction between neck torque and impact location on shear force represented as two different graphs based on impact angle (zero and 13.5 degrees).

When analyzing the three way interaction effect, there was a statistically significant simple two-way interaction between neck torque and impact location with a small effect size, $F(8, 510)= 4.337$, $p< .005$, $\eta^2= .064$ on shear force for zero-degree impacts. As depicted in Figure 29, the interaction between neck torque and impact location on shear force differs between locations. At the Side and Front Boss locations, the mean peak shear force is greater at the 12 in-lb condition and smaller for the other two neck torques. The Front location shows the

opposite trend, where the 12 in-lb neck torque resulted in the lowest peak shear force relative to the other neck torque settings. The Rear and Rear Boss impact locations, however, show a gradual increase in mean peak shear force as the neck torque is increased but not by a large degree.

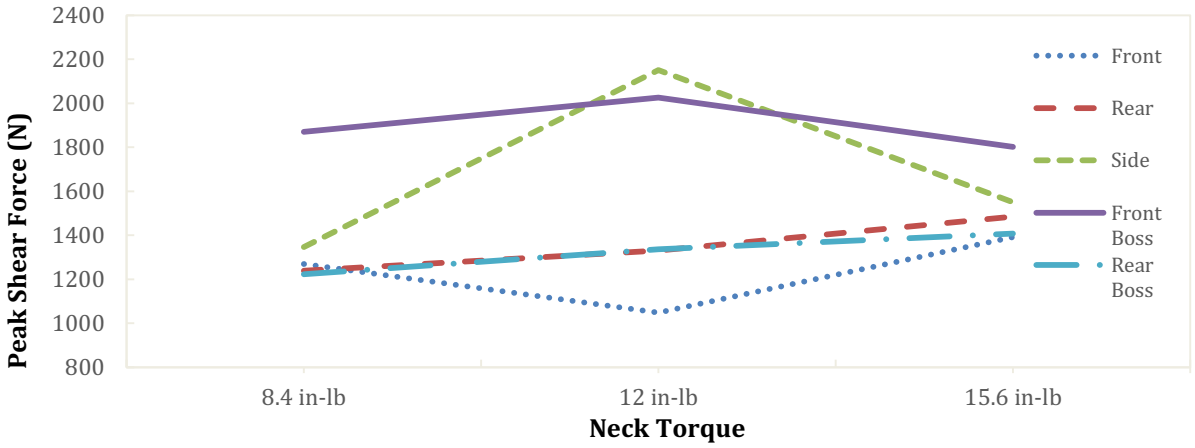

Figure 27. Neck torque and impact location interaction effect when measuring mean peak shear force for the zero-angle impacts. The figure shows the difference in mean peak shear force across impact location and neck torque settings.

There was also a statistically significant simple two-way interaction between neck torque and impact location with a small effect size, $F(8, 510)= 2.019$, $p= .043$,$\eta^2= .031$ for 13.5-degree impacts. As depicted in Figure 28, the Front and Rear impact locations show an increase in mean peak shear forces for the neck torque settings at 8.4 in-lb and 15.6 in-lb. The Rear Boss and Side locations show an opposite trend. That is, impacts with a 12 in-lb torque setting resulted in the lowest relative mean peak shear force when compared to 8.4 in-lb and 15.6 in-lb. The Front Boss location shows a gradual increase in mean peak shear force, similar to the trend shown by the Rear Boss location during the zero-degree impacts. Across the two different angles, there was not a similar trend observed for each impact location, meaning the angle of impact further influences the relationship between neck torque and impact location on shear force measures.

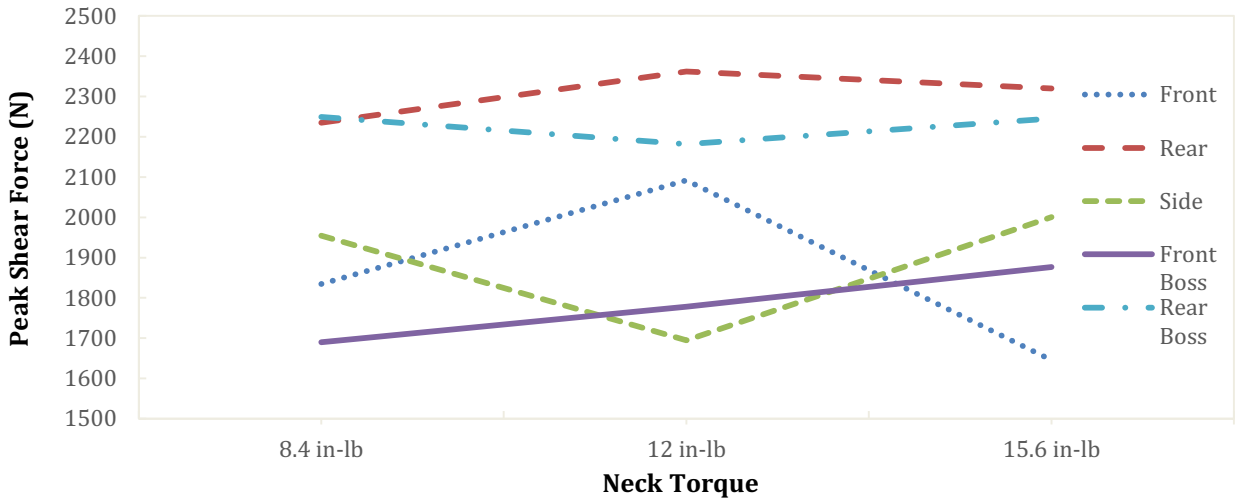

Figure 28. Neck torque and impact location interaction effect when measuring mean peak shear force for the 13.5-angle impacts. The figure shows the difference in mean peak shear force across impact location and neck torque settings.

Furthermore into this analysis, a statistically significant two-way interaction between impact angle and impact location with a medium effect size was observed, $F(4, 510)= 28.106$, $p<0.005$, $\eta^2= .181$. Figure 31 shows the interaction of impact angle and impact location when measuring mean peak shear force during impact. The general trend indicates that as the impact angle is increased, there is a large increase in the mean peak shear force at all impact locations with the exception of the Front Boss location. The greatest increase can be seen at the Rear location, where there is an increase from M=1351.802 N at the zero-angle impacts to M=2305.522 N during the 13.5-degree impacts. The increase is much less pronounced at the Side impact location.

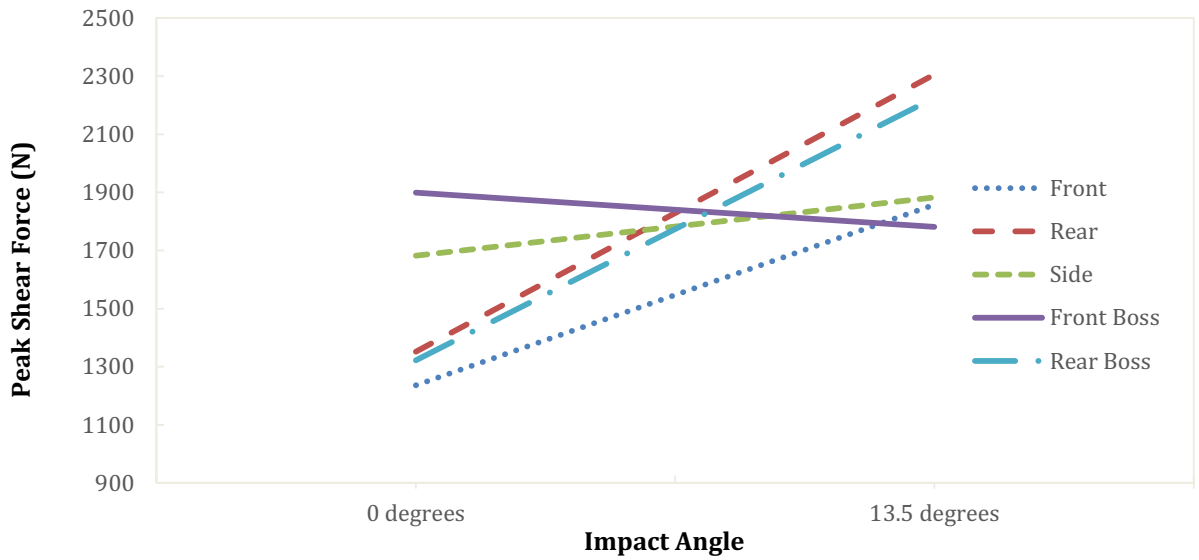

Figure 29. Neck torque and impact location interaction effect when measuring mean peak shear force. The figure shows the difference in mean peak shear force across impact location and neck torque settings.

The simple main effect for impact location was statistically significant for both the zero-degree, $F(4, 510)= 20.785$, $p< .005$ and 13.5-degree, $F(4, 510)= 14.856$, $p< .005$. All pairwise comparisons were completed for each impact angle (zero and 13.5 degrees) using a Bonferroni adjustment. For the zero-degree impacts, statistically significant differences were observed between the Side and Front impact locations (445.433 N, 95% CI [201.673, 689.193], $p< .005$), Side and Rear impact locations (330.422 N, 95% CI [84.864, 575.981], $p< .005$), Side and Rear Boss impact locations (359.901 N, 95% CI [116.141, 603.661], $p< .005$),Front Boss and Front impact locations (662.401 N, 95% CI [418.641, 906.161], $p< .005$),Front Boss and Rear impact locations (840.190 N, 95% CI [596.430, 1083.950], $p< .005$),and Front Boss and Rear Boss impact locations (547.390 N, 95% CI [301.831, 792.949], $p< .005$). For the 13.5-degree impacts, statistically significant differences were observed between the Rear and Front impact locations (448.555 N, 95% CI [204.795, 692.315], $p< .005$), the Rear and Side impact locations (422.435 N, 95% CI [178.675, 666.195], $p< .005$), the Rear and Front Boss impact locations (523.849 N,

95% CI [280.089, 767.609], $p < .005$), the Rear Boss and Front impact locations (368.460 N, 95% CI [124.701, 612.220], $p < .005$), the Rear Boss and Side impact locations (342.340 N, 95% CI [98.580, 586.100], $p = .001$), and between the Rear Boss and Front Boss locations (443.754 N, 95% CI [199.994, 687.514], $p < .005$).

The simple main effect for impact angle was statistically significant for the Front ($F(1, 510) = 50.699$, $p < .005$), Rear ($F(1, 510) = 119.898$, $p < .005$), Side ($F(1, 510) = 5.318$, $p = .021$), and the Rear Boss impact location ($F(1, 510) = 107.510$, $p < .005$). All pairwise comparisons were completed for these impact angles using a Bonferroni adjustment. The magnitude of statistically significant differences in shear force between impact angles were of 620.175 N, 95% CI [450.311, 790.039], $p < .005$ at the Front; 952.719 N, 95% CI [782.602, 1124.837], $p < .005$) at the Rear; 200.862 N, 95% CI [30.998, 370.726], $p = .021$ at the Side and 903.103 N, 95% CI [733.239, 1072.967], $p < .005$ at the Rear Boss location.

Research Question #2:

To determine the extent to which impact energy loading can be predicted based on shear force, impact angle, neck stiffness, peak linear acceleration, and impact location, a multiple regression analysis was conducted. First, a Shapiro-Wilk test for normality was conducted to ensure the data was normally distributed for each impact condition on the continuous variables (peak linear acceleration and shear force). That is, the test was conducted for every combination of neck torque, impact location, and impact angle on peak linear acceleration and shear force. In all cases, the Shapiro-Wilk statistic revealed that all distributions were normal, and the null hypothesis of having a normally distributed sample was accepted, $p > .05$, see Table 6 and Table 7. In addition, no significant outliers or high leverage points that required removal were detected.

Table 6

Normality Testing using Shapiro-Wilk statistic for Zero-Degree Impacts

Neck Torque (in-lb)	Location	Measure	Shapiro-Wilk Statistic	Sig.
8.4	Front	Peak Shear Force	.984	.981
		Peak Linear Acceleration	.969	.774
	Front Boss	Peak Shear Force	.949	.413
		Peak Linear Acceleration	.946	.364
	Side	Peak Shear Force	.971	.823
		Peak Linear Acceleration	.977	.913
	Rear Boss	Peak Shear Force	.970	.802
		Peak Linear Acceleration	.967	.730
	Rear	Peak Shear Force	.955	.513
		Peak Linear Acceleration	.958	.567
12	Front	Peak Shear Force	.961	.618
		Peak Linear Acceleration	.959	.578
	Front Boss	Peak Shear Force	.953	.471
		Peak Linear Acceleration	.952	.453
	Side	Peak Shear Force	.980	.954
		Peak Linear Acceleration	.971	.820
	Rear Boss	Peak Shear Force	.947	.386
		Peak Linear Acceleration	.960	.596
	Rear	Peak Shear Force	.971	.811
		Peak Linear Acceleration	.971	.814
15.6	Front	Peak Shear Force	.982	.968
		Peak Linear Acceleration	.964	.678
	Front Boss	Peak Shear Force	.930	.193
		Peak Linear Acceleration	.953	.481
	Side	Peak Shear Force	.973	.845
		Peak Linear Acceleration	.969	.787
	Rear Boss	Peak Shear Force	.968	.762
		Peak Linear Acceleration	.972	.835
	Rear	Peak Shear Force	.951	.448
		Peak Linear Acceleration	.958	.566

Table 7

Normality Testing using Shapiro-Wilk statistic for 13.5-Degree Impacts

Neck Torque (in-lb)	Location	Measure	Shapiro-Wilk Statistic	Sig.
8.4	Front	Peak Shear Force	.952	.465
		Peak Linear Acceleration	.914	.102
	Front Boss	Peak Shear Force	.933	.216
		Peak Linear Acceleration	.938	.264
	Side	Peak Shear Force	.983	.976
		Peak Linear Acceleration	.966	.718
	Rear Boss	Peak Shear Force	.962	.639
		Peak Linear Acceleration	.973	.856
	Rear	Peak Shear Force	.949	.412
		Peak Linear Acceleration	.925	.155
12	Front	Peak Shear Force	.925	.157
		Peak Linear Acceleration	.904	.067
	Front Boss	Peak Shear Force	.923	.145
		Peak Linear Acceleration	.918	.120
	Side	Peak Shear Force	.953	.467
		Peak Linear Acceleration	.947	.387
	Rear Boss	Peak Shear Force	.966	.726
		Peak Linear Acceleration	.972	.826
	Rear	Peak Shear Force	.929	.187
		Peak Linear Acceleration	.916	.108
15.6	Front	Peak Shear Force	.933	.222
		Peak Linear Acceleration	.901	.060
	Front Boss	Peak Shear Force	.936	.244
		Peak Linear Acceleration	.913	.097
	Side	Peak Shear Force	.975	.882
		Peak Linear Acceleration	.958	.561
	Rear Boss	Peak Shear Force	.964	.688
		Peak Linear Acceleration	.949	.407
	Rear	Peak Shear Force	.961	.628
		Peak Linear Acceleration	.904	.067

To test for independence of observations, the Durbin-Watson statistic was used. This statistic allows for the detection of autocorrelation in the residuals (error term). The test ensures that each error term is not related to the error term of its predecessor. In effect, the test is detecting whether or not there is “first-order correlation”. The statistic itself ranges from zero to four. A small value close to zero implies positive autocorrelation while a large value close to 4 implies negative autocorrelation of the residuals. From the analysis, it was determined that there was independence of observation, as assessed by a Durbin-Watson statistic of 1.418. This finding suggests that data points are independent of each other as they do not exhibit a strong positive or negative autocorrelation.

To test for linearity in the data, the unstandardized predicted energy loading values were

plotted against the studentized residuals using SPSS computer software. The resulting scatterplot revealed a linear relationship between the dependent and independent variables. The assumption of homoscedasticity was also assessed to determine if the residuals are equal for all values of the predicted dependent variable. Homoscedasticity refers to the variability of the data about the regression line. A line that shows homoscedasticity will have a relatively equal distribution of values about the regression line. Using the same studentized residual and unstandardized predicted value, it can be seen that there is a general homoscedasticity in the residuals.

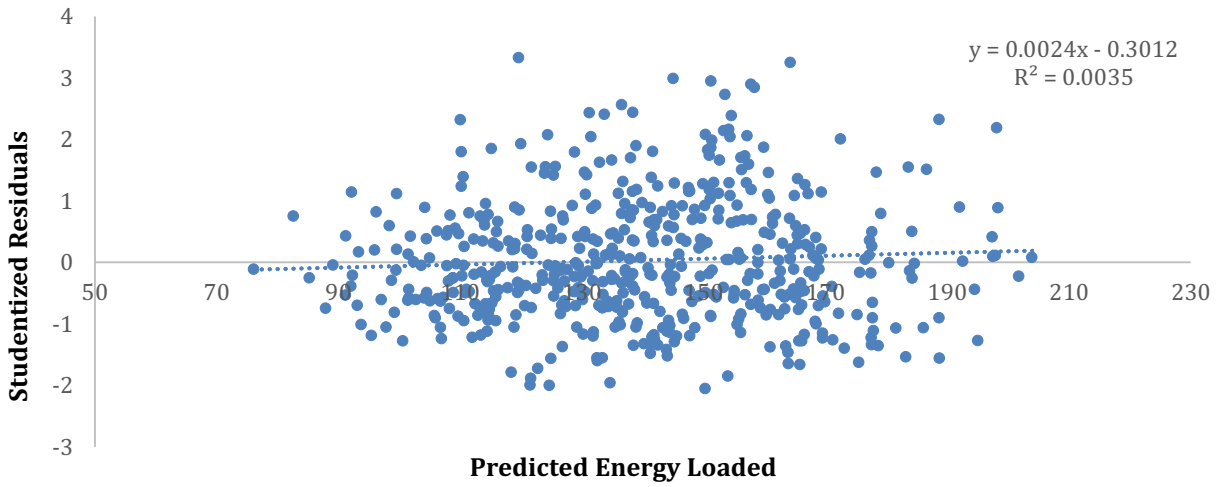

Figure 30. Predicted energy loaded against studentized residuals. The figure was used to test for linearity in the data. The slope of the line-of-best fit, as shown in the equation on the figure, indicates linearity in the data as well as homoscedasticity.

In addition, partial regressions were conducted for the continuous independent variables of peak shear force and peak linear acceleration, see Table 8. This analysis revealed a linear relationship between both of these independent variables and the energy loading dependent variable.

Table 8

Partial Correlations

Independent Variable	Correlation with Loading Energy	Sig.
Peak Linear Acceleration	.299	$p < .0001$
Peak Shear Force	.449	$p < .0001$

Multicollinearity was also assessed to determine if there were any independent variables that are highly correlated with each other, see Table 9. Ensuring there is no multicollinearity allows for accurate statements to be made about which variables contribute to the variance in the dependent variable. When analyzing the Spearman's rho correlations between the independent variables, none of the independent variables appear to be strongly correlated to each other, with the largest coefficient appearing to be between peak linear acceleration and peak shear force, $r = .472$, $p < .005$.

Table 9

Test for Multicollinearity

Independent Variable	Neck Torque	Impact Angle	Impact Location	Peak Linear Acceleration	Peak Shear Force
Neck Torque	1.000	.000	.000	.026	.057
Impact Angle	.000	1.000	.000	-.318	.458
Impact Location	.000	.000	1.000	-.043	.148
Peak Linear Acceleration	.026	-.318	-.043	1.000	.472
Peak Shear Force	.057	.458	.148	.472	1.000

In addition, Variance Inflation Factor (VIF) values were considered to determine if there was multicollinearity in the data, see Table 10. All VIF values were below 2.766, meaning there is no significant multicollinearity in the data and the assumption has not been violated and the analysis could proceed.

Table 10

Variance Inflation Factors for Independent Variables

Independent Variable	Variance Inflation Factor (VIF)
Impact Angle	2.361
Front	1.657
Rear	1.672
Side	1.630
Rear Boss	1.696
Peak Linear Acceleration	2.487
Peak Shear Force	2.766

Since impact location and neck torque are non-binomial categorical variables, a dummy coding procedure similar to that of Alkharusi (2012) was used to determine how each level contribute to the model. The regression analysis determined a multiple correlation coefficient of R= .645. As such, a moderate correlation exists between the predicted energy loading and measured energy loading onto the system. The coefficient of determination, R^2= .416 and an adjusted R^2= .409, states that nearly 41% of the variance in energy loading can be explained by the independent variables. This model leaves 59% of the variance unexplained. Table 11 shows a summary of the regression analysis.

Table 11

Summary of Multiple Regression Analysis

Variable	Unstandardized regression coefficient	Standard error of the coefficient	Standardized coefficient	Sig.
Intercept	22.324	10.272		.030
Front	43.076	5.534	.332	.000
Rear	28.619	5.560	.220	.000
Side	-20.833	5.489	-.160	.000
Rear Boss	27.582	5.599	.212	.000
Impact Angle	12.058	5.286	.111	.023
Peak Linear Acceleration	.256	.063	.181	.000
Peak Shear Force	.031	.005	.349	.000

According to the model, impact angle, all impact locations except the Front Boss location, peak shear force, and peak linear acceleration statistically significantly predicted energy

loading, $F(5, 535) = 54.190$, $p < .005$. Predictors including Impact Angle, all impact locations except the Front Boss location, Peak Linear Acceleration, and Peak Shear Force were found to contribute significantly to the model, $p < .05$. It was determined that the Neck Torque settings did not contribute significantly to the model, $p > .05$and neither did the Front Boss, $p > .05$ so they were not included in the analysis. The following equation was created in order to predict energy loading from the independent variables used in the analysis:

$$\text{LoadingE} = 22.324 + (12.058 \cdot \text{Angle}) + (43.076 \cdot \text{Front}) + (28.619 \cdot \text{Rear}) - (20.833 \cdot \text{Side}) + (27.582 \cdot \text{RearBoss}) + (0.256 \cdot \text{PeakLA}) + (0.031 \cdot \text{Shear}) \quad (16)$$

where:

Loading E= Predicted energy loading
Angle = Impact angle
Front = Front impact location
Rear = Rear impact location
Side = Side impact location
RearBoss = Rear Boss impact location
PeakLA = Peak linear acceleration
Shear = Peak shear force

Using this model, 41% of the energy loaded onto the system can be explained using the independent variables as predictors. In the case of the continuous variables, for one "g" of peak linear acceleration, there is a predicted increase of 0.256 J of energy loaded onto the system when the rest of the predictors are held constant. Similarly for an increase of 1 N of shear force there is an increase of 0.031 J of energy loaded onto the system when the other regressors are held constant. Based on these outcomes, linear impact acceleration produces higher energy loading into the system than shear forces.

The angle of impact possesses a regression coefficient of 12.058. According to the model, a unit value of 1 results in a predicted increase of 12.058 J of energy loaded onto the system when all other predictors are held constant. The regression coefficient shows that when the angle

of impact is increased from zero-degrees to 13.5-degrees, the predicted energy contribution increases from 12.058 J to 24.106 J

For impact location, Front, Side, Rear Boss, and Rear Boss possess different regression coefficients. According to the model, impacts to the Front contribute 43.076J or energy loaded onto the system, a much larger coefficient than the Rear (28.619 J), Side (-20.833 J), and the Rear Boss impact location (27.582J). Knowing all these impact characteristics in addition to the measured peak linear acceleration and peak shear force allows for a statistically significant prediction of the energy loaded onto the system.

Research Question #3:

Another objective of this study was to analyze how the energy loaded onto the system was related to the previously established and widely-used Severity Index in order to determine whether or not the energy loaded onto the head and neck could be used as a predictor of injury risk. To analyze the strength of the linear relationship between impact energy loading and Injury Severity Index, a Pearson product-moment correlation was conducted. A statistically significant moderate correlation was determined between loading energy and Severity Index, $r = .340$, $p < .05$. It was determined that the relationship between Severity Index and loading energy statistically explained 11.56% of the variability in the loading energy, $r^2 = .1156$. Figure 31 shows the linear relationship between the two variables. Based on this relationship, a linear model was created to predict the Severity Index by the energy loaded onto the system.

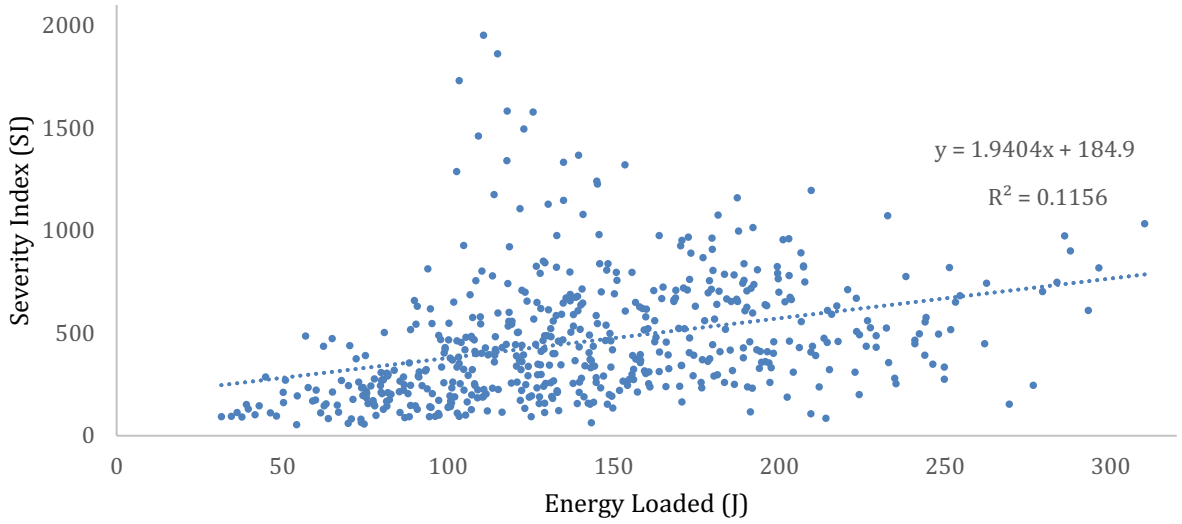

Figure 31. Relationship between Severity Index and loading energy. The figure shows the calculated loading energy and severity index for all 540 impacts.

The following interpolation function was determined from the correlation analysis:

$$\mathrm{SI} = 1.9404 * \mathrm{Loading\ E} + 184.9 \quad (17)$$

where:

Loading E = Energy loaded onto the system
SI = Severity Index

Using this interpolation function, the risk of injury (Severity Index) can be predicted based on the energy loaded onto the system for a given impact. The slope of the equation indicates that for every increase in 1 J of energy loaded, there is a predicted increase in Severity Index of 1.9404 SI when other regressors are held constant. This model presents a simple approach to estimating the injury risk based on the amount of energy loaded onto the system and shows that the two variables are in fact related.

Chapter Five - Discussion

The results of the current study are discussed using theoretical and empirical rationale to explain differences in the dependent variables across different impact conditions as well as the relationship between the variables of the study. Repetitive impact testing and static neck testing will be discussed first, followed by a discussion for each of the three research questions. In addition, there will be a discussion about the limitations of the study, conclusions, and recommendations for future research.

Repetitive Impact testing

The purpose of performing repetitive impact testing was to gain insight into the performance deterioration characteristics of the helmet being used in the study. After conducting 200 impacts per location (Front and Rear), the results as depicted in Figure 12 and Figure 13 revealed trends in the ability of the helmet to manage impact forces over a large number of impacts.

The impacts occurred repetitively, with nearly 2 impacts per second, much more rapidly than the impacts experienced in the actual study. For impacts to the front location, it was revealed that the performance was very stable up to 189 impacts at the intensity tested. After this point, there was a steep increase in measured impact force, or a decrease in the helmets ability to manage the impact forces. This finding suggests that the performance of the helmet at the front location was enduring, and could sustain a significant number of impacts before a performance concern was noticed.

For repetitive impacts to the rear location, a different trend was observed. Over the course of the impacts, a gradual increase in the measured impact force meant a slow and gradual decline of the helmet performance. When observing the equation of the line of best fit, a slope of

0.4023N/impact was determined. Although the decline was observable, a difference of 0.4023N/impact is not a significant decrease in performance to merit concern for 18 impacts.

These repetitive impact results can be compared relative to the number of impacts athletes sustain while playing hockey. In a study by Brainard et al. (2012), female athletes sustained M=105 SD=17.5 impacts to the head per season while male athletes sustained M=347.3 SD=170.2 impacts to the head per season. Among the male participants, only 5% of all impacts resulted in a peak linear acceleration greater than 47.5g, suggesting the majority of these individual impacts fell below the threshold of a 25% risk of concussion to the impacted athletes (Zhang, Yang, & King, 2004). Among these impacts, 30% were incurred to the front while 33% of all impacts occurred to the rear impact location, the two tested for repetitive impact resistance. In the current study, the number of impacts applied to the helmet and headform represents the number a female athlete may be expected to experience over a two season period to these locations, while roughly two thirds of a season for males. From the analysis conducted in the current study, it can be expected that female athletes may experience a decrease in helmet performance before the completion a two season period. Male athletes, on the other hand, may experience a decrease in helmet performance before the completion of one season.

From the data collected in the current study, performance deterioration was observed at both impact locations over 200 impacts; although, neither location showed rapid or significant changes in the measured impact force. This information was used to determine the number of helmets used in the study. Using this information and taking into consideration the number of helmets available to the researcher, a total of six helmets were used over the 540 impacts in the study. Each of the six helmets was exposed to only 18 impacts per location, alleviating concern that the performance of the helmet would experience a significant decrease on force absorption

over the course of the study and influence the data. The researchers were satisfied with the results of this preliminary testing before the actual study was conducted and with the number of impacts chosen per location.

Static Neck Testing

The purpose of analyzing the stiffness of the neckform was to quantify the difference in stiffness created by increasing, or reducing, the torque setting on the neck and quantifying how it influences dynamic response during impact. This analysis served to compare how a softer neck may compare to a stiffer neck in terms of injury risk reduction. It has been stated that during an impact, a stiffer neck can be expected to reduce the transfer of force and accelerations (Rousseau & Hoshizaki, 2009). The rationale is that a stiff neck can increase the "effective mass" of the receiving body, allowing the head to resist some of the force transmission (Rousseau & Hoshizaki, 2009). The comparison can also be operationalized to compare an athlete suspecting and bracing for impact (stiff) against an athlete who does not anticipate the impact (soft), similar to the analysis conducted by Rousseau and Hoshizaki (2009). An athlete anticipating the impact may have a greater amount of time to contract their neck muscles, aiding in the resisting of the impact.

Figure 14, Figure 15, and Figure 16 show the torque required to bend the neckform through a short range of extension, lateral flexion, and flexion, respectively. By testing the torque required to bend the neck, it is possible to quantify the difference between the "soft" 8.4 in-lb, the "normal" 12 in-lb, and the "stiff" 15.6 in-lb neck torque settings. For future research, using these results, comparisons between suspecting and unsuspecting athletes can be made, much like the research by Rousseau and Hoshizaki (2009), while being able to quantify the difference between neck torque settings. This type of analysis could allow for the comparison of impact

severity and injury risk across individuals but also aid in the reconstruction of injuries using the drop system. By measuring the neck stiffness of an individual who suffered an injury, a more accurate recreation of their impact can be completed by adjusting the neckform torque and stiffness accordingly. Using the equations for the lines-of-best-fit will allow for the estimation of the amount of torque required to flex, extend, and laterally flex a “soft”, “average”, and “stiff” neck.

Figures 15 and 16 shows the amount of torque required to extend and flex these “soft”, “average”, and “stiff” neck torque settings. Both figures show a relationship between neck torque setting and the amount of torque required to induce bending. This finding was expected because as the torque of the neck is increased, there is a slight compression of the discs of the neck, reducing the amount of allowable rotation and flex. For example, using the equation for the line-of-best-fit, to flex the neckform 20 degrees, a torque of 61.93 Nm would be required for the 8.4 in-lb setting, while 72.06 Nm and 87.14 Nm would be required for the 12 in-lb and 15.6 in-lb settings, respectively. This finding suggests that a tighter torque setting such as 15.6 in-lb resulted in a neckform with greater resistance to bending, and acts like a stiffer neck than the 8.4 in-lb and 12 in-lb torque settings.

Figure 15, shows the difference in torque required to laterally flex the neckform. The results reveal a different and unexpected trend. That is, the 8.4 in-lb setting required the smallest amount of torque to induce bending, however, the 15.6 in-lb setting required a smaller amount than the traditional torque setting of 12 in-lb used as a standard setting in previous research literature. The difference between 12 in-lb and 15.6 in-lb settings is small. For example, the predicted torque required to bend the neck 20 degrees is 113.53 Nm for the 12 in-lb and 107.521 Nm for 15.6 in-lb settings. This outcome indicates that a stiffer neck setting requires more torque

to bend the neck 20 degrees when compared to a lower neck stiffness of 8.4 in-lb, which only requires 83.61 Nm to bend the neck. It is possible, however, that the unexpected result may be due to some degree of measurement error during the manual bending procedure of the neckform or that more data points are required to ensure greater accuracy. Regardless of the previous outcomes, when comparing the torque measures between neck lateral flexion and neck flexion/extension, it appears that neck stiffness has a higher influence on lateral flexion as higher torque values are obtained for a 20 degrees neck bend.

The previously discussed static neck testing has not been observed in the literature. No previous studies could be found analyzing the influence neckform torque has on dynamic response and only one could be found to examine the influence neck stiffness has during simulated impacts (Rousseau & Hoshizaki, 2009). The analysis showed that neck torque had a significant influence on overall neck stiffness and can provide future research an avenue to control and examine the influence of neck stiffness without having to purchase or develop separate neckforms, as was done in the study by Rousseau and Hoshizaki (2009), or aid in injury reconstruction research by matching athletes to a particular neck torque setting to increase the accuracy of reconstructions.

The following discussion addresses each of the research questions.

Research Question 1:

Peak linear acceleration. This measure is commonly used in the literature to assess head impact severity because of its association with brain injuries like a skull fracture (Gurdjian, Lissner, & Evans, 1961; Post et al., 2011). Peak linear acceleration has also been used to predict risk of injury such as concussion (Zhang, Yang, & King, 2004). One of the main challenges with using peak linear acceleration to predict a concussion is to figure out which threshold peak linear

acceleration values can be used to determine the risk of concussion in order to conduct simulated studies. Based on head injury reconstruction guidelines for American football players, Zhang, Yang & King (2004) proposed a threshold of peak linear acceleration to determine potential risk of brain injury for any given impact. According to their proposed threshold, peak linear accelerations of 66g, 82g, and 106g corresponded to 25%, 50%, and 80% risk of concussion. According to these guidelines, the results of the current study indicate that the mean peak linear acceleration values for all zero-degree impact conditions were above 80% risk of concussion. For the 13.5-degree impacts, only impacts to the Side with an 8.4 in-lb neck torque (M=116.501g, SD=34.065g), to the Side with a 15.6 in-lb neck torque (M=119.879g, SD=34.372g), and to the Rear with a 15.6 in-lb neck torque (M=114.646g, SD=28.666g) were above the 80% risk of concussion threshold. According to the proposed threshold by Zhang. Yang, and King (2004), zero-degree impacts resulted in a greater risk of concussion when compared to the 13.5-degree impacts. The difference exists due to the vector of the force being applied to the headform. During the angled impacts, the force is not directed through the centre of mass of the headform, resulting in a lower peak linear acceleration measure being felt by the accelerometers within the headform. As will be discussed later, this highlights a shortcoming in focusing on linear acceleration measures because of the large amount of rotational acceleration created during angled impacts.

In order to properly assess head impact severity on measures of peak linear acceleration and develop appropriate headgear to minimize the risk of head injury, it is important to understand the mechanism of injury by taking in consideration the location of the impact, the stiffness of the neck and the angle of the impact (Walsh et al., 2011), but more importantly, how these factors affect one another for a given impact on measures of peak linear acceleration to

properly assess the risk of injury.

The results of the current study revealed that there was no three-way interaction effect between angle, location, and torque on peak linear acceleration measures. There were, however, significant differences for impact location, $F(1, 510)= 74.143$, $p< .005$ and impact angle, $F(4, 510)= 6.236$, $p< .005$. These outcomes are consistent with the research conducted by Zhang et al., (2011), which found that impact location influences the amount of peak linear acceleration felt by the headform during linear impacts. Similarly, Walsh et al. in 2011, found that the side impact location resulted in the greatest amount of peak linear acceleration (M=132.8g, SD=3.8g) when compared to the front, front boss, and rear impact locations on a headform. More specifically, Walsh et al. in 2011 found that the rear boss impact location resulted in the smallest amount of peak linear acceleration when compared to the front boss (M=102.1g, SD=5.1), the rear (M=116.9g, SD=2.0g), and the front impact locations (M=121.3g, SD=5.6g).

While the results of the current study show that the front boss impact location resulted in the highest peak linear acceleration followed by the front, side, rear, and rear boss instead of the side location follow by the front, rear, front boss, and rear boss as found by Walsh et al. in 2011, the differences may be due to the mechanism of impact used in both research studies. For instance, Walsh et al. in 2011 used a pneumatic “projectile” impact system, whereas, the results of the current study are based on a drop tower head impact system. To further support this rationale, Nishizaki et al. (2014) examined the main effect of impact location on peak linear acceleration measures using a monorail drop system. Similar to the results of the current study, Nishizaki et al. (2014) found that the front boss impact location resulted in the greatest amount of peak linear acceleration followed by the side and rear boss locations at impact velocities of 2, 4, and 6 m/s. Some discrepancies, however, may be related to helmet, headform, and neckform

behavior properties across impact locations. These outcomes suggest that injury risk may be elevated at certain impact locations when compared to others. This rationale will be further addressed later in the discussion section related to injury Severity Index across locations. Regardless, these outcomes highlight the need to further improve helmet designs to minimize linear impact acceleration across locations and therefore, reduce injury risk, especially sensitive location such as the side, which has been identified as one of the most dangerous locations to cause brain injuries.

The results of the current study also show a main effect due to impact angle when measuring peak linear acceleration. For impacts performed at zero and 13.5-degree angled conditions, peak linear acceleration differs across impact locations. For the 13.5 degree impacts, the peak linear acceleration values appear to be similar across impact locations, however, smaller in magnitude than during the zero-degree impacts. This outcome also supports the research work of Walsh et al. (2011), which found a reduction in peak linear acceleration when an impact angle of 45-degrees was introduced. This work, however, was conducted using a pneumatic impactor as opposed to a drop system. Unfortunately, no previous research studies could be found analyzing hockey helmet impacts to an angled surface. Neither previous studies analyzing impacts to smaller angles. That being said, the difference in peak linear acceleration created by a change in impact angle is due to the direction of the force being applied to the headform. The force applied to the headform is not directly through the centre of mass during angled impacts. Since force is not directed through the centre of mass, peak linear acceleration may not fully describe the impact injury risk. With less force being directed through the centre of mass and more being directed tangentially from the impact surface in the form of shear force, the result is a greater angular acceleration of the headform (McLean & Anderson, 1997). This finding suggests

that focusing on peak linear acceleration alone to determine injury risk and using it as criteria for helmet designs may not be accurate in minimizing the effect of tangential forces on the severity of brain injuries.

In the past, the influence of variables such as location of impact, angle of impact, and neck stiffness on peak linear acceleration measures has been assessed independently (Daniel, Rowson, & Duma, 2012; Haldin & Kleiven, 2013; Rousseau & Hoshizaki, 2009; Walsh, Rousseau, & Hoshizaki, 2011), but not to the extent of how they interact with one another. Since each of these impact characteristics represent unique stresses, it is important to analyze how these variables interact to influence the dynamic response of the neck and helmet and therefore, provide better information on the prevention of head injury and possibly reveal shortcomings of current helmet designs. In the current study no significant three-way interaction effect was found between impact angle, impact location, and neck torque setting. There was, however, a two-way interaction between impact angle and impact location. This finding suggests that there is a significant difference in peak linear acceleration depending on the combination of impact angle and impact location, with the differences varying in magnitude. This outcome is interesting to note as changes in peak linear acceleration are not equal across impact locations when the angle is changed, suggesting that the angle of impact influences the behavior of the helmet properties differently depending on where the impact occurs.

It is possible that differences in peak linear acceleration measures found in the current study could arise because of the asymmetry of the neckform caused by the slits in the anterior side and the cut-outs in the posterior portion of the neckform. The asymmetry of the neckform, however, is necessary to allow for different flexion and extension responses to better simulate a human neck (Ashrafiuon et al., 1996). Previous research work has also shown that neck

asymmetry may contribute to changes in peak linear acceleration outcomes across locations (Foreman, 2010), but such outcomes more likely mimic the response behaviour of a human neck. The differences in compliance in neck flexion, extension, and lateral flexion may also contribute to different dynamic responses seen in the results across impact angle and location. Given this rationale, it is possible to think that the results obtained in the current study may be somewhat influenced by the presence of a custom neckform, as opposed to using a Hybrid III neckform, which is a standard in current literature. The outcome from a pilot study conducted before the actual research, however, revealed strong correlations between the custom neckform and the Hybrid III when using the same protocol with both devices, which indicates that the behaviour of the custom neckform is similar to the Hybrid III neckform when the headform is impacted at different locations.

Besides neck asymmetry possibly influencing measures of peak linear acceleration across location, differences may also arise due to the shape of the head and the helmet itself (Halstead, 1998). Current helmets, for example, have been identified as being "square" in geometry with many external ridges (Halstead, 1998). This traditional design of hockey helmets may have led to shortcomings in performance, especially on the flatter portions of the helmet such as the side impact location. As stated by Halstead (1998), at the flatter portions, the helmet is not as effective in spreading and attenuating the impact accelerations (Halstead, 1998).

It is interesting, however that no main effect was observed for neck torque on measures of peak linear acceleration during the analysis, $F(2, 510)= 1.941$, $p= .145$. This outcome is contradictory to the results obtained by Rousseau and Hoshizaki (2009) on measures of peak linear acceleration across different neck stiffness. In their study, a significant difference was determined between the "soft", "median", and "stiff" neckforms. More specifically, Rousseau

and Hoshizaki found that peak linear acceleration was statistically significantly greater for the "stiff" neck condition. The fact that the results of the current study do not match the results of the study by Rousseau and Hoshizaki (2009) on measures of peak linear acceleration across different neck stiffness may be due to the nature of the impact systems used in both studies. As previously stated, the current study used a drop system as opposed to a pneumatic impactor as well as a different method for controlling compliance. In the research work conducted by Rousseau and Hoshizaki (2009), three separate neckforms were used; changing the material properties to control the stiffness. In the current study, neck torque was adjusted using the same neckform to achieve differences in stiffness. It is possible that Rousseau and Hoshizaki (2009) had a greater difference between their neck compliance conditions than in the current study, which may have contributed to the difference in their results. In summary, neck torque did not influence the data as expected in the current study and since there is still a gap in existing literature on the effect of neck stiffness for simulated impacts involving a neckform, more research is still required to explain how neck compliance influences peak linear acceleration.

Energy loaded. While Peak linear acceleration is the most commonly used measure to assess helmet performance, this measure does not provide enough information on helmet's ability to load and unload forces to account for the deformation of helmet material and more accurately assess the risk of brain injury when wearing these protective devices. As stated by Chajari & Galvanetto (2013), there is a need to develop a more robust criterion to more accurately assess helmet performance in reducing the risk of injury. The energy loaded onto the system may offer an avenue to fill this gap in current literature.

In order to address the concerns with peak linear acceleration measures and develop a more robust measure to assess the risk of injury during a head impact, it is important to evaluate

the ability of helmets in combination with the head and neck to manage the energy loaded on the whole system due to an impact. This approach can be accomplished by taking in consideration certain mechanisms of injury related to impact location, angle of impact, and neck stiffness. More importantly, it is crucial to examine how the interaction of these mechanisms of injury affects the energy loaded on the system. Unfortunately, no previous research studies could be found analyzing the amount of energy loaded on the helmet during a simulated fall in combination with the head and neck during a simulated impact. The current study, however, addresses the interaction effect of mechanisms of injury related to impact location, angle and neck stiffness on the amount energy loaded on the system due to an impact. While no three-way interaction was observed between these three mechanisms of injury, main effects were observed for both impact angle, $F(1, 510)= 29.453$, $p< .005$, and impact location, $F(4, 510)= 28.589$, $p< .005$ when measuring the amount of energy loaded onto the system.

When analyzing the main effect between angles, the impacts conducted at a greater angle were shown to have statistically significantly greater amount of energy loaded onto the system. This increase in energy loaded onto the system means that there is a larger requirement on the ability of the helmet in combination with the neck and head to manage the energy loaded on the system to reduce injury. While hockey helmets are not ideal energy absorbers, not all of the energy will be dissipated by the helmet shell and crushable foam and in effect, more energy will be applied to the head and brain (Cui, Kiernan, & Gilchrist, 2009; McLean et al., 1997; Monthatipkul, Iovenitti, & Sbarski, 2012). The exact amount of energy dissipated by the helmet cannot be determined by this analysis, however, the severity and stress applied to the system was determined to be greater when the angle of impact was increased.

When analyzing the main effect between locations on energy measures, the results of the

current study revealed that the location of the impact on the head influences the amount of energy loaded onto the helmet, headform, and neck. While there is not information in the literature to address differences across head impact locations on energy loading when using a helmet in combination with the head and neck, the findings of the current study add to existing literature and indicate that the helmet in combination with the head and neck do not manage the impact energy equally across impact locations. One explanation for this outcome may be that the asymmetry in neck compliance and helmet structure may contribute to this difference. For example, at certain locations, the neck and helmet geometry may allow for a greater loading in energy, which may explain the difference. As stated by Halstead (1998) differences in helmet geometry may result in different energy management ability and in effect, varying degrees of energy being transferred onto the system. Furthermore, it has been stated by researchers that improvements in helmet external geometry is a need to create better helmets and it is a recommendation that helmet manufacturers should consider in future designs (Halstead, 1998). Other factors to consider, yet not addressed in this study relate to the effect of helmet designs and fitting on energy loading and should be examined to ensure that current helmet designs function adequately in reducing energy transfer to the head and brain to better protect athletes from injury.

When analyzing the main effect between neck stiffness settings on energy measures, the results of the current study indicate not significant differences across neck torque settings, $F(2, 510)= .745$, $p= .475$. This finding suggests that there was no significant difference in the amount of energy loaded onto the helmet in combination with the neck and head across different neck torque settings and in effect, neck compliance. Although previous research has not yet examined the extent to what neck stiffness influences energy loading on a helmet in combination with the head and neck, from a theoretical perspective, it was expected that a greater amount of neck

stiffness would result in a reduction of impact forces transmitted to the head and consequently a greater dispersion of energy if the head was held rigidly during helmeted impacts, as stated by Cantu (1992) and Johnston, McCrory, Mohtadi, and Meeuwisse (2001). This theoretical concept, however, has not been proven in real-life impacts (Johnston, McCrory, Mohtadi, & Meeuwisse, 2001), which indicates that future research is still required to determine whether neck stiffness can influence the amount of energy transferred to the head and neck during helmeted impacts.

An interaction effect between impact angle and impact location on energy loading, however, revealed that impacts to the rear, side, front boss, and rear boss had a larger amount of energy loading for the 13.5-degree impacts when compared to the zero-degree impacts, except of the front location which manifested the opposite. This outcome indicates that angle of impact influences the degree of energy loading into the system and it is dependent on impact location. This finding is important, especially in helmet designs as they are usually evaluated across locations without considering angle of impacts to ensure the helmet can manage impact energy adequately to reduce injury risk.

An interaction effect between neck torque and impact angle on energy loading was also found, which revealed that the energy loaded onto the system is influenced differently depending on the combination of neck torque and impact angle. As depicted in Figure 23, the loading energy is greater for the 13.5-degree impacts for all neck torque settings when compared to the zero-degree impacts. This outcome is the opposite of what was observed for peak linear acceleration; peak linear acceleration was decreased when the angle was increased. It appears that at the zero-degree impacts, there is a linear relationship between neck torque and energy loaded onto the system in that as the torque is increased, there is an increase in the energy loaded. This finding is not consistent with expectations stated in the literature (Magee,

Zachazewski, Quillen & Manske, 2011). It is described by Magee et al. that a stiff neck produces a "sum of masses", allowing for a more effective transfer of mechanical energy away from the head or headform during a projectile type impact (Magee, Zachazewski, Quillen & Manske, 2011). This finding was also shown in a study by Coulson & Hoshizaki (2011), where impacts to a stiffer, less compliant neck resulted in a smaller amount of total energy transferred to the headform and neck for unhelmeted impacts. Both of these previous analyses were conducted on "projectile" impacts, where in the stationary head is impacted, as opposed to falling to the impact surface like the current study. This finding may highlight a difference in helmet and neck impact energy management depending on mechanism of the impact. For the 13.5-degree impacts on the other hand, there is an increase in energy loaded from 8.4 in-lb to 12 in-lb, however, a large decrease at 15.6 in-lb. This interaction shows that helmet research and design may need to consider how impact angle and neck compliance influence the amount of energy transferred to the person during falls in greater detail. Helmet performance should ideally give all athletes protection against injury during any impact they may experience during regular play; these findings suggest they may not.

Shear force. Besides energy loading, it is also crucial to consider the role that shear forces play during a head impact. As stated in the literature, the brain and axons have a high susceptibility to shearing forces (National Research Council (U.S.), 2014). In the case of brain injuries, shear forces are thought to be of particular concern because they can cause vessel rupturing or swelling (McLean & Robert, 1997; National Research Council (U.S.), 2014). In the current study, the amount of shear force applied to the head during different impact conditions was examined using a forceplate. This measurement approach could not be found in the literature for hockey helmet impact testing as the majority of the testing protocols are based on measures

of peak linear acceleration (Zhang, Yang, & King, 2004). The analysis conducted on the current study, however, serves to investigate the interaction that impact angle, impact location, and neck stiffness have on the amount of shear force applied to the head. The analysis of this interaction effect also serves to provide more information about injury mechanisms to build on existing literature and possibly generate additional information for helmet testing designs to protect against brain injury induced by shear forces.

When examining the injury mechanisms related to angle of impact, neck torque and helmet locations, the results of the current study revealed a statistically significant three-way interaction between impact angle, neck torque, and impact location on shear forces. To better interpret the three way interaction, simple two-way interactions between neck torques and impact locations on shear force were used for each impact angle. These two way interactions were found to be significant for zero-degree impacts, $F(8, 510)= 4.337$, $p< .005$ and 13.5 degree impacts, $F(8, 510)= 2.019$, $p= .043$. The interactions reveal that the helmet and neckform cannot manage the amount of shear forces being applied to the head equally across conditions.

Since shear forces generate rotational accelerations, it is the general consensus that large amounts of shear forces contribute to the occurrence of concussion and diffuse axonal injuries (King et al., 2003). In the current study, some helmet locations are more affected than others due to neck stiffness and angle of impact as shown in Figures 29 and 30. For example, the Rear Boss and Rear locations showed an increase in peak shear force when the neck torque was increased for zero-degree impacts but did not show the same trend for 13.5-degree impacts. The front location also differs greatly across impact angles, as it shows the opposite trend for angled impact as it did for zero-degree impacts. The results from the analysis are not consistent with the literature. It would be expected that during impacts with a stiffer neck, less shear force and

angular motion would be applied to the head when compared to the more compliant neck torque settings (Magee et al., 2011; Rousseau & Hoshizaki, 2009). In the study by Rousseau and Hoshizaki (2009), the expected finding was confirmed for direct "projectile" impacts when manipulating neckform stiffness. The interaction effect observed in the current study revealed that the system reacts differently for simulated falls and that the system may not manage shear forces the same way when the angle of impact is increased.

While shear forces have not been considered extensively in helmet testing protocols and designs and it is shown in the literature that these forces can certainly increase angular acceleration causing vessel rupturing or swelling, leading to brain injuries(McLean & Robert, 1997; National Research Council (U.S.), 2014).The interaction effects found in this analysis certainly open an avenue to develop new helmet testing protocols to better examine helmet ability to manage shear forces cause by mechanisms of injury related to impact location, neck strength and angle of impact.

Severity Index. Although measures of peak linear acceleration, energy loading, and shear forces provide very useful information for helmet testing protocols and designs when examined across different mechanisms of injury, it is also of great benefit for the clinician, researcher, athlete and coach to have information on the ability of the helmet to minimize the risk of injury. One commonly measure used to predict injury risk in simulated and real-life impact scenarios is the Severity Index calculation (Higgins et al., 2007; Greenwald et al., 2009). The Severity Index calculation is based entirely on linear accelerations. It is a simple and useful tool in predicting risk of injury for any given impact. Even though there is not perfect measure of injury risk, previous studies have shown that linear acceleration has been found to be the most highly correlated measure with clinical diagnosis of concussion (Greenwald et al., 2009). Lower

head accelerations, however, have been shown to result in lower incidence of head and brain injuries like concussion (Rowson & Duma, 2013). Based on the results from the current study, it is clear that at zero-degree impacts, collisions to the front boss location resulted in the greatest risk of injury, with some of the impact exceeding the 1200 SI maximum determined by NOCSAE. This finding is consistent with those determined by Wonnacott and Fournier (2013) wherein impacts to the Front Boss location resulted in the highest risk of injury as estimated by Severity Index. The opposite result was obtained for the 13.5-degree impacts, where the front boss location resulted in the lowest risk of injury as estimated by the Severity Index, suggesting impact locations' ability to manage injury risk depend largely on the angle of impact.

While Severity Index has been analyzed across impact characteristics in the past, the performance of this index across mechanisms of injury such as impact angle, impact location, and neck stiffness has not yet been examined (Greenwald et al., 2008; Higgins et al., 2007). Each of these impact characteristics create unique impact conditions that influence the dynamic response of the head and brain and should be analyzed together (Clark, 2015). As a researcher, clinician and helmet manufactures, it is important to consider how this index performs across impact characteristics including impact angle, impact location, and neck compliance to better understand the degree to which the interaction of these mechanisms of injury influences the risk of injury in real life situations to ensure athletes are provided with the best possible protection.

While there was not a three-way interaction between neck torque, impact angle, and impact location on measures of Severity Index, a significant main effect was determined for impact angle, $F(1, 510)= 40.953$, $p< .005$. The influence that impact angle has on Severity Index as found in this study during simulated falls builds on existing literature (Higgins et al., 2007; Greenwald et al., 2009) by suggesting that the risk of injury is significantly greater for zero-

degree impacts and less for impacts induced at an angle such as13.5-degree. This outcome is opposite to the effect of angle on shear forces as higher shear forces were found for the 13.5 degree impacts. The outcome suggests, however, that it is possible to reduce the risk of injury during a head impact if the helmet and neck are able to manage the magnitude of linear accelerations and shear forces during direct and tangential impacts applied to the head.

In the current study, there was also a significant main effect of impact location on Severity Index, $F(4, 510)= 8.847$, $p< .005$. The influence that impact location has on Severity Index has been assessed in the past (Wonnacott & Fournier, 2013). The outcome of the current study supports the literature, highlights significant differences in injury risk across the five impact locations tested and suggests that the head and brain may be more susceptible to severe injury at certain locations as stated by Greenwald et al., (2009), specifically the Front Boss and Front locations. Said differently, this finding identifies that helmet performance in terms of linear acceleration reduction is non-uniform across impact locations and that athletes may be at a greater risk of injury when falls result in contact with the Front and Front Boss locations.

More research is required, however to determine the reason for this difference across locations on Severity Index. Some rationales for this difference may be attributed to neck asymmetry, as well as, the geometric shape of hockey helmets themselves as previously stated when discussing measures of peak linear acceleration, energy, and shear forces.

The results of the current study, however, revealed no significant main effect of neck torque when measuring Severity Index, $F(2, 510)= 1.229$, $p= .294$. This outcome is consistent with the research study conducted by Rousseau & Hoshizaki (2009). In their study, neck stiffness had a significant effect on linear and rotational acceleration, however, Severity Index measures did not differ significantly between the “soft”, “median”, and “stiff” neck conditions. The effect

of neck stiffness has not been research extensively in the past, so it is difficult to say why this may have occurred. When comparing these results to the previously discussed analysis of peak linear acceleration, the results are similar. The similarity between analyses makes sense due to the fact Severity Index relies on linear acceleration for its calculation. What the peak linear acceleration analysis fails to consider is the total transfer of acceleration across the entire impact duration. The non-significant main effect of neck torque on Severity Index implies that the impact duration may not have been affected by neck compliance.

Although no significant three-way interaction between impact angle, neck torque and impact location was obtained on Severity Index, a significant two-way interaction between impact angle and impact location was obtained, $F(4, 510)= 12.795$, $p< .005$.The interaction effect between impact angle and impact location suggests that the angle of impact affects the injury risk differently depending on where the impact is occurring. Current analyses of helmets testing only ensure the helmet is adequately protective at all relevant impact locations, but does not consider the angle of impact (NOCSAE, 2014). This finding, however, adds to existing literature and suggests that the helmet and neck have a different ability to manage the risk of injury across different combinations of impact angle and location, meaning it cannot reduce injury risk to the same degree. This finding is a consideration that should be taken into account when designing new helmets and determining if they are suitably protective for athletes. That is, designing helmets that are able to reduce the effect of shear forces, rotational accelerations, linear accelerations, and energy loadings on the head and brain tissue across impact angles, helmet locations and neck stiffness may help minimize the risk of concussions and brain injuries during head impacts. The outcome of this study supports the desire of other researchers in the past in terms of improving helmet evaluations techniques. As stated by Walsh et al., 2011,

helmet evaluation techniques should incorporate varying impact angles and a greater number of dynamic response variables to adequately assess protective performance.

Research Question 2:

The concepts of energy absorption, dissipation, and loading have been researched scarcely in the past and the research conducted did not simulate real-life human head impacts because the researchers did not include a neckform. The findings, however, have provided useful information about headgear and helmet performance protocols during impact testing (Marsh, McPherson, & Zerpa, 2008; Monthatipkul, Iovenitti, & Sbarski, 2012). One reason for the exclusion of energy in the analyses among the literature may be the complexity and time consuming process when calculating energy, as demonstrated by Equations 11 to 15 in the procedure section of the current study. The creation of a model to predict the energy loaded onto the headform can ease this taxing process to make it more accessible for researchers, clinicians, athletes, and coaches when assessing helmet performance and simulating injuries.

Based on the above rationale and limitations of current computational techniques to assess helmet performance on measures of energy loading, the purpose of this analysis was to determine how much weight each measure of shear force, impact angle, impact location, and peak linear acceleration has in predicting the amount of energy loaded onto the helmet in combination with the head and neck during an impact. From the calculated coefficients and t-values, it is clear that all of the variables contributed significantly to the prediction of energy loaded, with the exception of neck torque, which was not included in the regression analysis.

In terms of the variables found to be significant, impact angle was found to contribute significantly to the amount of energy loaded onto the system. Based on the regression coefficient, 12.058 J of energy is loaded onto the system when the angle is increased from zero

to 13.5-degrees. This is a small increase in energy, however, the model identified that as the angle of impact is increased, more energy is loaded onto the system. This factor greatly influences the vector of force travelling through the headform and the amount of linear and rotational acceleration felt by the brain. Because of the non-centric application of force, the neckform and helmet may not be able to effectively manage the impact energy as well when impacted at an angle, resulting in the increase in energy loaded onto the system during the angled impacts.

While angle of impact was found to contribute significantly to the model, the location was also found to significantly influence the amount of energy loaded onto the system. The impact location coefficients determined that when the location is changed, different amounts of energy loaded is contributed to the model. After dummy coding was conducted for the impact locations, the Front Boss was not found to contribute significantly, and as such serves as the reference to which the others can be compared. The coefficients determined for each impact location indicated that when compared to the Front Boss location, impacts to the Front resulted in a predicted 43.076 J more energy loaded onto the head when all other variables were held constant. The coefficient for the Front was larger than the Rear (28.619 J), the Side (-20.833 J), and the Rear Boss (27.582 J). The model identified that the location of impact has a large influence on the predicted energy loaded onto the system.

In addition to impact angle and location, the regression coefficients of the two continuous variables included, peak linear acceleration and peak shear force, were both determined to be significant. Despite being small coefficients, both values are present in significant amount for each impact, meaning they both in fact contribute greatly to the amount of energy loaded onto the helmet, headform, and neckform. For example, for every unit of shear force (N), there is an

increase in 0.031 J of energy being loaded onto the system when all other factors are held constant. In addition, for every unit of peak linear acceleration (g), there is an increase of 0.256 J of energy loaded onto the system. The model identified that these two variables statistically significantly influence the amount of energy transferred to the system.

The model was found to be significant and can predict a significant amount of the variance, $R^2 = .416$, in the energy loaded based on significant predictors such as impact location, impact angle, peak linear acceleration, and peak shear force. That is, the model is only able to account for 41.6% of the variance. There is, however, 58.4 % of the variance not accounted for by this model, which may be related to other factors or predictors not identified in the current model. In the future, the strength of the model may be improved by further manipulating characteristics of the impact. For example, a greater number of angles and impact velocities could be used in addition to using the drop system's ability to control inbound mass, similar to a study by Karton, Hoshizaki, and Gilchrist (2014).The addition of more impact characteristics may aid in predicting the amount of energy loaded onto the system. Nevertheless, this model can be used in future research as a starting point to better understand and explain the effect of these predictors on injury reconstructions during falling incidents related to concussions.

Research Question 3:

Severity Index is a widely-used measure to predict injury risk based on linear acceleration applied to the headform throughout an impact (NOCSAE, 2014; O'Brien & Meehan, 2015; Oukama, 2013; Rousseau & Hoshizaki, 2009). It is a useful measure in determining injury risk, however, there should be a broader focus in assessing protection and injury risk against brain injuries such as concussion (Chajari & Galvanetto, 2013). Measures of energy transfer and dissipation have been identified as useful variables in determining injury risk

(Monthatipkul, Iovenittie, & Sbarski, 2012), but have never been compared directly to injury risk assessment tools based on other impact variables, like Severity Index.

Based on the above rationale, the purpose of this analysis was to determine if the energy loaded onto the system compared to the widely used Severity Index. The strength of association between the two variables was determined to be moderate between the energy loaded and the Severity Index, r= .340. The moderate correlation suggests that higher levels of energy loaded is associated with higher Severity Index and in effect, a greater risk of injury. The correlation is significant between the two variables, with 11.56% of the variance in energy loaded being explained by the relationship. There is still a large amount of variance not being accounted for in the relationship, which may be due to the fact that Severity Index is based entirely on linear acceleration. It has been shown previously that the amount of energy loaded onto the system is influence by shear forces as well, a variable not considered in Severity Index. According to the analysis, the amount of energy loaded onto the system is fact related to the risk of injury as predicted by Severity Index.

Limitations

There are a number of limitations to the study including: the headform, drop system, and neckform. The results obtained from the study are specific to the testing conditions. Meaning the results may only be directly comparable to real-life falls onto a flat or 13.5-degree impact surface. The results obtained from the accelerometer within the simulated headform can only create estimated values of linear acceleration and Severity Index that a human brain would experience during the impacts. It is difficult to say that a human would experience the exact obtained values for certain. The neckform was designed by the Lakehead Mechanical Engineering Department to closely mimic the response of the Hybrid III neckform, however, it

cannot be said that a human neck would respond exactly as the simulated neck did during the impact conditions.

When conducting the repetitive impact testing to determine helmet deterioration threshold values, the force used was much lower than the maximum force experienced during the actual testing. Ideally, a researcher would use the maximum impact force to determine the critical point at which the helmet would fail. This approach was not possible in the current study in order to minimize the wear and tear of the neckform mechanism. The technique, however did not affect the current results, as helmets were changed after 18 impacts per location.

Limitations with the drop system exist in the durability of some of the smaller parts and their ability to withstand the rigors of a study requiring a significant amount of impacts. Although no major issues arose with the system, minor issues including a few bearings breaking were experienced. It is unlikely that these small issues affected that data, however, the system should be improved to avoid having to change parts.

In addition, the only angle achievable through the resources available was 13.5-degrees. Ideally, more angles would be tested to create more meaningful and in depth comparisons of the dependent variables across impact angle.

Strengths

The primary strength of the study lies in the comparison of impact dynamics and injury across different neck torque settings. No prior studies could be found analyzing the difference in neck torque and very few analyzing the difference neck compliance can have on impact characteristics (Rousseau & Hoshizaki, 2009; Rousseau, Hoshizaki, Gilchrist, & Post, 2010). In addition, the study analyzed impacts by measuring the amount of energy being applied to the headform, helmet, and neckform as well as the shear force by using a forceplate; no prior studies

could be found performing this type of analysis for hockey-helmeted impacts despite the large potential they have to describe impact severity.

Conclusion

This study examined the influence of neck torque, impact angle, and impact location when measuring peak linear acceleration, shear force, energy loaded, and Severity Index as well as create a model by which energy loaded onto the system could be predicted and determine the relationship between energy loaded and Severity Index. The study was conducted because it was evident that there were gaps in the literature in terms of determining how neck stiffness and impact angle influence injury risk and the amount of peak linear acceleration applied to the headform. Head and brain injuries remain to be very common within the sport of hockey and addressing these gaps may help reduce injury rates. In addition, the study served to examine addition dependent variables that could provide greater insight into impact severity an injury risk.

The data presented in the current study helps provide a better understanding of injury risk and potential for future injury prevention strategies and research. Improving the understanding of injury mechanisms as well as the interplay of impact characteristics can benefit the development of hockey helmets. The information may also provide an understanding of preventative measures that can be taken by athletes such as neck strength training.

The study found many interaction effects between neck torque, impact angle, and impact location as well as many simple main effects explaining significant differences in peak linear acceleration, shear force, Severity Index, and energy loaded onto the system. The differences support and build on previous literature analyzing hockey helmet impacts (Aldman, 1984; Bishop & Arnold, 1993; Greenwald et al., 2008; Kendall et al., 2012, Rousseau & Hoshizaki,

2012). The study also determined how many different impact characteristics can be used to predict energy loaded onto the head and neck and determined that a relationship existed between energy loading and risk of injury as estimated by Severity Index. The study served to create an avenue to better assess differences in impact severity across conditions as well as attempted to gain a greater understanding of how different characteristics of impacts can influence the risk of injury for athletes sustaining a fall.

Future Research

Future research should focus on analyzing impacts in a broader sense than focusing on peak linear or peak rotational acceleration like much of the current literature. Studies should continue to analyze the effects of impact forces as well as internal measures on acceleration and Severity Index to determine injury risk. In addition to greater consideration of dependent variables, studies should also focus on comparing different impact conditions and the influence they can have on the dynamic response of the head. Focusing on the differences created by a wide degree of impact angles, neck stiffness, and impact locations could aid in the future development of helmets as well as aid in developing more rigorous testing protocols.

Future research could also be conducted to isolate the performance differences of the helmet itself during a simulated impact, rather than the system as a whole. Future research should focus on quantifying the direct influence the helmet is having on the impact. Future research focusing on helmet performance directly could give more insight into what areas of development need to be improved. Research could be conducted to compare helmet performance by conducting an unhelmeted impact and a helmeted impact for the same condition and comparing the results to determine the energy reduction or dissipation characteristics of the helmet.

In summary, this study analyzed the influence that neck stiffness, impact angle, and impact location can have on traditional helmet analysis variables such as peak linear acceleration and Severity Index. In addition, unconventional analysis was conducted by analyzing the peak shear force being applied to the head as well as the amount of energy loaded onto the system of the helmet, headform, and neckform which were not previously analyzed in the literature despite the known role they may play injury risk and occurrence (Gurdjian, 1972; Holbourn, 1943; Kleiven, 2013; Monthatipkul, Iovenitti, Sbarski, 2012). The study revealed many relationships between impact angle, neck stiffness, and impact location when measuring variables such as peak linear acceleration, peak shear force, energy loaded, and Severity Index. In addition, some unique main effects were identified, showing how the helmet and neck managed the impact differently depending on the nature of the impact, although, not entirely consistently with previous research. The results provided insight into helmet performance under many unique conditions, highlighting shortcomings and helmet performance and design.

The study also revealed that a model could be created to predict the amount of energy loaded onto the head and neck by using the angle of impact, the location of impact, the shear force, and peak linear acceleration to a statistically significant degree and can predict the severity of the impact in terms of energy transferred to the helmet, head, neck, and brain. A gap exists in the literature regarding energy loading analysis; this model serves to aid in filling this gap and provide a simpler avenue to compare energy loading across impact conditions. The model can now be used to predict the amount of energy loaded onto the system for future research using the Lakehead University drop system.

The study also compared the energy loaded with measures of Severity Index to determine how the amount of energy transferred to the head was related to the risk of injury, as predicted

by the Severity Index criteria. Severity Index is designed to estimate the risk of injury based solely on the linear acceleration transferred to the headform over the course of the impact (NOCSAE, 2014). The results revealed an association between the two variables, suggesting that a large amount of energy loaded onto the system is related to a large risk of injury as estimated using linear acceleration. From a theoretical perspective, the results indicate that there is a relationship between the linear acceleration transferred throughout the impact to the amount of energy loaded onto the system. This suggests that the variables are related during simulated falls, although, not entirely, as only 11.56% of the variance in Severity Index can be explained by the relationship.

Finally, it can be said that the study served to analyze common dynamic impact variables across impact conditions that are not often manipulated. In addition, the study uses a non-traditional analysis of shear force and energy transfer to assess how they change across impact conditions. These outcomes provide an avenue to further assess helmet performance and build on previous research attempting to determine injury risk that athletes are exposed to.

References

Agel, J., & Harvey, E. (2010). A 7-year review of men's and women's ice hockey injuries in the NCAA. *Canadian Journal Of Surgery*, *53*(5), 319-323.

Aldman, A. (1984). A method for the assessment of the load distributing capacity of protective helmets. Goteborg, Chalmers University of Technology.

Alkharusi, H. (2012). Categorical Variables in Regression Analysis: A Comparison of Dummy and Effect Coding. *IJE*, 4(2).

Andriessen, T., Jacobs, B., & Vos, P. (2010). Clinical characteristics and pathophysiological mechanisms of focal and diffuse traumatic brain injury. *Journal of Cellular And Molecular Medicine*, *14*(10), 2381-2392.

Arciniegas, D., Anderson, A., Topkoff, J., & McAllister, T. (2005). Mild traumatic brain injury: a neuropsychiatric approach to diagnosis, evaluation, and treatment. *Neuropsychiatric Disorder Treatment*, *1*(4), 311-327.

Ashrafiuon, H., R. Colbert, L. Obergefell and I. Kaleps (1996). "Modeling of a deformable manikin neck for multibody dynamic simulation." Mathematical and Computer Modelling 24(2): 45-56

Avalle, M., Belingardi, G., & Montanini, R. (2001). Characterization of polymeric structural foams under compressive impact loading by means of energy-absorption diagram. *International Journal of Impact Engineering, 25*, 455-472.

Bailes, J., Petraglia, A., Omalu, B., Nauman, E., & Talavage, T. (2013). Role of subconcussion in repetitive mild traumatic brain injury. *Journal of Neurosurgery, 119*(5), 1235-1245.

Barth, J., Freeman, J., Broshek, D., & Varney, R. (2015). Acceleration-deceleration sport-related concussion: The gravity of it all. *Journal of Athletic Training*, *36*(3), 253–256.

Benson, B., Hamilton, G., Meeuwisse, W., McCrory, P., & Dvorak, J. (2009). Is protective equipment useful in preventing concussion? A systematic review of the literature. *British Journal of Sports Medicine, 43*(Suppl 1), I56-I57.

Benson, B., Mieeuwisse, W., Rizos, J., Kang, J., & Burke, C. (2011). A prospective study of concussions among National Hockey League players during regular season games: the NHL-NHLPA Concussion Program. *Canadian Medical Association Journal, 183*(8), 905-911.

Biasca, N., Wirth, S., & Tegner, Y. (2002). The availability of head and neck injuries in ice hockey: A historical review. *British Journal of Sports Medicine, 36*, 410-427.

Biesbroek, J., Rinkel, G., Algra, A., & van der Sprenkel, J. (2012). Risk Factors for Acute Subdural Hematoma From Intracranial Aneurysm Rupture. *Neurosurgery*, *71*(2), 264-269.

Bishop PJ, Arnold J. The effectiveness of hockey helmets in limiting localized loading on the head, in *Safety in Ice Hockey*, pp. 175–182, CR Castaldi, PJ Bishop, EF Horner (Eds), American Society for Testing Materials, Philadelphia, USA, 1993.

Brainard, L., Beckwith, J., Chu, J., Crisco, J., McAllister, T., Duhaime, A., . . . Greenwald, R. (2012). Gender differences in head impacts sustained by collegiate ice hockey players. *Medicine & Science in Sports & Exercise,44*, 297-304.

Cantu, R. (1992). GUidelines for return to contact sports after cerebral concussion. *Phys Sportsmed,14*, 64-74.

Caswell, S., & Deivert, R. (2002). Lacrosse helmet designs and the effects of impact forces. *Journal of Athletic Training,37*(2), 164-171.

Chamard, E., Theoret, H., Skopelja, E., Forwell, L., Johnson, A., & Echlin, P. (2012). A

prospective study of physician-observed concussion during a varisty university hockey season: Metabolic changes in ice hockey players. Part 4 of 4. *Neurosurgical Focus, 33*(6), 1-7

Chartrand, D. (2001). *Patent No. 6298497.* USA.

Cobb, B. (2013). Measuring head impact exposure and mild traumatic brain injury in humans.*Brain Injuries and Biomechanics, 1*, 1-8.

Concannon, L., Kaufman, M., & Herring, S. (2014). Counseling athletes on the risk of chronic traumatic encephalopathy. *Sports Health,6*(5), 396-401.

Concussion. (2015). Retrieved from http://www.mayoclinic.org/diseases-conditions/concussion/basics/symptoms/con-20019272

Cronbach, L., & Meehl, P. (1955). Construct validity in psychological tests. *Psychological Bulletin*, *52*(4), 281-302.

Cui, L., Kiernan, S., & Gilchrist, M. (2009). Designing the energy absorption capacity of functionally graded foam materials. *Materials Science and Engineering, 30*, 3405-3413.

Dalong, G., & Wampler, C. (2009, December 1). Head Injury Criterion: Assessing the Danger of Robot Impact. *IEEE Robotics & Automation Magazine*, 71-74.

Daniel, R., Rowson, S., & Duma, S. (2012). Head Impact Exposure in Youth Football. *Annals Of Biomedical Engineering*, *40*(4), 976-981.

Davenshvar, D., Nowinski, C., McKee, A., & Cantu, R. (2011). The epidemiology of sport-related concussion. *Journal of Sports Medicine, 30*(1), 1-17.

Dissipation. (2015). In *Oxford Dictionaries.* Retrieved from http://www.oxforddictionaries.com/definition/english/dissipation

Drost, E. (2011). Validity and reliability in social science research. *Education Research And Perspectives*, *38*(1), 105-123.

Eppinger, R., Sun, E., Bandak, F., Haffnerm M., Khaewpong, N., Maltese, M., Kuppa, S., Nguyen, T., Takhounts, E., Tannous, R., Zhang, A., & Saul, R. Development of improved injury criteria for the assessment of advanced automotive, restraint systems- II. Supplement to NHTSA Docket, 199804405-9, National Highway Traffic Safety Administration, US Department of Transportation, Washington, DC, USA, 1999

Filley, C. (2012). White matter dimentia. *Therapeutical Advances In Neurological Disorders*, *5*(5), 267-277.

Flik, K., Lyman, S., & Marx, R. (2005). American collegiate men's ice hockey: an analysis of injuries. *American Journal of Sports Medicine, 33*(2), 183-187.

Foreman, S. G. (2010). The Dynamic Impact Response of a Hybrid III Head- and Neckform under Four Neck Orientations and Three Impact Locations. M.Sc. MR74136, University of Ottawa (Canada).

Gadd, C. Use of a weighted impulse criterion for estimating injury hazard. In: *Proceedings of the 10th Stapp Car Crash Conference,* Society of Automotive Engineering, 1966, pp 95-100.

Gennarelli, T. (1983). Head injury in man and experimental animals: Clinical aspects. *Acta Neurochirurgica Supplement, 32*, 1-13

Gennarelli, T., Ommaya, A., & Thibault, L. (1971). Comparison of translational and rotational head motions in experimental cerebral concussion. *Stapp Car Crash Conference,* 797-803.

Gennarelli, T., Thibault, L., Adams, J., Graham, D., Thompson, C., & Marcincin, R. (1982). Diffuse axonal injury and traumatic coma in the primate. *Annals Of Neurology*, *12*(6), 564-574.

Ghajari, M. & Galvanetto, U. The impact attentuation test of motorcycle helmet standards. *Proceedings of the 1st International Conference on Helmet Performance and Design,* 2013, pp 16-26

Gimbel, G., & Hoshizaki, T. (2008). A comparison between vinyl nitrile foam and new air chamber technology on attenuating impact energy for ice hockey helmets. *International Journal of Sports Science and Engineering, 2*(3), 154-161.

Giza, C., & Hovda, D. (2001). The Neurometabolic Cascade of Concussion. *Journal of Athletic Training, 36*(3), 228-235.

Graham, R., Rivara, P., Ford, M., & Spicer, C., (2014). *Sports-Related Concussion in Youth.* Washington, DC: The National Academies Press.

Greenwald, R., Gwin, J., Chu, J., & Crisco, J. (2008). Head impact severity measurement for evaluating mild traumatic brain injury risk exposure. *Neurosurgery,62*(4), 789-798.

Gurdjian, E. (1972). Recent advances in the study of the mechanism of impact injury the head--a summary. *Clinical Neurosurgery, 19*, 1-42.

Gurdjian, E., Hodgson, V., Thomas, L., & Patrick, L. (1968). Significance of relative movements of scalp, skull, and intracranial contents during impact injury of the head. *Journal of Neurosurgery, 29*(1), 70-72.

Gurdjian, E., Lissner, H., Evans, F. (1961). Intracranial Pressure and Acceleration Accompanying Head Impacts in Human Cadavers. *Surgery, Gynecology, and Obstetrics*, *112*,185-190

Gurdjian, E., Roberts, V., & Thomas, L. (1966). Tolerance curves of acceleration and intracranial pressure and protective index in experimental head injury. *Journal of Trauma,6*, 600-604.

Gurdjian, E., & Webster, J. (1945). Linear acceleration causing shear in the brain stem in trauma of the central nervous system. *Mental Advances in Disease,* 24-28.

Gurdjian, E., Webster, J., & Lissner, H. (1955). Observations on the mechanism of brain concussion, contusion, and laceration. *Journal of Surgery, Gynecology, and Obstetrics, 101*(6), 680-690.

Gwin, J., Chu, J., McAllister, T.,& Greenwald, R. (2009). In situ measures of head impact acceleration in NCAA Division I mean's ice hockey: Implications for ASTMF1045 and other ice hockey helmet standards. *Journal of ASTM International, 6*(6), 1-10.

Hall, R., Hall, R., & Chapman, M. (2005). Definitions, diagnosis, and forensic implications of post concussion syndrome. *Psychosomatics, 46*(3), 195-202.

Halldin, P. & Kleiven, S. The development of next generation test standards for helmets. *Proceedings of the 1st International Conference on Helmet Performance and Design,* 2013, pp 1-8.

Halstead, D. (2001). Performance testing updates in head, face, and eye protection. *Journal of Athletic Training, 36*(3), 322-327.

Halstead, D., Alexander, C., Cook, E., & Drew, R. (1998). "Hockey Headgear and the Adequacy of Current Design Standards". Safety in Ice Hockey, ASTM STP 1341, Ashare, A., B., Ed., ASTM International, West Conshohocken, PA, 2000, pp. 93-100.

Halstead, M., Walter, K., & American Academy of Pediatrics Council on Sports Medicine. (2010). Sport-related concussion in children and adolescents. *Pediatrics, 126*(3), 597-

615.

Hannon, P., & Knapp, K. (2006). *Forensic Biomechanics* (p. 126). Lawyers & Judges Publishing Company.

Hardy, W., Foster, C., Mason, M., Yang, K., King, A., & Tashman, S. (2001). Investigation of head injury mechanisms using neural density technology and high-speed biplanar x-ray. *Stapp Car Crash Journal, 45*, 337-368.

Higgins, M., Halstead, D., Snyder-Mackler, L., & Barlow, D. (2007). Measurement of impact acceleration: Mouthpiece accelerometer versus helmet accelerometer. *Journal of Athletic Training, 42*(1), 5-10.

Hodgson, V (1975). National Operating Committee on Standards for Athletic Equipment football helmet certification program. *Medicine and science in sports. 7*(3):225.

Holbourn, A. (1943). Mechanics of head injuries. *Lancet,* 438-441

Honey, C. (1998). Brain injuries in ice hockey. *Clinical Journal of Sports Medicine, 8*(1), 43-46.

Hoshizaki, T., & Brien, S. (2004). The science and design of head protection in sport. *Neurosurgery, 55*(4), 956-967.

Hoshizaki, B., & Chartrand, D. (Eds.). (1995). *Proceedings from ISBS-1995: 13th International Symposium on Biomechanics in Sport*. Thunder Bay, ON: Bauer.

Hoshizaki, B., Post, A., Kendall, M., Karton, C., Brien, S. (2013). The relationship between head impact characteristics and brain trauma. *Journal of Neurology Neurophysiology* 5(1), 1-8.

Hoshizaki, T.B., "The relationship between helmet standards and head protectors safety in ice hockey", in *IIHF International Symposium on Medicine and Science in Hockey*, Biasca, N., Montag, W., & Gerber, C., University of Zurich, Zurich, 1995, pp. 90-95

Johnston, K., McCrory, P., Mohtadi, N., & Meeuwisse, W. (2001). Evidence-Based Review of Sport-Related Concussion: Clinical Science. *Clinical Journal Of Sport Medicine*, *11*(3), 150-159.

Karton, C., Hoshizaki, T., & Gilchrist, M. (2014). In *Mechanism of Concussion in Sport* (pp. 23-44). West Ponshonhocken: ASTM International.

Katz, D., Cohen, S., & Alexander, M. (2015). Mild traumatic brain injury. *Handbook Of Clinical Neurology*, *127*, 131-56.

Kelly, K., Lissel, H., Rowe, B., Vinventen, J., & Voaklander, D. (2001). Sport and recreation-related head injuries treated in the emergency department. *Clinical Journal of Sports Medicine, 11*(2), 77-81.

Kendall, M., Post, A,Rousseau, P., Gilchrist, M., & Hozhiaki, B., (Eds). (2012). A comparison of dynamic impact response and brain deformation metrics within the cerebrum of head impact reconstructions representing three mechanisms of head injury in ice hockey. *Proceedings from IRCOBI 2012*: *International Research Council on the Biomechanics of Injury*. Dublin, Ireland: University of Dublin.

Kimpara, H., & Iwamoto, M. (2012). Mild traumatic brain injury predictors based on angular accelerations during impacts. *Annals of Biomedical Engineering,40*(1), 114-126.

King, A., Yang, K., Zhang, L., & Hadry, W. (Eds). (2003). Is head injury caused by linear or rotational acceleration? Proceedings from IRCOBI 2003: *International Research Council on the Biomechanics of Injury.* Lisbon, Portugal.

Kis, M., Saunders, F., Kis, M., Irrcher, I., Tator, C., Bishop, P., & Hove, M. (2013). A method of evaluating helmet rotational acceleration protection using the Kingston Impact Simulator (KIS Unit). *Clinical Journal of Sports Medicine, 23*(6), 470-477.

Kleiven, S. (2013). Why Most Traumatic Brain Injuries are Not Caused by Linear Acceleration but Skull Fractures are. *Front. Bioeng. Biotechnol.*, *1*.

Landro, L., Sala, G., & Olivieri, D. (2002). Deformation mechanisms and energy absorption of polystyrene foam for protective helmets. *Polymer Testing, 21*, 217-228.

Lissner, H., M, L., & Evans, F. (1960). Experimental studies on the relation between acceleration and intracranial changes in man. *Surg., Gynecol. Obstet.,111*, 329-338.

Magee, D. (2001). *Athletics and sport issues in musculoskeletal rehabilitation.* St. Louis, Mo.: Elsevier/Saunders

Marsh, P., McPherson, M., & Zerpa, C. (Eds.). (2004). *Proceedings from ISBS-2004: 22nd International Symposium on Biomechanics in Sport*. Ottawa, ON.

McAllister, A. (2013). Surrogate Head Forms for the Evaluation of Head Injury Risk. *Brain Injuries And Biomechanics*.

McAllister, T., Sparling, M., Flashman, L., & Saykin, A. (2001). Neuroimaging finding in mild traumatic brain injury. *Journal of Clinical and Experimental Neuropsychology, 23*(6), 775-791.

McLean, A., FIldes, B., Kloeden, C., Digges, K., Anderson, R., Moore, V., Simpson, D., "Prevention of Head Injuries to Car Occupants: An Investigation of Interior Padding Options," University of Adelaide, 1997.

McIntosh, A., & Janda, D. (2003). Evaluation of cricket helmet performance and comparison with baseball and ice hockey helmets. *British Journal of Sports Medicine, 37*(4), 325-330.

Meaney, D., & Smith, D. (2011). Biomechanics of concussion. *Clinics in Sports Medicine, 30*(1), 19-31.

Menon, D., Schwab, K., Wright, D., & Maas, A. (2010). Definition of traumatic brain injury. *Physical Medicine and Rehabilitation, 91*(11), 1637-1640.

Monthatipkul, S., Iovenitti, P., & Sbarski, I. (2012). Design of facial protection gear for cyclists. *Journal of Transportation Technologies, 2*, 204-212.

Mihalik, J., Guskiewicz, K., Marshall, S., Blackburn, T., Cantu, R., & Greenwald, R. (2012). Head impact biomechanics in youth hockey: Comparisons across playing position, event types, and impact locations. *Annals of Biomedical Engineering, 40*(1), 141-149.

Mills, N., Wilkes, S., Derler, S., & Flisch, A. (2009). FEA of oblique impact tests on a motorcycle helmet. *International Journal Of Impact Engineering*, *36*(7), 913-925.

Namjoshi, D., Good, C., Cheng, W., Panenka, W., Richards, D., Cripton, P., & Wellington, C. (2013). Towards medical management of traumatic brain injury: a review of models and mechanisms from a biomechanical perspective. *Disease Models and Mechanisms, 6*(6), 1325-1338.

Nath, S. (2013). Best Split-Half and Maximum Reliability. *IOSRJRME*, *3*(1), 01-08.

National Operating Committee on Standards for Athletc Equipment. (2014). *Standard PerformanceSpecifications for Newly Manufactured Hockey Helmets. Overland Park, USA: NOCSAE.*

National Operating Committee on Standards for Athletc Equipment. (2014). *Standard Test Method and Equipment Used in Evaluating the Performance Characteristics of Headgear/Equipment. Overland Park, USA: NOCSAE.*

National Research Council (U.S.).,. (2014). *Review of Department of Defense Test Protocols for Combat Helmets*. National Academies Press.

Nishizaki, Kyle, Marino, Wayne, Hoshizaki, T. Blaine, Post, Andrew, Oeur, Anna, Walsh, Evan S., Gilchrist, Michael D., and Kendall, Marshall, "Evaluation of Dynamic Response and Brain Deformation Metrics for a Helmeted and Non-Helmeted Hybrid III Headform Using a Monorail Centric/Non-Centric Protocol," Mechanism of Concussion in Sports, STP 1552, Alan Ashare and Mariusz Ziejewski, Eds., pp. 171–186, doi:10.1520/STP155220120169, ASTM International, West Conshohocken, PA 2014.

O'Brien, M., & Meehan, W. (2016). *Head and Neck Injuries in Young Athletes* (p. 97). New York: Springer.

Oeur, A., Hoshizaki, T., Gilchrist, M. The influence of impact angle on the dynamic response of a Hybrid III headform and brain tissue deformation. 2012, ASTM conference 2012, published by ASTM International.

Ommaya, A., Grubb, R., & Naumann, R. (1971). Coup and contre-coup injury: Observations on the mechanics of visible brain injuries in the rhesus monkey. *Journal of Neurosurgery, 35*, 503-516.

Ouckama, R. (2013). *Time series measurement of force distribution in ice hockey helmets during varying impact conditions.* Unpublished doctoral dissertation, McGill University, Montreal, Canada

Ouckama, R., & Pearsall, D. (2012). Impact performance of ice hockey helmets: Head acceleration versus focal force dispersion. *Journal of Sports Engineering and Technology,226*(3/4), 185-192.

Ouckama, R., & Pearsall, D., (Eds). (2014). Projectile impact testing of ice hockey helmets: headform kinematics and dynamic measurement of localized pressure distribution. *Proceedings from IRCOBI 2014: International Research Council on the Biomechanics of*

Injury. Berlin, Germany

Pearsall, D., Hakim-Zadeh, R. (Eds.). (2005). *Proceedings from International Society of Biomechanics XXth Congress*. Cleveland, Ohio.

Petraglia, A., Dashnaw, M., Turner, R., & Bailes, J. (2014). Models of mild traumatic brain injury: translation of physiological and anatomic injury. *Neurosurgery*, *4*, 34-49.

Post, A., Oeur, A., Hoshizaki, B., & Gilchrist, M. (2011). Examination of the relationship between peak linear and rotational accelerations to brian deformation metrics in hockey helmet impacts. *Computer Methods in Biomechanics and Biomedical Engineering, 16* (5), 511-519.

Reilly, P. & Bullock, R. (1997). *Head Injury* (pp. 25-37). London: Chapman & Hall.

Rousseau, P., & Hoshizaki, T. (2009). The influence of deflection and neck compliance on the impact dynamics of a Hybrid III headform. *Proceedings Of The Institution Of Mechanical Engineers, Part P: Journal Of Sports Engineering And Technology*, *223*(3), 89-97.

Rousseau, P., Hoshizaki, T., Gilchrist, M., & Post, A. (2010). Estimating the influence of neckform compliance on brain tissue strain during a helmeted impact. *Stapp Car Crash Journal*, *54*, 37-48.

Rousseau, P., Post, A., & Hoshizaki, T. (2009). The effects of impact management materials in ice hockey helmets on head injury criteria. *Journal of Sports Engineering and Technology, 223*, 159-165.

Rowson S, Duma S. The temperature inside football helmets during head impact: a five-year study of collegiate football games. *Proceedings of the Institution of Mechanical Engineers, Part P: Journal of Sports Engineering and Technology*. 2013;*227*(1):12-19.

Rowson, B., Rowson, S., & Duma, S. (2015). Hockey STAR: A methodology for assessing the biochemical performance of hockey helmets. *Annals Of Biomedical Engineering*, *43*(10), 2429-2443.

Rueda, M., & GIlchrist, M. (2012). Computational analysis and design of components of protective helmets. *Journal of Sports Engineering and Technology, 0*(0), 1-12.

Schmahmann, J., Smith, E., Eichler, F., & Filley, C. (2008). Cerebral white matter. *Annals Of The New York Academy Of Science*, *1142*, 266-309.

Shaw, N. (2002). The neurophysiology of concussion. *Progress In Neurobiology*, *67*(4), 281-344. http://dx.doi.org/10.1016/s0301-0082(02)00018-7

Spittle, E., Miller, D., Shipley, B., & Kaleps, I. (1992). *Hybrid II and Hybrid III Dummy Neck Properties for Computer Modeling*. Ft. Belvoir: Defense Technical Information Center.

USA Hockey. (2011). *Official Rules of Ice Hockey*. Colorado, Colorado Springs: USA Hockey.

Vatansever, F., & Hamblin, M. (2012). Far infrared radiation (FIR): its biological effects and medical applications. *Photonics Lasers Med.*, *1*(4), 255-266.

Walsh, E., Rousseau, P., & Hoshizaki, T. (2011). The influence of impact location and angle on the dynamic impact response of a Hybrid III headform. *Sports Eng*, *13*(3), 135-143.

Wennberg, R., & Tator, C. (2003). Nation Hockey League reported concussions, 1986-87 to 2001-02. *Canadian Journal of Neurological Science, 30*(3), 206-209.

Wilcox, B., Beckwith, J., Greenwald, R., Chu, J., McAllister, T., Flashman, L., . . . Crisco, J. (2014). Head impact exposure in male and female collegiate ice hockey players. *Journal of Biomechanics,47*(1), 109-114.

Wonnacott, M., & Fournier, E. (2013). *Linear Impactor Testing of Hockey Helmets to Determine the Effects of the MIPS System on Head Response* (Tech. No. R13-02). Ottawa, ON: Biokinetics and Associates

Yoganandan, N., & Pintar, F. (2004). Biomechanics of temporo-parietal skull fracture. *Clinical Biomechanics, 19*(3), 225-239.

Zhang, L., Yang, K., & King, A. (2011). Comparison of brain responses between frontal and lateral impacts by finite element modeling. *Journal Of Neurotrauma*, *18*(1), 21-30.

Appendix A

Evidence of reliability and validity for the use of a helmet impact drop system

Concurrent-related evidence of validity and reliability for linear impact acceleration measured of Lakehead University drop system were examined via a plot study. Concurrent validity is studied when the measures of a test are proposed to be a substitute for the measures of another test, previously established as criteria (Cronbach & Meehl, 1955). In this case, the Lakehead University linear impact measure drop system, shown in Figure 32, was compared to the University of Ottawa Neurotrauma Science research lab impact acceleration measures drop system, shown in Figure 33, to provide concurrent-related evidence of validity.

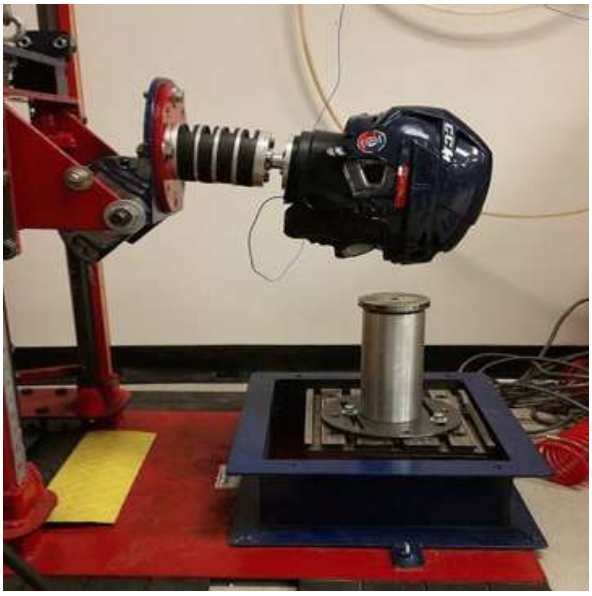

Figure 32. Lakehead University Impact Drop system. The drop system used at Lakehead University, with the headform positioned for frontal impact.

Figure 33. University of Ottawa drop system. The figure shows the system mounted with a NOCSAE headform and CCM Vector V08 helmet, as tested at Lakehead University. The system uses a monorail design; as opposed to the dual-rail design of the Lakehead University drop system. All other conditions were maintained to the best of the researchers' ability.

Identical protocol was conducted at both institutions. The protocol included five helmet locations, three identical helmets, and three linear impacts for each helmet location. The helmet impact locations were: front, front boss, side, rear boss, and rear, as shown in Figure 1. A total of 45 impacts were collected across three identical CCM Vector V08 helmets; 15 impacts per helmet.

Helmets were properly fitted prior to all impacts, as described above, measuring 5.5 cm from the brim of the helmet to the bridge of the nose on the NOCSAE headform, as shown in Figure 10. All impacts were conducted using an inbound velocity of 4.5 m/s; meaning a drop height of 1.03 m was used. Drop height and velocity were determined using the law of conservation of energy. By assuming that the potential energy at release would be the same as the kinetic energy at impact, the drop height for a velocity of interest was determined as shown in Equation 18.

$$\begin{aligned} PE &= KE \\ mgh &= (1/2)mv^2 \\ gh &= v^2/2 \end{aligned} \tag{18}$$

where:

PE= Potential Energy
KE=Kinetic Energy
m= mass
v= velocity
g= acceleration due to gravity

Intra-class correlations were used to provide evidence of concurrent-related validity for each helmet impact location. For frontal impacts, the Lakehead University drop system captured a mean resultant acceleration of M=112.23g, SD=6.14g, as shown in Figure 13. For the same condition, Ottawa University's drop system captured a mean of M=149.33g, SD=14.24g. Using intraclass correlation, strong significant correlation coefficients of ICC=0.922, $p<0.005$ was determined, providing evidence of concurrent-related validity for frontal impacts.

For the Front Boss location, Lakehead University data had a mean of M=136.41g, SD=17.36g while the Ottawa system showed a mean of M=153.04g, SD=14.67g, as shown in Figure 13. According to ICC values, the Lakehead system showed strong concurrent-related validity for the front boss impact location, ICC=0.844, $p<0.005$ (shown in Figure 14), provided evidence of concurrent-related validity for this impact location.

For the side location, Lakehead University data had a mean of M=108.39g, SD=6.83g, while the Ottawa University system collected data with a mean of M=125.1g, SD=8.26g, as shown in Figure 13. An intraclass correlation of ICC=0.934, $p<0.005$ (shown in Figure 14), provided evidence of concurrent-related validity for the side impact location.

For the rear boss location, Lakehead University data had a mean of M=125.38g, SD=3.74g, while the Ottawa University system had a mean of M=149.58g, SD=12.56g, as

shown in Figure 13. Intraclass correlation coefficients, ICC=0.952, $p<0.005$, showed strong significant correlation between systems, provided evidence of concurrent-related validity for the rear boss location, as shown in Figure 14.

Finally, for the rear impact location, Lakehead University data had a mean of 125.1g, SD=4.31g, while the Ottawa system had a mean of M=114.47g, SD=7.21g, as shown in Figure 13. The intraclass correlation coefficient, ICC=0.932, $p<0.005$, provided evidence of concurrent-related validity for the rear impact location.

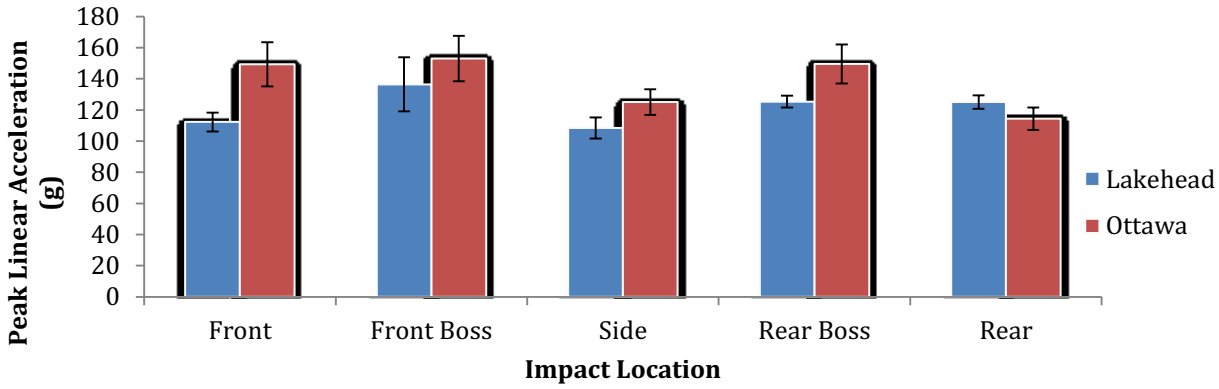

Figure 34. Summary of Peak Resultant Acceleration Values Obtained. Figure 13 shows the peak measures of resultant acceleration for each location at each of the two testing facilities. The figure also displays error bars signifying the standard deviation of values obtained over the three impacts per location. The figure shows discrepancy between the two facilities at each of the locations; therefore, Lakehead University data was scaled to match the mean and standard deviation of the previously validated University of Ottawa system's data.

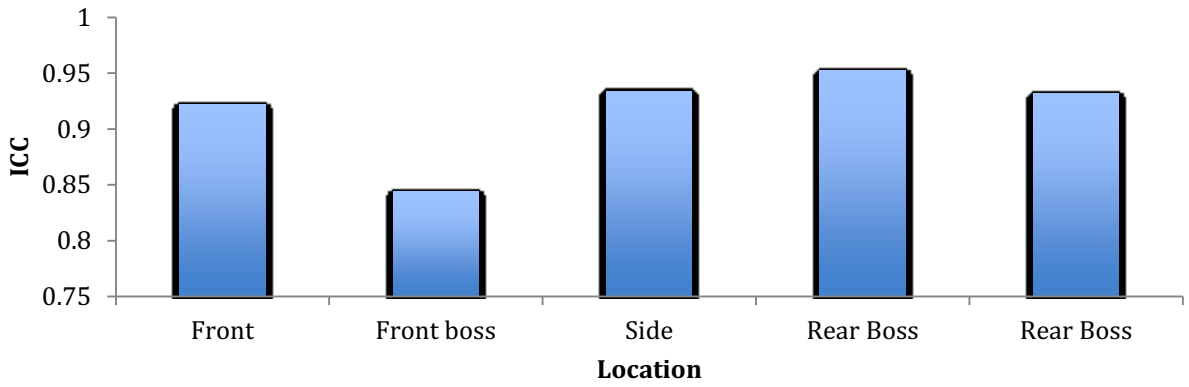

Figure 35. ICC coefficients for each of the five locations. Figure 14 summarizes the high degree of correlation between the data collected on the Lakehead University system and the University of Ottawa system. Analysis revealed strong significant (p<0.005) ICC values for all locations, ranging from ICC= 0.844 for the front boss location to as high as ICC=0.952 for the rear boss location. The findings provide evidence of concurrent validity at all locations tested.

The scaled values are important to future research. Since Lakehead University data was scaled to the established Ottawa University system, future data will also be scaled to these values to allow for valid data collection and analysis. Another important aspect of the drop system is its test-retest reliability, which was also previously determined using reliability analysis in SPSS computer software.

Reliability of the system's impact measures is also important to research using the Lakehead University drop system. Reliability is the extent to which the measurement is consistent and repeatable (Drost, 2011), in that the same result can be obtained from the drop system with different operators, on different occasion, and repeated trials. Reliability of the system's impact measures was determined by conducting 100 impacts to the rear location of a single helmet at an inbound velocity of 3.13 m/s. This velocity was achieved by raising the system up to a height of 50 cm before each trial. The helmet chosen was a new CCM Vector V08 helmet, identical to those used in the validity analysis. This protocol allowed for the determination of consistency of the acceleration values captured by the accelerometers across

replications.

An impact accelerations mean of M=86.44g, SD=3.02g was obtained over 100 impacts at the speed of 3.13 m/s. Strong evidence of reliability were found across replication of the protocol, r=0.922, $p<0.005$ when using the split-half technique. The split-half method is used when the results from a single measure is randomly divided into two equal halves. The two halves are then correlated to determine reliability of the scores from the measure (Nath, 2013). This correlation result provides evidence of consistency of the drop system and acceleration measures across identical trials.